DEVELOPMENT OF NIOSOME CONTAINING ACE INHIBITOR/CYCLODEXTRIN COMPLEXES AS AN OPHTHALMIC DELIVERY FOR LOWERING INTRAOCULAR PRESSURE

Miss Hay Marn Hnin -

จุฬาลงกรณ์มหาวิทยาลัย
Chulalongkorn University

A Thesis Submitted in Partial Fulfillment of the Requirements
for the Degree of Master of Science in Pharmaceutical Sciences and Technology
Common Course
FACULTY OF PHARMACEUTICAL SCIENCES
Chulalongkorn University
Academic Year 2019
Copyright of Chulalongkorn University

การพัฒนานิโอโซมบรรจุตัวยับยั้งเอซีอี/ไซโคลเดกซ์ทรินเชิงซ้อนเพื่อการนำส่งทางตาสำหรับลดความดันในลูกตา

น.ส.เฮย์ มาร์น ฮนิน -

จุฬาลงกรณ์มหาวิทยาลัย
CHULALONGKORN UNIVERSITY

วิทยานิพนธ์นี้เป็นส่วนหนึ่งของการศึกษาตามหลักสูตรปริญญาวิทยาศาสตรมหาบัณฑิต
สาขาวิชาเภสัชศาสตร์และเทคโนโลยี ไม่สังกัดภาควิชา/เทียบเท่า
คณะเภสัชศาสตร์ จุฬาลงกรณ์มหาวิทยาลัย
ปีการศึกษา 2562
ลิขสิทธิ์ของจุฬาลงกรณ์มหาวิทยาลัย

Thesis Title	DEVELOPMENT OF NIOSOME CONTAINING ACE INHIBITOR/CYCLODEXTRIN COMPLEXES AS AN OPHTHALMIC DELIVERY FOR LOWERING INTRAOCULAR PRESSURE
By	Miss Hay Marn Hnin -
Field of Study	Pharmaceutical Sciences and Technology
Thesis Advisor	Phatsawee Jansook, Ph.D.
Thesis Co Advisor	Assistant Professor Dusadee Charnvanich, Ph.D.

Accepted by the FACULTY OF PHARMACEUTICAL SCIENCES, Chulalongkorn University in Partial Fulfillment of the Requirement for the Master of Science

..... Dean of the FACULTY OF PHARMACEUTICAL SCIENCES
(Assistant Professor RUNGPETCH SAKULBUMRUNGSIL, Ph.D.)

THESIS COMMITTEE

..... Chairman
(Associate Professor ANGKANA TANTITUVANONT, Ph.D.)

..... Thesis Advisor
(Phatsawee Jansook, Ph.D.)

..... Thesis Co-Advisor
(Assistant Professor Dusadee Charnvanich, Ph.D.)

..... Examiner
(VARIN TITAPIWATANAKUN, Ph.D.)

..... External Examiner
(Associate Professor Rathapon Asasujarit, Ph.D.)

CHULALONGKORN UNIVERSITY

เฮย์ มาร์น ฮนิน - : การพัฒนานิโอโซมบรรจุตัวยับยั้งเอซีอี/ไซโคลเดกซ์ทรินเชิงซ้อนเพื่อการนำส่งทางตาสำหรับลดความดันในลูกตา. (DEVELOPMENT OF NIOSOME CONTAINING ACE INHIBITOR/CYCLODEXTRIN COMPLEXES AS AN OPHTHALMIC DELIVERY FOR LOWERING INTRAOCULAR PRESSURE) อ.ที่ปรึกษาหลัก : อ. ภก. ดร.ภาสวีร์ จันทร์สุก, อ.ที่ปรึกษาร่วม : ผศ. ภญ. ดร.ดุษฎี ชาญวาณิช

วัตถุประสงค์ในการศึกษานี้เพื่อพัฒนายาหยอดตานิโอโซมที่มีความคงตัวบรรจุตัวยับยั้งแองจิโอเทนซิน-คอนเวอร์ติงเอนไซม์ (เอซีอี) สำหรับลดความดันในลูกตา ในการศึกษานี้ใช้ตัวยับยั้งเอซีอีสามชนิดได้แก่ แคปโตพริล ควินาพริล และโฟซิโนพริล (FOS) ประเมินการเกิดสารประกอบเชิงซ้อนของยาดังกล่าวกับไซโคลเดกซ์ทริน (CD) ต้นแบบ ได้แก่ alphaCD betaCD และ gammaCD พบว่ายาทุกตัวแสดงการเกิดสารประกอบเชิงซ้อนกับไซโคลเดกซ์ทรินทุกชนิดในอัตราส่วน 1:1 โดยสารประกอบเชิงซ้อน FOS/gammaCD มีค่าคงที่ของการเกิดสารประกอบเชิงซ้อนสูงที่สุด การศึกษาจลนศาสตร์ของการสลายตัวยืนยัน FOS สลายตัวได้น้อยที่สุดเมื่อมี gammaCD อยู่ด้วย ผลการวิเคราะห์สารประกอบเชิงซ้อนในสถานะสารละลายและสถานะของแข็งรวมถึงการจำลองการจับกันให้การสนับสนุนการเกิดสารประกอบเชิงซ้อนระหว่าง FOS และ gammaCD อย่างแท้จริง การศึกษาความคงตัวทางความร้อนของ FOS ผ่านวิธีโซนิคเคชัน พบว่าช่วยเพิ่มความคงตัวเมื่อมี gammaCD อยู่ด้วยและสามารถป้องกันการเสื่อมสลายอย่างมีนัยสำคัญเมื่อเติมสารต้านออกซิเดชันสองชนิดได้แก่ อีดีทีเอ และ โซเดียม เมทาไบซัลไฟต์ เพื่อเพิ่มความคงตัวทางเคมีของ FOS ในสารละลายน้ำมากขึ้น จึงพัฒนาสูตรตำรับรูปแบบนิโอโซม ประเมินผลของไซโคลเดกซ์ทริน ชนิดของสารลดแรงตึงผิวและสารเพิ่มความคงตัว/เหนี่ยวนำให้เกิดประจุต่อคุณสมบัติทางเคมีฟิสิกส์และเคมีของนิโอโซมที่เตรียมได้ ค่าพีเอช ขนาดอนุภาคเฉลี่ย การกระจายขนาดอนุภาค และความต่างศักย์ไฟฟ้า อยู่ในช่วงที่ยอมรับได้ สูตรตำรับนิโอโซมทั้งหมดมีคุณสมบัติไฮเปอร์โทนิกเล็กน้อยและมีความหนืดต่ำ สูตรตำรับที่มีสแปน 60 ไดซีทิล ฟอตเฟส ร่วมกับมีและไม่มี gammaCD เป็นองค์ประกอบ ได้รับการคัดเลือกเป็นสูตรที่เหมาะสม เนื่องจากมีความสามารถกักเก็บยาได้มากและมีค่าความต่างศักย์ไฟฟ้าที่เป็นลบประกอบกับสามารถควบคุมการปลดปล่อยตัวยาแบบนอกกายได้ การศึกษาการซึมผ่านเนื้อเยื่อในสภาพแวดล้อมภายนอก ค่าฟลักซ์และสัมประสิทธิ์การซึมผ่านของ FOS มีค่าต่ำสุดในสูตรตำรับนิโอโซมที่มี gammaCD เป็นองค์ประกอบ ซึ่งยืนยันว่าสารประกอบเชิงซ้อนของ FOS/gammaCD ถูกบรรจุภายในชั้นน้ำตรงกลางของนิโอโซมและสามารถปกป้องตัวยาจากการเสื่อมสลายโดยปฏิกิริยาไฮโดรไลซิสได้ ข้อมูลการศึกษาความคงตัวพบว่า FOS ที่บรรจุในนิโอโซมมีความคงตัวทางกายภาพและเคมีโดยเฉพาะสูตรตำรับที่มี gammaCD ร่วมด้วย เป็นเวลาอย่างน้อยสามเดือนเมื่อเก็บในสภาวะอุณหภูมิ 4 องศาเซลเซียส

จุฬาลงกรณ์มหาวิทยาลัย
CHULALONGKORN UNIVERSITY

สาขาวิชา	เภสัชศาสตร์และเทคโนโลยี	ลายมือชื่อนิสิต .....
ปีการศึกษา	2562	ลายมือชื่อ อ.ที่ปรึกษาหลัก .....
		ลายมือชื่อ อ.ที่ปรึกษาร่วม .....

6176129733 : MAJOR PHARMACEUTICAL SCIENCES AND TECHNOLOGY
KEYWORD: FOSINOPRIL / CYCLODEXTRIN / NIOSOME / OPTHALMIC DELIVERY / STABILITY

Hay Marn Hnin - : DEVELOPMENT OF NIOSOME CONTAINING ACE INHIBITOR/CYCLODEXTRIN COMPLEXES AS AN OPHTHALMIC DELIVERY FOR LOWERING INTRAOCULAR PRESSURE. Advisor: Phatsawee Jansook, Ph.D. Co-advisor: Asst. Prof. Dusadee Charnvanich, Ph.D.

The purpose of this study was to develop a stable niosomal eye drop containing angiotensin converting enzyme (ACE) inhibitor for lowering intraocular pressure. Three ACE inhibitors i.e., captopril, quinapril and fosinopril (FOS) were used in this study. Their inclusion complexes formation with parent CDs i.e., alphaCD, betaCD and gammaCD were determined. All drugs represented 1:1 stoichiometry inclusion complex with each CD. Of these, FOS/gammaCD complex showed the highest stability constant. Kinetic degradation study confirmed that FOS showed the lowest degradation in the presence of gammaCD. The obtained results of solution- and solid-state characterizations including molecular docking supported the true inclusion complex formation of FOS with gammaCD. Thermal stability of FOS through heating by sonication method was improved in the presence of gammaCD and significantly protected it from the degradation was found by the addition of two antioxidants, EDTA and sodium metabisulfite. In order to further enhance the chemical stability of FOS in aqueous solution, niosomal formulations were developed. The effects of CD, surfactant type and membrane stabilizer/charged inducers on physiochemical and chemical properties of niosome were evaluated. The pH value, average particle size, size distribution and zeta potentials were within the acceptable range. All niosomal formulation showed slightly hypertonic with low viscosity. Span®60/dicetyl phosphate niosomal formulations in the presence and absence of gammaCD were selected as the optimum formulations according to high % entrapment efficiency and negatively zeta potential values as well as *in-vitro* controlled release profile. The lowest flux and apparent permeability coefficient values of FOS in niosome containing gammaCD in *ex-vivo* permeation confirmed that FOS/gammaCD complex was encapsulated within the inner aqueous core of niosome and could be protected it from hydrolytic degradation. The stability data revealed that FOS loaded niosomal preparation exhibited good physical and chemical stability especially of that in the presence of gammaCD for at least three months at storage condition of 4ºC.

Chulalongkorn University

Field of Study:	Pharmaceutical Sciences and Technology	Student's Signature .....
Academic Year:	2019	Advisor's Signature .....
		Co-advisor's Signature .....

ACKNOWLEDGEMENTS

First of all, I would like to express my deepest gratitude to my advisor, Phatsawee Jansook, Ph.D for his valuable guidance, helpfulness and encouragement throughout my study. His systematic mentorship helped me to extend my knowledge and to accomplish my research on time. I would like to say special thanks to my co-advisor, Asst.Prof. Dr. Dusadee Charnvanich for her valuable suggestions and greatly support of dicetylphosphate and stearylamine in niosome preparation.

I also would like to offer my sincere thanks to Assoc.Prof. Dr. Angkana Tantituvanont for kindly support porcine eyes from slaughterhouse, and all of my thesis committee for their valuable suggestions and comments.

Moreover, I am extremely grateful to the Thailand International Cooperation Agency (TICA) for granting the financial support to fulfill my study. My sincere thanks are also provided to the 90th Anniversary of Chulalongkorn University under Rachadapisek Somphot Fund for financially supported in this project.

Furthermore, I would like to thank to Asst.Prof. Dr. Thanyada Rungrotmongkol and Dr. Panupong Mahalapbutr from Structural and Computational Biology Research Unit, Department of Biochemistry, Faculty of Science, Chulalongkorn University for their kindly supported in molecular docking study.

Special thanks are giving to each teacher and staff in the Department of Pharmaceutics and Industrial Pharmacy, Faculty of Pharmaceutical Sciences, Chulalongkorn University for their facilities and instruments support. I would like to pay heartfelt thanks to all lab members especially Ms. Hayman Saung Hnin Soe and Ms. Phyo Darli Maw for their suggestion and helpfulness throughout the study years.

I am also grateful to Ministry of Health and Sports, Myanmar and Department of Food and Drug Administration, Myanmar for giving permission to study a Master of Science (Pharmaceutical Science and Technology) program in Chulalongkorn University.

Finally, I would like to express my deepest thanks to my parents, my sister and my friends, especially Ms.Theingi Tun for their never-ending support and encouraging talk which are valuable and precious for me to finish my study.

Hay Marn Hnin -

จุฬาลงกรณ์มหาวิทยาลัย
CHULALONGKORN UNIVERSITY

TABLE OF CONTENTS

Page

..... iii

ABSTRACT (THAI) iii

.....iv

ABSTRACT (ENGLISH).....iv

ACKNOWLEDGEMENTS.....v

TABLE OF CONTENTS.....vi

LIST OF TABLES..... viii

LIST OF FIGURES x

LIST OF ABBREVIATION.....xii

CHAPTER I INTRODUCTION.....1

CHAPTER II LITERATURE REVIEWS 6

1. Glaucoma.....6

2. ACE inhibitors.....7

2.1 Mechanism of action 7

2.2 Physicochemical properties and chemical stability of ACE inhibitors 9

3.Ocular drug delivery system.....13

3.1 Anatomy of the eye 13

3.2 Topical drug delivery to eye.....13

4.Cyclodextrins (CDs) 15

4.1 Drug/CD complex formation.....17

4.2 CD in ocular drug delivery.....19

4.3 Role of CD in stability enhancement 20

5. Niosome.....21

6. Drug-in-CD-in-niosome 23

CHAPTER III MATERIALS AND METHODS 27

จุฬาลงกรณ์มหาวิทยาลัย
Chulalongkorn University

Materials 27
Equipments 29
Methods 31
CHAPTER IV RESULTS AND DISCUSSION.....45
1. Stoichiometry determination by Job's Plot method.....45
2. Stability constant determination 46
3. Kinetic degradation study 47
4. Effect of CD on thermal stability of FOS 49
5. Effect of antioxidants on thermal stability of FOS 51
6.Characterization of FOS/γCD inclusion complex 52
7.Physicochemical and chemical characterization of niosomal formulations containing fosinopril.....62
8. Transmission electron microscopy (TEM) 73
9. *In-vitro* release study 74
10. *Ex-vivo* permeation study 76
11. Physical and chemical stability studies of FOS 78
CHAPTER V CONCLUSIONS 87
REFERENCES 89
APPENDIX HPLC VALIDATION.....110
VITA 119

จุฬาลงกรณ์มหาวิทยาลัย
Chulalongkorn University

LIST OF TABLES

Page

Table 1 Physicochemical properties of ACE inhibitors (60, 61, 68-71).....12

Table 2 Some physicochemical properties of parent CDs and CD derivatives (modified from Ref (87)).....17

Table 3 Some observations of niosome encapsulated drug/CD complex 25

Table 4 Conditions for stoichiometric determination 31

Table 5 Compositions of FOS loaded niosomal formulations.....40

Table 6 Stability constant ($K_{1:1}$) of the drug/CD complexes in ultrapure water (mean values, n=3).....47

Table 7 Degradation rate constant (k) of FOS in pure water or in CD complexing media (mean values, n=3).....49

Table 8 The percentage of FOS remaining in pure water or 5% (w/v) aqueous γCD solution after one to three heating cycles by autoclaving or sonication in ultrasonic bath (n=3, mean±S.D.).....50

Table 9 The percentage of FOS remaining in 5% (w/v) aqueous γCD solution with antioxidants after one to three heating cycles by sonication in ultrasonic bath at 60°C for 30 min (n=3, mean±S.D.).....52

Table 10 ^{1}H-NMR chemical shifts (ppm) of FOS alone and in the presence of γCD ..54

Table 11 pH value, osmolality and viscosity of the formulations (n=3, mean±S.D.) .67

Table 12 Mean particle size, size distribution and zeta potential of the formulations (n=3, mean±SD).....70

Table 13 Total drug content and entrapment efficiency of niosomal formulations (n=3, mean±S.D.) 72

Table 14 The flux and apparent permeation coefficient (P_{app}) of FOS loaded niosomal preparation in the presence and absence of γCD, and aqueous FOS/γCD complex solution, through porcine cornea or sclera (n=4, ± S.D.).....78

Table 15 pH values of FOS niosomal preparation and FOS/γCD complex storage at 4°C, 30±2 °C (75±5% RH) and 40±2 °C (75±5% RH) for 0, 1,3 and 6 months (n=3, mean±S.D.) 81

จุฬาลงกรณ์มหาวิทยาลัย
Chulalongkorn University

Table 16 The average particle size and size distribution (PDI) of FOS niosomal preparation and FOS/γCD complex storage at 4°C, 30±2 °C (75±5% RH) and 40±2 °C (75±5% RH) for 0, 1, 3 and 6 months (n=3, mean±S.D.).....82

Table 17 The average zeta potential values (ZP) of FOS niosomal preparation and FOS/γCD complex storage at 4°C, 30±2 °C (75±5% RH) and 40±2 °C (75±5% RH) for 0, 1, 3 and 6 months (n=3, mean±S.D.) 84

Table 18 Total FOS content (%) of FOS niosomal preparation and FOS/γCD complex storage at 4°C, 30±2 °C (75±5% RH) and 40±2 °C (75±5% RH) for 0, 1, 3 and 6 months (n=3, mean±S.D.).....85

จุฬาลงกรณ์มหาวิทยาลัย
Chulalongkorn University

LIST OF FIGURES

Page

Figure 1 Schematic diagram showing the main components of the renin- angiotensin system (56).....9

Figure 2 Anatomy of the eye (https://cyclolab.hu.com) 13

Figure 3 The chemical structure and the conical shape of cyclodextrin molecule (85, 86) 16

Figure 4 Schematic diagram showing permeation of free drug or drug/CD complex from the ocular membrane surface (99, 100).....20

Figure 5 The structure of niosome encapsulating hydrophilic and lipophilic drugs (117) 22

Figure 6 Stoichiometric determinations of (a) quinapril (b) fosinopril sodium (c) captopril; αCD (left), βCD (middle) and γCD (right). Data represented means of three determinations.....45

Figure 7 The first-order plots for degradation of FOS alone or with CDs in aqueous solution (n=3, mean±S.D.); (a) at 25°C (b) at 40°C; (●) FOS alone; (○) αCD; (▲) βCD; (△) γCD. The error bars are smaller than the symbol size at 40°C. 48

Figure 8 Partial counter plot of 500 MHz, 2D ROESY spectrum of 1:1 FOS/γCD complex in D_2O, showing cross peaks of aromatic protons of FOS with inner protons of γCD cavity.....55

Figure 9 Geometry of inclusion complex of FOS with γCD through the insertion of aromatic ring of FOS from secondary hydroxyl rim of γCD (a) overview, (b) side view. Grey backbone represents FOS moiety whereas grey with red backbone represents γCD moiety. 56

Figure 10 DSC thermograms of (a) pure FOS, (b) pure γCD, (c) PM FOS/γCD, (d) FD FOS/γCD.....57

Figure 11 PXRD spectra of (a) pure FOS, (b) pure γCD, (c) PM FOS/γCD, (d) FD FOS/γCD.....59

Figure 12 FT-IR spectra of (a) pure FOS, (b) pure γCD, (c) PM FOS/γCD, (d) FD FOS/γCD.....61

จุฬาลงกรณ์มหาวิทยาลัย
Chulalongkorn University

Figure 13 The proposed conformations of 1:1 FOS/γCD inclusion complex 62

Figure 14 The appearance of FOS loaded Span® 60 and Brij® 76 niosomes in the presence and absence of γCD 63

Figure 15 Polarized light microscopic images of FOS loaded niosomal formulations in the presence of Span® 60 surfactant with or without 5% γCD; (a) F1; (b) F2; (c) F3; (d) F4; (e) F5 ; (f) F6 (Magnification of 10×40) 64

Figure 16 Polarized light microscopic images of FOS loaded niosomal formulations in the presence of Brij®76 surfactant with or without 5% γCD; (a) F7; (b) F8; (c) F9; (d) F10; (e) F11; (f) F12 (Magnification of 10×40) 65

Figure 17 TEM micrographs of FOS loaded niosomes (a) F1, (b) F2, (c) F4 and (d) F5 74

Figure 18 The release profiles of FOS niosomal preparations and FOS/γCD loaded niosomal preparation through semipermeable membrane with MWCO 12000-14000 Da (n=3, mean±S.D.).....76

Figure 19 The proposed drawing of (a) FOS loaded niosomes and (b) FOS/γCD loaded niosome 86

จุฬาลงกรณ์มหาวิทยาลัย
Chulalongkorn University

LIST OF ABBREVIATION

%	percentage
°C	degree Celsius
µg	microgram (s)
µl	microliter (s)
µm	micrometer (s)
µM	micromolar (s)
αCD	α-cyclodextrin
βCD	β-cyclodextrin
γCD	γ-cyclodextrin
Å	angstrom
ACE	angiotensin-converting enzyme
AH	aqueous humor
AMD	age-related macular degeneration
Ang	angiotensin
CAP	captopril
CD	cyclodextrin
CHO	cholesterol
D_2O	deuterium oxide
Da	dalton
DCP	dicetylphosphate
DSC	differential scanning calorimetry
DLS	dynamic light scattering
EDTA	disodium edetate
Eq	equation
FD	freeze-dried

จุฬาลงกรณ์มหาวิทยาลัย
CHULALONGKORN UNIVERSITY

FT-IR	fourier transform infrared spectroscopy
FOS	fosinopril sodium
HLB	hydrophilic-lipophilic balance
HPβCD	2-hydroxylpropyl-βCD
HPγCD	2-hydroxylpropyl-γCD
HPLC	high-performance liquid chromatography
^{1}H-NMR	proton nuclear magnetic resonance
ICH	International Conference on Harmonisation
IOP	intraocular pressure
K	stability constant
k	degradation rate constant
min	minute (s)
mL	milliliter (s)
MLV	multilamellar vesicles
mM	micromolar (s)
mm	millimeter (s)
mV	millivolts
MWCO	molecular weight cut-off
Na-MS	sodium metabisulfite
nm	nanometer (s)
P_{app}	permeation coefficient
PDI	polydispersity index
PXRD	powder X-ray diffraction
PM	physical mixture
QUI	quinapril
RAS	renin-angiotensin system
R^2	coefficient of determination

จุฬาลงกรณ์มหาวิทยาลัย
Chulalongkorn University

RMβCD	randomly methylated-βCD
ROESY	rotating frame overhauser enhancement spectroscopy
rpm	revolution per minute
s	second (s)
SBEβCD	sulfobutylether-βCD
SC24	solulan ® C24
SD	standard deviation
STA	stearylamine
TEM	transmission electron microscopy
ULV	unilamellar vesicles
UV/VIS	ultraviolet/visible
VEGF	vascular endothelium growth factor
v/v	volume by volume

จุฬาลงกรณ์มหาวิทยาลัย
Chulalongkorn University

CHAPTER I
INTRODUCTION

Glaucoma is one of the leading causes of irreversible blindness worldwide. It is characterized by progressive optic neuropathy in association with damaging of optic nerve head and subsequently, visual loss if it is left untreated (1, 2). According to the recent data, the researchers predicted that the global glaucoma prevalence will be risen up to 80 million people in 2020 and 11.2 million will be blind bilaterally as the result of glaucoma (3). It was predicted that India will become the second greatest number of people with glaucoma, surpassing Europe by 2020 (3). The national health and nutrition examination survey (2005–2008) suggested that the lower bound estimate is 2.9 million people in the United States were affected by glaucoma (4). The elevation of intraocular pressure (IOP), usually greater than 20.5 mmHg is considered a major risk factor for glaucoma (1, 5). Glaucoma can occur in any age but the prevalence is exponentially increased with age (6). Glaucoma can be found in several variants depending on the underlying etiology, but the two main types are open-angle glaucoma and close-angle glaucoma (1). The underlying cause is excessive aqueous humor (AH) retention in an anterior chamber due to imbalance between AH production and outflow within the eyes (2). AH is physiologically produced by processing of ciliary-body. It flows into the anterior chamber to nourish the cornea before leaving through the trabecular meshwork into the venous system. Only a small volume of AH is existed by the way of uveoscleral channels (1, 7). Close-angle glaucoma is caused due to the obstruction AH outflow by the closure of the angle between the iris and cornea. In primary open-angle glaucoma, the

จุฬาลงกรณ์มหาวิทยาลัย
Chulalongkorn University

trabecular meshwork-Schlemm's canal system increases the resistance of AH outflow, which in turn leads to an elevated IOP (1, 8).

Currently, treatment for management of glaucoma includes topical and oral medical therapies, laser therapies, and surgical operation, all are aimed to lower IOP (2). Effective drug therapies include the drugs that reduce the rate of AH production and/or enhance its drainage. Several classes of drugs are available in managing long-term treatment of glaucoma such as prostaglandin analogues, carbonic anhydrase inhibitors, α-adrenergic agonists, β-adrenergic blockers, and cholinergic agonists (1, 2).

Angiotensin-converting enzyme (ACE) inhibitors have recently paid attention as a new class of drug for the treatment of glaucoma. ACE is responsible for the conversion of the biologically inactive angiotensin I (Ang I) to the potent vasopressor, angiotensin II (Ang II) as well as the breakdown of bradykinin. Inhibition of ACE leads to the accumulation of bradykinin and promote the synthesis of prostaglandins, which could in turn lower IOP by increasing the uveoscleral outflow (9). Additionally, the blockage of Ang II formation leads to increase the level of Ang I as well as Ang (1–7), which has opposite effects to Ang II (10-13). Recent study showed that both Ang I and Ang (l-7) stimulate for prostaglandin release (13).

จุฬาลงกรณ์มหาวิทยาลัย
Chulalongkorn University

Earlier studies proved that ACE inhibitors had the ability to lower IOP (14-17). They also have beneficial effect on retarding the progression of diabetic retinopathy in types diabetic patients (18, 19). Moreover, ACE inhibitors showed beneficial effect in age-related macular degeneration (AMD) through suppression of inflammatory responses of renin-

angiotensin system (RAS) signaling pathway (20, 21). However, the literatures reported that ACE inhibitors produce various side-effects when given systemically (22-24). Topical and localized application could provide beneficial effects on targeted eyes with lower systemic side-effects.

ACE inhibitors possess difference chemical structures in their active moieties. The different unique structure of ACE inhibitors reveals for their certain types of degradation such as cyclization via internal nucleophilic reaction to form substituted diketopiperazines, oxidation and/or hydrolysis of the ester side chain group (25-28). Therefore, most ACE inhibitors are available only in solid oral dosage forms.

Several studies have been reported that cyclodextrins (CDs) improve the chemical stability of many labile drugs in aqueous solution (29-32). CDs are cyclic (α-1,4)-linked oligosaccharides of α-D-glucopyranose units formed by the action of certain enzymes on starch. The most common natural CDs are α-cyclodextrin (αCD), β-cyclodextrin (βCD), and γ-cyclodextrin (γCD), which consist of six, seven, and eight glucopyranose units, respectively. CDs possess truncated conical shapes with hydrophobic central cavities and hydrophilic exterior edges imparted by hydroxy group networks (33, 34). Due to these unique structural features, CDs form inclusion complexes with a variety of organic guest substrate, and thereby increase the solubility of the drug, improve stability, enhance the transmembrane permeation and minimizes the ocular irritation (35, 36). It was reported that CD induced enhancement of drug stability may be a result of providing a molecular shield by encapsulating chemically labile

จุฬาลงกรณ์มหาวิทยาลัย
Chulalongkorn University

moiety of drug molecule at the molecular level and protecting them against various process of degradation (34).

Recently, colloidal drug delivery has been introduced as alternative formulation approaches for problematic drug candidates. Numerous colloidal carriers such as liposome, niosome, nanoparticle, microemulsion and micelles have been developed, which are applicable not only to solve the problems of poor solubility and stability but also to provide specific drug targeting, optimized drug release properties and reduce toxicity (37). Vesicular carrier, niosome has gained attention because of its advantages as follows: (i) enhance solubility and permeability; (ii) improve chemical stability; (iii) simple and cost-effective fabrication; (iv) low toxicity and high compatibility because of their non-ionic nature (38).

Niosomes are non-ionic surfactant vesicles, arisen from the self-assembly of nonionic amphiphiles in aqueous media. The spherical shaped niosomes are capable of entrapping lipophilic molecules within the lipid bilayer by interacting with alkyl chains of non-ionic surfactants, whereas hydrophilic drug molecules are located within an aqueous core by interacting with polar head groups of non-ionic surfactants (39, 40). Numerous studies reported the successful uses of niosome as ocular drug delivery carriers (41-45). Vesicular delivery systems used in ophthalmic offer targeting at the site of action, improving chemical stability of encapsulated drug and providing controlled release action at the corneal surface (46, 47). Vyas et al. (1998) reported that the ocular bioavailability of niosome entrapped water-soluble drug i.e., timolol maleate was increased as compared to timolol maleate solution (41). This can be

จุฬาลงกรณ์มหาวิทยาลัย
Chulalongkorn University

explained that surfactants behave as penetration enhancers by removing the mucus layer and breaking junctional complexes (48).

In this study, the effect of CD on the formation of ACE inhibitors inclusion complexes and their thermal stability were determined. The solution-state and solid-state characterizations of selected fosinopril (FOS)/γCD complexes were investigated. Then, niosomal preparations containing FOS/γCD inclusion complex were developed. This combined strategy i.e., Drug/CD inclusion complex and incorporation of inclusion complex into niosomal vesicle was applied to increase the chemical stability and to provide controlled drug release action. The physiochemical and chemical properties of niosomal formulations were evaluated. In addition, *in-vitro* release, *ex-vivo* permeation and physical and chemical stability studies were also determined.

The main objectives of this work are as follows:

1. To determine the effect of CD on the formation of ACE inhibitors inclusion complexes and the thermal stability of drug
2. To prepare the drug/CD complexes and evaluate by solution and solid-state characterizations
3. To develop and characterize niosomal formulation containing drug/CD complex
4. To determine the physical and chemical stability of niosomal formulation containing drug/CD complex

จุฬาลงกรณ์มหาวิทยาลัย
Chulalongkorn University

CHAPTER II
LITERATURE REVIEWS

1. Glaucoma

Glaucoma is a multifactorial long-term ocular neuropathy, which is associated with a progressive loss of visual field, structural abnormalities of retinal nerve fiber and cupping of optic nerve head (1, 2). Nowadays, it become the second leading cause of blindness worldwide after cataract (3).The pressure within the eye is physiologically maintained by a balance of AH formation and out-flow. In healthy human eye, AH is secreted with the flow rate of 2 µl/min from the posterior chamber by the non-pigmented ciliary epithelial cells lining the ciliary processes (1, 5). It flows around the lens and then into anterior chamber, from which it leaves the eye principally through the trabecular meshwork. Only a smaller portion is drained out by uveoscleral out-flow (1). If any blockage or slow drainage of the channels, there is excessive accumulation of AH which leads to increase pressure within the eyes, damaging to the optic nerve head and as a result, permanent vision loss if untreated condition. The normal IOP is 15.5 (±2.6) mmHg and the elevation of IOP greater than 20.5 (± 2.0) mmHg is considered as a glaucoma (1, 5).

จุฬาลงกรณ์มหาวิทยาลัย
Chulalongkorn University

Several types of glaucoma are found depending on the underlying etiology, but the most common types are open-angle glaucoma and close-angle glaucoma. Open-angle glaucoma is found in the case of slow drainage or resistance to the outflow of AH despite the angle is opened whereas the drainage angle is blocked in angle closure glaucoma (1, 8). Currently, IOP is the major known risk factor for glaucoma. However, there are many predictors such as age, positive family history, race,

myopia, exfoliation syndrome (49). Moreover, glaucoma is usually associated with various systemic vascular diseases including low systemic blood pressure, transient nocturnal decreases in blood pressure, hypertension, migraine, vasospasm and diabetes has been reported (50-53). Systemic hypertension is the most common coexisting vascular disorders found in patients with chronic open-angle glaucoma (54).

Currently used all medical management for glaucomatous treatment are aimed to lower IOP. Treatment options involve oral and topical medications, laser therapy and surgical operation. Medication is the first line treatment and laser therapies are used to help the fluid drain out of the eyes. If medication and laser therapy are not enough various types of surgical operations are applied to drain out of the fluid. Medications involve the drugs that reduce AH production and/or enhance its drainage such as prostaglandin analogues, carbonic anhydrase inhibitors, α-adrenergic agonists, β-adrenergic blockers, and cholinergic agonists (1, 2).

จุฬาลงกรณ์มหาวิทยาลัย
Chulalongkorn University

2. ACE inhibitors

2.1 Mechanism of action

ACE inhibitors is a potent vasodilator which is widely used in the treatment of hypertension, congestive heart failure and diabetic nephropathy (55). It is well-known that ACE plays an important role in the control of blood pressure and electrolyte homeostasis of renin-angiotensin system (RAS). ACE (kininase II) is a bivalent dipeptidyl carboxyl metallopeptidase, presents as a membrane-bound form in endothelial cells,

epithelial or neuroepithelial cells, and as a soluble form in blood and numerous body fluids (55). ACE is responsible for the conversion of the biologically inactive angiotensin I to the potent vasopressor, angiotensin II as well as the breakdown of bradykinin, a physiological stimulus of prostaglandin production. Inhibition of ACE leads to the accumulation of bradykinin and promote the synthesis of prostaglandins, a potent vasodilator which could in turn lower IOP by increasing the uveoscleral outflow (9). Additionally, ACE inhibition is associated with significant elevations of Angiotensin (1–7). The blockade of ACE activity diverts the pathway of Ang II formation and increase in Ang I level as well as degradation of Ang I into Ang (1–7) (10, 11). Figure 1 shows the main components of RAS. Recent study also showed that both Ang I and Ang (l-7) stimulated PG release (13). Ang (1–7) has the opposite effects to Ang II. It promotes vasodilation, possibly by increasing nitric-oxide formation, release of prostaglandins and/or potentiation of the vasodilatory actions of bradykinin (12, 13). Therefore, mechanisms of ACE inhibitors-induced IOP lowering are resemble to those of prostaglandin analogs by increasing uveoscleral outflow of AH.

จุฬาลงกรณ์มหาวิทยาลัย
Chulalongkorn University

There are several reported that ACE inhibitors have anti-vascular endothelium growth factor (VEGF) on retinal cells in retarding the progression of diabetic retinopathy (18, 19), AMD (20, 21) and other VEGF induced neovascular conditions of the eye (56-58).

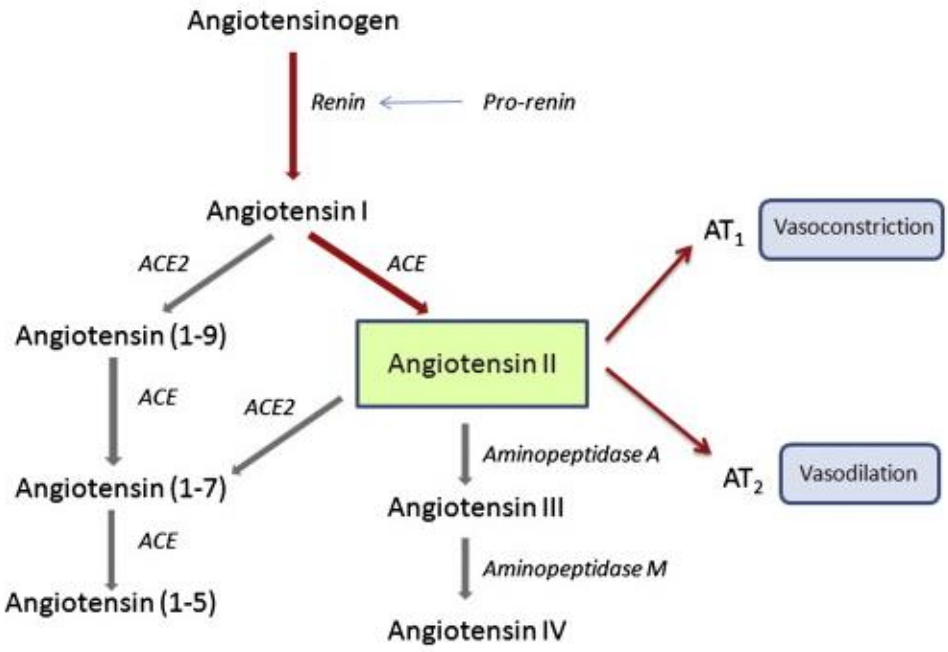

Figure 1 Schematic diagram showing the main components of the renin- angiotensin system (56).

2.2 Physicochemical properties and chemical stability of ACE inhibitors

จุฬาลงกรณ์มหาวิทยาลัย
Chulalongkorn University

The physicochemical properties of captopril (CAP), quinapril hydrochloride (QUI) and fosinopril sodium (FOS) are shown in Table 1. All these drugs studied are very soluble in water with high Log $P_{o/w}$ values except for CAP (Log $P_{o/w}$ 0.34). Practically most ACE inhibitors contain acidic functional groups in addition to their fundamental carboxyl group. Therefore, most ACE inhibitors exhibit with two p*K*a values. In CAP, the presence of carboxylic acid group represents as p*K*a 3.7 and a second p*K*a value of 9.8 is due to the weakly acidic thiol group (59). Dicarboxyl group of QUI behaves as a strong acid (p*K*a 2.8) and secondary amine exhibits p*K*a 5.4 (60). For FOS, phosphinic group is more acidic (p*K*a 3.7)

than the carboxyl group (p*K*a 4.1) (61). According to the Biopharmaceutics Classification System (BCS), QUI and FOS are including in BCS class I and CAP is classified as BCS class I/III system (60, 62).

CAP is the first generation of orally active sulfhydryl containing ACE inhibitor. It subjects to some degree of oxidative degradation due to the presence of sensitive thiol group. The rate of oxidation is promoted in the presence of contaminant metal ions. As the captopril molecule also includes an amide function group, degradation via hydrolysis is also possible. The pH dependent stability of CAP shows maximum stability below pH 4.0 (27).

QUI is an ester prodrug and rapidly hydrolyzed *in vivo* into more active diacid form, quinaprilat (63). Like other ACE inhibitors, QUI is unstable in aqueous solution and degrades approximately 9 % after 24 h at room temperature (64). Previous study reported that QUI is stable only a narrow range of pH 5.5-6.5 (64). The two major degradants formation of QUI is pH dependent, quinaprilat is formed in basic condition and intramolecular cyclization product is formed in acid condition. (64, 65).

จุฬาลงกรณ์มหาวิทยาลัย
Chulalongkorn University

FOS is the ester prodrug of fosinoprilat, the first orally active phosphorus-containing ACE inhibitor. It is converted into active moiety, fosinoprilat *in vivo* by hydrolysis of diester side chain (66). According to the literature, degradation of FOS occurs in two distinct pathways, i.e., ion-mediated degradation and hydrolysis. The metal ion-mediated degradation of FOS was found especially with magnesium (28). Hydrolysis degradation of FOS was found in all conditions i.e., acidic, basic and neutral whereas the greater extent in basic condition (67). The photostability studies revealed that degradation product was found in photo-acidic condition i.e.,

in 0.1 N HCl (67). Because of this, the development of aqueous formulations of FOS has been retarded. Recently, literature reported that concentration dependent stability of FOS in phosphate buffer (pH 7), increasing in FOS concentration resulted decreasing in hydrolysis rate. This was due to the formation of micellar shield by the ester linkage and protected from attacking by phosphate or hydroxy ions (68).

จุฬาลงกรณ์มหาวิทยาลัย
Chulalongkorn University

Table 1 Physicochemical properties of ACE inhibitors (60, 61, 68-71)

Drugs	Chemical structure	Molecular weight	Melting point (°C)	p*K*a	Log$P_{o/w}$ [a]	S_0 (mg/ml) in water (at RT [b])
Captopril	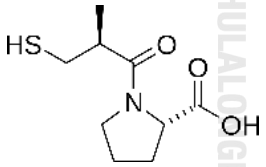	217.29	106	3.7, 9.8	0.34	160
Quinapril Hydrochloride	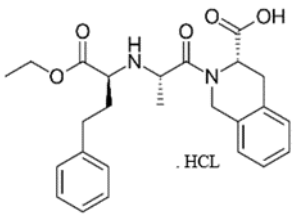	474.98	167	2.8, 5.4	3.72	>100
Fosinopril sodium	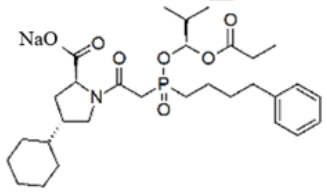	585.7	196	3.7, 4.1	6.19	~ 350

[a]The logarithm of the octanol/water partition coefficient

[b]Room temperature at 25 °C

3.Ocular drug delivery system

3.1 Anatomy of the eye

A complexed unique structure of the eye can be divided into two portions: the anterior segment which occupies one-third portion of the eye and the remaining two-third portion of the eye refers to posterior segment (Figure 2). Anterior segment comprises cornea, conjunctiva, aqueous humor, iris, ciliary body, and lens while sclera, vitreous humor, retina, choroid, and optic nerve are belonged to the posterior segment (72).

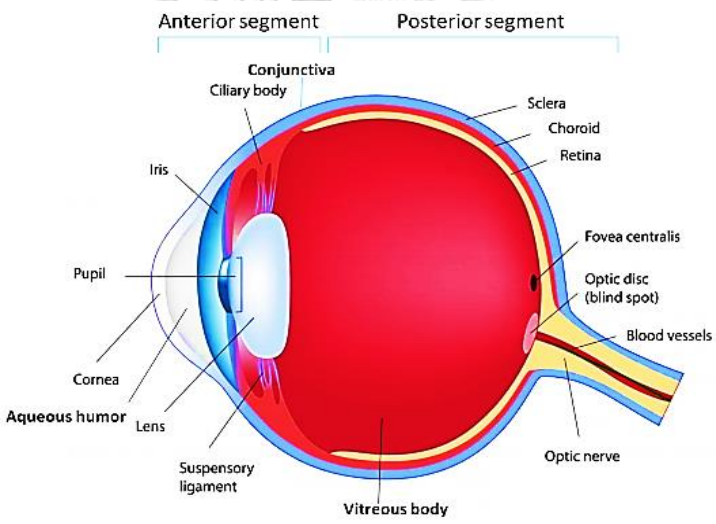

Figure 2 Anatomy of the eye (https://cyclolab.hu.com)

3.2 Topical drug delivery to eye

Ocular drug delivery via the topical administration typically involves the conventional dosage forms, such as solutions, suspensions and ointments, and about 90% of these are currently marketed ophthalmic formulations. Although topical administration is a patient-friendly route,

its ocular bioavailability is generally <5% of applied dose (35). The main barriers that involving in topical drug delivery to the eye are lacrimal or tear fluid drainage system, the mucus layer on the eye surface and membrane barrier, i.e., cornea and conjunctiva/sclera. Tear film contributes to a majority of the drug loss due to its high turnover rate of 0.5–2.2 µL/min. A healthy human eye has approximately 7–9 µL of a tear volume and cul-de-sac can transiently keep up to 30 µL. The excess volume upon topical administration is drained either via the nasolacrimal duct into systemic circulation or lost by reflex blinking (5–7 blinks/min) (73). Moreover, mucus layer on the eye surface also forms an unstirred aqueous layer and behaves as an aqueous barrier to passive diffusion of dissolved drug molecules.

As we known, the cornea represents as the main absorption path for most of ophthalmic preparations. It is generally composed of three main layers i.e., epithelium, stroma and endothelium. The cornea epithelial forms a primary barrier to the drug absorption via topical administration. Due to its lipid nature, corneal epithelium gives a significant resistance to the permeation of hydrophilic drugs (74). The corneal stroma is embedded in mucopolysaccharides matrix and highly hydrated with collagen fibrils. Due to its hydrophilic nature, corneal stroma acts as a major barrier for permeation of lipophilic drug (74). The innermost endothelium is a separating barrier between stroma and aqueous humor, which allows the passage of even macromolecules due to the leakage of their junctions (74). Therefore, corneal epithelial and stroma are considered as the main barriers for ocular drug delivery and at the same time, the drug molecule should have amphipathic nature i.e., appropriate hydrophilic and lipophilic properties in order to permeate these barriers (75). Although the corneal

permeation is favorably depended on lipophilicity of the drug molecule, the permeation through conjunctiva/sclera is mainly controlled by the molecular size of a drug molecule, where permeation is inversely proportional to molecular size (76, 77). Moreover, due to the presence of conjunctival blood capillaries and lymphatics, there is a significant drug loss into systemic absorption and decreasing the overall drug available for therapeutic action (78).

Achieving the desired concentration of a drug at the targeted eye with prolonged duration of time is the main challenge faced by the researchers worldwide. Numerous ophthalmic nano-scaled drug delivery systems have been exploited to improve ocular bioavailability such as liposome, niosome, microsphere, ocular insert and polymeric nanoparticle (76). CDs has been gained interesting as an alternative approach in topical ophthalmic formulations for increasing solubility and permeability of poorly water-soluble drugs (79, 80). CDs act as the potential drug carrier by protecting the drug in solution and enhancing the ocular bioavailability by increasing the drug availability at the ocular surface (81).

จุฬาลงกรณ์มหาวิทยาลัย
Chulalongkorn University

4.Cyclodextrins (CDs)

Complexation with CD has been successfully used in pharmaceutical field for enhancing solubility, stability, bioavailability and reduce the side effects of a variety of drugs (34, 82, 83). CDs are cyclic (α-1,4)-linked oligosaccharides, obtained by glycotransferase enzyme-induced degradation of starch. The three most common natural CDs, named αCD, βCD and γCD consists of 6, 7 and 8 glucopyranose units

respectively. The cone shaped structure of CDs present hydrophilic outer surface due to secondary hydroxy groups facing outwards from the wider edge and primary hydroxy groups from the narrower edge (Figure 3) whereas lipophilic character of central activity is given by linking of skeletal carbons with ethereal oxygen of the glucose units (34, 84). This unique structural feature brings about the use of CD as a solubilizer for poorly water-soluble drug.

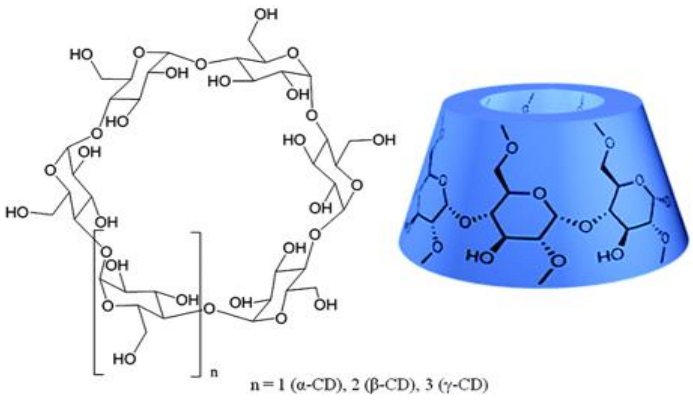

Figure 3 The chemical structure and the conical shape of cyclodextrin molecule (85, 86)

จุฬาลงกรณ์มหาวิทยาลัย
Chulalongkorn University

Due to the limited aqueous solubility of nature CDs, especially with βCD, intra-molecular hydrogen bonds between adjacent secondary hydroxyl groups reduce their interactions with the water molecule. Therefore, a number of modified CD derivatives such as hydroxypropyl derivatives of βCD and γCD, randomly methylated-βCD and sulfobutylether-βCD are synthesized. CD molecules are relatively large (molecular weight ranging from almost 1000 to >2000 Da) with numerous hydrogen bond donors and acceptors, and therefore, they are poorly

absorbed through biological membranes (87). The physicochemical properties of natural CDs and some CD derivatives are shown in Table 2.

Table 2 Some physicochemical properties of parent CDs and CD derivatives (modified from Ref (87))

Cyclodextrin	Substitution[a]	Molecular weight (Da)	Solubility in water[b] (mg/mL)
α-cyclodextrin (αCD)	-	972	145
β-cyclodextrin (βCD)	-	1135	18.5
γ-cyclodextrin (γCD)	-	1297	232
2-hydroxylpropyl-βCD (HPβCD)	0.65	1400	>600
Randomly methylated-βCD (RMβCD)	1.8	1312	>500
Sulfobutylehter-βCD (SBEβCD)	0.9	2163	>500
2-hydroxylpropyl-γCD (HPγCD)	0.6	1576	>500

[a]average number of substituents by glucopyranose per repeat unit
[b]solubility in pure water at about 25 °C

จุฬาลงกรณ์มหาวิทยาลัย
Chulalongkorn University

4.1 Drug/CD complex formation

In aqueous solution, CD forms inclusion complexes with a variety of organic guest molecules by inserting lipophilic moiety or the whole molecule within its inner cavity (87). There is no covalent bond formation during the complexation and the free drug molecules are in equilibrium with the molecule bound within the CD cavity. The hydrophobic

interaction, Van der Waals' forces, hydrogen bond formation, electrostatic interaction as well as the release of conformational strain and charge-transfer interaction contribute in a cooperative way to the inclusion mechanism (34). The release of high enthalpy water molecules from the hydrophobic CD cavity upon complexation in aqueous media has been assigned as the driving force for complex formation (88).

Numerous physicochemical methods are applied to characterize the entrapment of drug molecule in hydrophobic CD cavity. The solution state characterizations involve solubility studies, spectroscopic methods such as UV/VIS spectroscopy, circular dichroism spectroscopy, fluorescence spectroscopy and nuclear magnetic resonance spectroscopy, pH-potentiometric titration, microcalorimetry and surface tension techniques (89). Differential scanning calorimetry (DSC), Fourier transform infrared spectroscopy (FT-IR), and powder X-ray diffraction analysis (XRD) are the most commonly used techniques to characterize the inclusion complex formation in solid-state (90). The ability of CDs to accommodate a variety of guest molecule within their cavities modify the physicochemical properties of the guest molecules, with consequent several benefits such as enhancement of drug solubility, stability and bioavailability, reduction in ocular and gastrointestinal irritation, and masking of unpleasant odor and taste (91).

4.2 CD in ocular drug delivery

In most cases, CDs are used to enhance aqueous solubility, reduce ocular irritation and improve ocular bioavailability of the drug, but in some cases, CDs are used as an alternative approach in topical ophthalmic formulations for stability enhancement of labile drugs (92, 93). Several studies proved that CD enhance the ocular bioavailability of drugs (94-96). However, using too much CD than it is required to solubilize the lipophilic drugs will decrease the ocular bioavailability. The optimum concentration of CDs for the aqueous eye drop preparations should be less than 15% (36). In case of multidose eye drop container, care should be taken to select the suitable preservative and its appropriate amount in formulation because CDs can reduce the efficiency of the preservatives (36).

Due to large molecular weight and hydrophilic outer surface, CDs are hardly permeated through the biological membrane. Moreover, relatively lipophilic membrane has low affinity for hydrophilic CD molecules and thus, they remain in the aqueous tear fluid. However, CD complexation increase the solubility of poorly soluble drug in tear fluid, resulting increase in drug concentration gradient over the mucus as shown in Figure 4. Consequently, increase the availability of free drug molecules at ocular epithelium surface by keeping the drug molecules in solution and delivering them to the eye surface, thereby improve the drug permeation and ocular bioavailability (91, 97, 98).

จุฬาลงกรณ์มหาวิทยาลัย
Chulalongkorn University

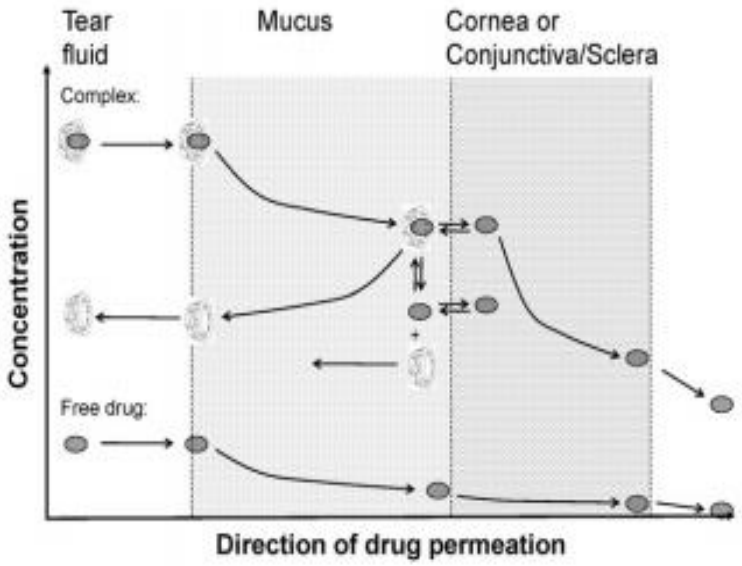

Figure 4 Schematic diagram showing permeation of free drug or drug/CD complex from the ocular membrane surface (99, 100)

4.3 Role of CD in stability enhancement

The feasibility of pharmaceutical formulation is usually limited by its stability issues. This is because therapeutic activity is frequently lost especially with aqueous formulations, the drugs are prone to be hydrolysis or oxidative degradation. In recent years, CD has gained a role in enhancing the stability of labile drugs. It was reported that CD-induced enhancement of drug stability may be a result of providing a molecular shield by encapsulating chemically labile moiety of drug molecule at the molecular level and protecting them against various process of degradation (34). There are numerous reported that CD complexation improves the chemical stability of many labile drugs in aqueous solution by hampering hydrolysis, oxidation, photodecomposition, isomerization and enzyme

catalyzed degradation of dissolved drugs solution (29-32, 101-103). It also enhances the solid-state stability of the drugs (104, 105).

However, CDs also accelerate the drug degradation in some cases (34, 101, 106-108). Indeed, the stabilization of the drug upon CD complexation is not only depend on the type and concentration of CD but also the portion of the drug that resides within the complex and the nature of the vehicle used (109-113). The magnitude of the stability constant of drug/CD complex plays a significant role in determining the extent of protection of drug against various degradations (114, 115).

5. Niosome

Niosome, one kind of colloidal particles, brings a promising way to increase the drug bioavailability, prevent degradation, reduce toxicity and transport to targeted sites (116). Niosomes are hydrated vesicular system, comprised of nonionic surfactants along with cholesterol and charged molecules. Nonionic surfactants consist of hydrophobic tail and polar head group, possessing high interfacial activity and form bilayer vesicle by self-assembly upon hydration. Niosomes that contain only one bilayer are designated as unilamellar vesicles (UV) and with more bilayers as multilamellar vesicles (MLV). Niosomes are able to encapsulate hydrophilic drugs in their interior hydrophilic core and hydrophobic drugs within the lipid bilayer (Figure 5) and thereby, provide better chemical stability of drug from various degradation process (39). The most common widely used non-ionic surfactants for niosome formulations are sorbitan fatty acid ester (Span®), polyoxyethylene sorbitol ester (Tween®) and polyoxyethylene cetyl ether (Brij®) (38).

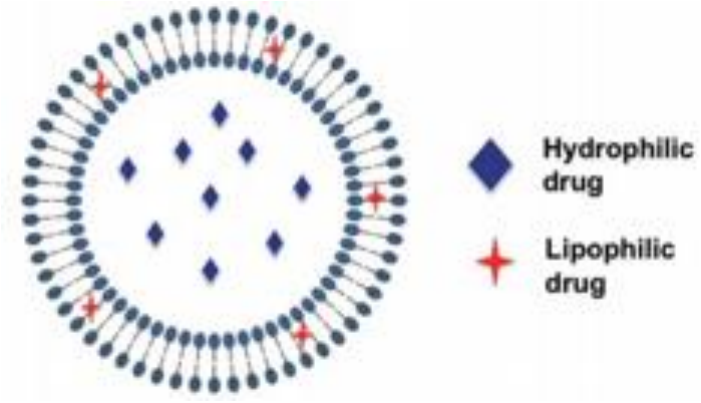

Figure 5 The structure of niosome encapsulating hydrophilic and lipophilic drugs (117)

Niosomes are usually prepared by various methods such as thin-film hydration method, reversed phase evaporation, ether injection, microfluidization, transmembrane pH gradient method, nitrogen bubble method and heating method (116). Among these methods, thin-film hydration method is most commonly used to avoid direct exposure of drug molecule to organic solvent. However, there are several factors that influence on physiochemical properties of niosomes such as type of surfactant, nature of drug, method of preparation, surfactant to lipid level and hydration temperature (118).

The level of surfactant/lipid used to prepare the niosomal dispersion is generally 10-30 mM (1-2.5% w/w) (39). Alteration in surfactant and water ratio during the hydration step may affect the structure and properties of niosome (119). Cholesterol is used mainly to improve the rigidity of the membrane which affects the fluidity and permeability of the bilayer. In general, a molar ratio of 1:1 between cholesterol and nonionic surfactant plays an optimal ratio for physically stable niosomal formulation. As HLB value of surfactants increase above 10, it is necessary to increase the

amount of cholesterol added for compensating the larger polar head group (39, 120).

Charged molecules are usually added to enhance the stability of the niosome by preventing aggregation of vesicles. Dicetylphosphate (DCP) and phosphatidic acid are known as negative charged molecules while stearylamine (STA) and cetylpyridinium chloride are used as positively charged molecules, respectively (42). Normally, charged molecules are added in the amount of 2.5-5 mol % because the higher concentration can inhibit the formation of niosomes (123). The other non-ionic membrane additive is cholesteryl ploy-24-oxyethylene ether (Solulan ® C24) and used in the range of 5-10 mol% to enhance membrane stability by steric effect (42).

6. Drug-in-CD-in-niosome

Drug-in-CD-in-niosome is a new strategy to encapsulate the drug molecules in the form of water-soluble drug/CD inclusion complexes into niosome vesicle. The coupling of these two delivery systems has been investigated to combine the relative advantages of both carriers into one system and to overcome some drawbacks associated with each separate system. Based on our knowledge, there are few literatures reported regarding to this system (122-128) and their observations are shown in Table 3.

It is well-known that CD itself increases the chemical stability of the drug molecule by encapsulating within its hydrophobic cavity (101). The

loading of the drug/CD complex into the inner aqueous core of niosome attributes better stability of encapsulated drug. The presence of double barriers offered by the lipid membrane of niosomal vesicle and hydrophobic cavity of CD reduce the exposure of unstable drug from various degradation environment and enhancement in stability (129).

Regarding to the drug release, incorporation of CD to niosomal system provides better controlled release of drug profile. The literature reported there are two possible ways for drug release. The one is that drug/CD inclusion complex can be transported from the inner aqueous core to the lipid bilayer of vesicle and then, release as the whole inclusion complex into the medium. The other way is the release of free drug which is in equilibrium with inclusion complexes in the inner aqueous core of niosome (130).

There are also beneficial that entrapment of drug/CD complex in inner aqueous core of niosome prevent possible drug displacement by other blood components which have higher affinity for the CD cavity. Moreover, the combined system can also overcome the problem of low drug-to-lipid mass ratio and destabilizing issue of niosomal lipid bilayer membranes due to incorporation of sparingly water-soluble drugs (131-133). Therefore, incorporation of drug/CD complexes into niosome provide as a promising strategy to join their respective beneficial effects into one carrier system.

จุฬาลงกรณ์มหาวิทยาลัย
Chulalongkorn University

Table 3 Some observations of niosome encapsulated drug/CD complex

Niosome loaded drug/CD complex	Composition[a]	Observations	Ref.
Ibuprofen/βCD	Tween®20/ CHO	faster drug release and rapid permeation rate than free drug loaded niosome in *in-vitro* study	(122)
Fluconazole/HPβCD	Span®60/ CHO	Enhanced both the drug flux and corneal permeation than free drug solution in *in-vitro* study, well tolerated with no corneal swelling or discharge, enhanced antifungal activity with a prolonged action	(124)
Methotrexate/βCD	Span®60/ CHO/ DCP	Provided a more stable niosome with higher %EE, slower *in-vitro* drug release and enhance anti-tumor activity as compared with free drug loaded niosome	(123)
Ciprofloxacin/βCD and norfloxacin/βCD	Tween®80/ CHO	A more sustained drug release with significant higher absorption in intestine in contrast with drug/CD complex solution	(125)

จุฬาลงกรณ์มหาวิทยาลัย
Chulalongkorn University

Table 3 Some observations of niosome encapsulated drug/CD complex (Con't)

Niosome loaded drug/CD complex	Composition[a]	Observations	Ref.
Pseudolaric acid B/ HPβCD	Tween®80/ CHO	Provided sustained drug release with 8.1 fold higher rat plasma stability than free drug solution	(126)
Pilocarpine/βCD	Span®60/ CHO/ DCP	Increased %EE, a slower and controlled drug release than free drug loaded niosome	(127)
Plumbagin/βCD	Span®60/ CHO/ DCP	Improved anticancer activity with faster drug release by comparing with plain drug loaded niosome	(128)

[a]CHO = cholesterol; DCP= dicetylphosphate

จุฬาลงกรณ์มหาวิทยาลัย
Chulalongkorn University

CHAPTER III
MATERIALS AND METHODS

Materials

The following materials were used as

- Acetonitrile HPLC grade (Burdisk & Jackson, Korea)
- Alpha-cyclodextrin (Wacker Chemie AG, Germany)
- Beta-cyclodextrin (Wacker Chemie AG, Germany)
- Brij® 76 (The East Asiatic Public Company Ltd, Thailand)
- Captopril (Dideu Industries Group Ltd, China)
- Chloroform (RCI Labscan Ltd, Thailand)
- Cholesterol (Sigma-Aldrich, USA)
- Dialysis membrane (Spectra/Por, Netherlands)
- Dicetyl phosphate (Sigma-Aldrich, USA)
- Disodium hydrogen phosphate (Ajax Finechem Pty Ltd, Australia)
- Ethylenediamine tetra-acetic acid disodium salt (Ajax Finechem Pty Ltd, Australia)
- Fosinopril sodium (Dideu Industries Group Ltd, China)
- Gamma-cyclodextrin (Wacker Chemie AG, Germany)
- Methanol HPLC grade (Burdisk & Jackson, Korea)
- Phosphoric acid (Carlo Erba Reagents, Germany)
- Potasssium chloride (Ajax Finechem Pty Ltd, Australia)
- Potassium dihydrogen phosphate (Ajax Finechem Pty Ltd, Australia)
- Quinapril hydrochloride (Dideu Industries Group Ltd, China)
- Sodium chloride (Ajax Finechem Pty Ltd, Australia)

จุฬาลงกรณ์มหาวิทยาลัย
Chulalongkorn University

- Sodium metabisulphite (Ajax Finechem Pty Ltd, Australia)
- Solulan® C-24 (Chemico inter Corporation Ltd, Thailand)
- Span® 60 (Chemico inter Corporation Ltd, Thailand)
- Stearylamine (Sigma-Aldrich, USA)
- Tetrahydrofuran (RCI Labscan Ltd, Thailand)

จุฬาลงกรณ์มหาวิทยาลัย
CHULALONGKORN UNIVERSITY

Equipments

- Analytical balance (Mettler Toledo AG285, Germany)
- Autoclave (Hirayama, HICLAVE HVE-50, Japan)
- Differential scanning calorimetry (NETZSCH, DSC204 F1 Phoenix, Germany)
- Franz diffusion cell (NK Laboratories Co. Ltd., Bangkok, Thailand)
- Freeze dryer (Labconco Lyophilizer, MO, USA)
- Fourier transform infrared spectroscopy (Thermo Scientific, model Nicolet iS10, USA)
- High performance liquid chromatography (HPLC) instrument equipped with
    - Liquid chromatography pump (quaternary pump, Agilent 1260 Infinity II, G7111A)
    - UV-VIS detector (Agilent 1260 Infinity II, G7115A)
    - Auto sampler (Agilent 1260 Infinity II, G7129A)
    - C18 column (Phenomenex Kinetex, 5µm, 150×4.5 mm ID reverse phase column)

จุฬาลงกรณ์มหาวิทยาลัย
Chulalongkorn University

- High speed refrigerator micro centrifuge (TOMY, MX-305, Japan)
- Nanosizer (Zetasizer, Nano-ZS with software version 7.11, Malvern, UK)
- Osmometer (Gonotec, OSMOMAT 3000 basic, Germany)
- pH meter (Mettler Toledo, Seven Compact, Germany)
- Polarized light microscope (Nikon Eclipse E200, Japan)
- Powder X-ray diffractometer (Rigaku model MiniFlex II, Japan)

- Proton nuclear magnetic resonance spectroscopy (^{1}H-NMR, BRUKER, model AVANCE III HD, USA)
- Rotary evaporator (BUCHI Rotavapor R-200, Switzerland)
- Shaking incubator (DLabTech, LSI-4018A, India)
- Transmission electron microscope (Model JEM-2100F, JEOL, USA)
- Thermostat circulating water bath (GRANT W6, England)
- Ultra-centrifuge (HITACHI CP100NX, Japan)
- Ultrasonic bath (GT sonic, China)
- UV-Visible spectrophotometer (Shimadzu UV-1800, Japan)
- Viscometer (Sine-wave Vibro SV-10, Japan)

จุฬาลงกรณ์มหาวิทยาลัย
Chulalongkorn University

Methods

1. Stoichiometry determination

The stoichiometry of the drug/CD inclusion complexes was determined by Job's Plot method of continuous variation (134). Equimolar solutions of drug and CD (i.e., αCD, βCD or γCD) were mixed in 10-mL volumetric flasks by varying the molar ratio (1 mL:9 mL; 2 mL:8 mL; and so on), while the total concentration was held constant. An analogous set of the drug solution was also carried out by using ultrapure water as a medium. After shaking for 24 h at room temperature, the absorbance was measured by Ultraviolet-Visible (UV-Vis) spectrophotometer (Shimadzu UV-1800, Japan) using 1.0-cm quartz cells. Absorbance values were measured at respective λ_{max} for each drug at 298.15 K. The absorbance variation in the presence and absence of CD was calculated as $\Delta A = A\text{-}A_0$. The values of ΔA was plotted against mole fractions R, where R =[Drug]/{[Drug]+[CD]}. Each sample was carried out in triplicate and the results presented are the average of all experiments. The conditions for stoichiometric determination of quinapril (QUI), fosinopril (FOS) and captopril (CAP)are shown in Table 4.

จุฬาลงกรณ์มหาวิทยาลัย
Chulalongkorn University

Table 4 Conditions for stoichiometric determination

Drugs	Concentration (mM)	Detection wavelength (nm)
Quinapril	1.14	258
Fosinopril	0.03	208
Captopril	0.07	210

2. Stability constant determination

Benesi-Hildebrand model was applied for determination of apparent stability constant of drug/CD inclusion complexes (135). The UV-Vis spectrophotometric measurement was performed by keeping the drug concentration as constant (i.e., 1.14, 0.03, 0.07 mM for QUI, FOS and CAP, respectively), whereas CD concentrations were varied from 0 to 5 mM. The absorption spectra were recorded in the range of 200–400 nm, using 1.0-cm quartz cells. The variation of the absorbance $\Delta A = A\text{-}A_0$ was calculated as the difference between the absorbance of drug at different CD concentrations and in the absence of CD. The stability constant value (K_s) was calculated using the following Eq. 1:

$$\frac{1}{\Delta A} = \frac{1}{[\text{Drug}] \cdot \Delta\varepsilon \cdot K_s} \cdot \frac{1}{[\text{CD}]} + \frac{1}{[\text{Drug}] \cdot \Delta\varepsilon} \qquad \text{Eq. 1}$$

Where, ΔA is change in absorbance, $\Delta\varepsilon$ is change in molar attenuation coefficient, and K_s is stability constant.

จุฬาลงกรณ์มหาวิทยาลัย
Chulalongkorn University

3. Kinetic degradation study

To investigate the effect of CD on kinetic degradation of the FOS, the experiment was carried out by adding 1% (w/v) FOS in ultrapure water or aqueous solutions containing 5% (w/v) CD (αCD, βCD or γCD) solutions. The samples were placed in vials, covered with screw caps, stored at the temperature of 25±1 °C and 40±1°C. At different time intervals, an aliquot (1.0 mL) was withdrawn and analyzed by validated high-performance liquid chromatography (HPLC) method. Each measurement was carried out in triplicate. By plotting of logarithms of the

percent drug remaining versus time, the slope value was obtained and from which degradation rate constant (*k*) was calculated by the following Eq. 2:

$$\text{Slope} = -k / 2.303 \qquad \text{Eq.2}$$

4. Quantitative analysis of FOS

4.1 Calibration curve of FOS

The accurate amount of FOS (10.0 mg) was weighed and dissolved in acetonitrile: water (70:30 v/v) to obtain 200 μg/mL of FOS as a stock solution. The solution was further diluted to be a concentration range of 20-200 μg/mL. Each concentration was subjected to HPLC analysis in triplicate. Peak area was recorded and the equation was calculated from the linear relationship between peak area of FOS and their concentrations.

4.2 Sample preparation

The sample was prepared by appropriately diluted with acetonitrile: water (70:30 v/v). A portion of sample was filtered through 0.45 μm nylon filter before subjected to HPLC analysis. The content of FOS in the sample was calculated from calibration curve of FOS.

4.3 HPLC condition

The quantitative determination of FOS was performed on a reversed-phase HPLC component system from Agilent 1260 Infinity II consisting of liquid chromatography pump (quaternary pump, G7111A), UV-VIS detector (G7115A), auto sampler (G7129A) with Chem Station software

version (E.02.02) and Phenomenex Kinetex 5µm C18 reverse-phase column (150 ×4.6 mm) with C18 guard cartridge column MG II 5µm, 4×10 mm. The HPLC conditions was as follows; mobile phase: aqueous solution containing 1% tetrahydrofuran with 0.05% phosphoric acid and acetonitrile (30:70 v/v); flow rate:0.9 mL/min; UV detector wavelength: 205 nm; oven temperature: 40°C; injection volume 20 µL; and run time: 6 min.

4.4 Validation for quantitative analysis of FOS

Specificity

The specificity of analyte was investigated by injecting of FOS, γCD, EDTA, Na-MS, blank niosome and mobile phase to demonstrate that there is no interference in analyte elution (see in Appendix). The components were properly diluted before determining by HPLC.

Linearity

Linearity was determined by injecting three sets of six concentrations (20-200 µg/mL) of FOS standard solutions. The calibration curves were constructed by plotting the peak area versus their concentration, and linear regression analysis was evaluated from coefficient of determination (R^2). R^2 value > 0.999 is regarded as indicating coefficient.

Precision

Within run precision

The within run precision was checked by analyzing five sets of three standard solutions of FOS within one day. The coefficient of variation of the peak area responses (% CV) for each concentration were determined.

Between run precision

The between run precision was determined by analyzing three standard solutions on three different days. Each concentration of FOS standard solution on three different days were compared and the coefficients of variation of the peak area responses (% CV) was calculated.

Accuracy

The accuracy of analytical method is the closeness of test result to the true value. The recovery of FOS from blank formulation was assessed by spiking blank formulation (all components except the drug) with the amount of FOS in formulation at three level spanning. The analysis was done in triplicate. The average recovery and the coefficient of variation (% CV) were then calculated.

5. Effect of CD on thermal stability of FOS

The thermal stability study was carried out according to Loftsson et al. (2005) (136). The small amount of FOS to be tested was dissolved in ultrapure water or 5% (w/v) aqueous γCD solution. Each solution was divided into four sealed vials and equilibrated at 30±1°C for 24 h under constant agitation. After equilibrium was attained, one sealed vial was left for no heating cycle and the other three sealed vials were heated in autoclave at 121°C for 20 min by one, two and three heating cycles. The analogue set was performed in ultrasonic bath by sonicating at 60 °C for 30 min. The experiment was performed in triplicate. The concentration of the drug remaining in each vial was determined by validated HPLC method.

6. Effect of antioxidants on thermal stability of FOS

The effect of antioxidants on thermal stability of FOS was determined by adding 0.1% (w/v) of disodium edetate (EDTA) or sodium metabisulfite (Na-MS) individually or their combination to the aqueous FOS solution containing 5% (w/v) γCD. Each solution was divided into four sealed vials and thermal stability was determined as described in section 5. The experiment was done in triplicate.

7. Solution-state characterization

7.1 ^{1}H-NMR spectroscopy

The NMR spectra were recorded at 500 MHz by ^{1}H-NMR spectrometer (BRUKER model AVANCE III HD, USA). The deuterium oxide (D_2O) solutions of pure FOS and γCD as well as binary FOS/γCD complex (i.e., 1:1 molar ratio of drug/CD) were equilibrated at constant agitation for 24 h and then were subjected to analysis. The residual solvent signal at 4.6500 ppm was used as internal reference. The chemical shift values (Δδ*) were expressed as ppm and calculated according to the following Eq. 3:

$$\Delta\delta^* = \delta_{(complex)} - \delta_{(free)} \qquad \text{Eq.3}$$

7.2 Rotating Frame Overhauser Enhancement Spectroscopy (ROESY)

Two-dimensional (2D) NMR spectroscopy was applied to investigate a more insight between the binding mode of FOS with γCD as

well as to confirm the structure of inclusion complexes proposed by ^{1}H-NMR. The experiment was carried out with a spectral width of 0-5500 Hz with 32 scans at 25°C. The acquisition time was 0.1835 s, the relaxation delay was 2.0 s, and the spin-lock mixing time was set to 200 ms. 2D NMR spectra was recorded for 1:1 molar ratio of FOS/γCD complex in D_2O in which at 4.6500 ppm was used as an internal reference.

8. Molecular docking study

The 3D structures of FOS and γCD were obtained by extracting from their crystal structures at Protein Data Bank in pdb file format. The geometries of FOS and γCD were optimized and inclusion complex was constructed using CDOCKER module implemented in Discovery Studio 2.5 software (Accelrys, Inc., San Diego, CA, USA). CHARMm force field was used to diminish the potential energy. A 10 Å radius sphere was defined around the bounded ligand to confirm the side chain of some residues of the receptor within the distance from the center of active site is free to move. After 100 docking runs, all possible inclusion conformations of FOS and γCD were generated.

จุฬาลงกรณ์มหาวิทยาลัย
Chulalongkorn University

9. Solid-state characterization

Sample preparation

Aqueous solution containing 1:1 molar ratio of the binary complexes i.e., FOS/γCD was prepared by heating in the sonicator at 60°C for 30 min. The sample was equilibrated at 30±1 °C for 24 h under constant agitation. After the equilibrium was attained, the sample was centrifuged (Thermo Fisher Scientific, MA, USA) at 13,000 rpm for 20 min. Then, the

supernatant was withdrawn, frozen at -80°C for 2 h and lyophilized at -52 °C for 48 h in a freezer-dryer (Labconco Lyophilizer, MO, USA) to obtain a solid complex freeze-dried powder (FD). Identical physical mixture (PM) was prepared by careful blending of FOS and γCD in a mortar with pestle. The samples were characterized in solid-state as follows: pure FOS and γCD, PM and FD of binary FOS/γCD complexes.

9.1 Differential Scanning calorimetry (DSC)

DSC thermograms was determined by a differential scanning calorimeter (NETZSCH, DSC204 F1 Phoenix, Germany). The samples (3-5 mg) were placed in sealed aluminium pans and heated with flow rate of 5.0 K/min from 30 to 300 °C under nitrogen. An empty aluminium pan was used as reference.

9.2 Powder X-ray diffraction (PXRD)

The PXRD patterns were recorded by powder X-ray diffractometer (Rigaku^{TM} model MiniFlex II, Japan). The analyses were performed at a voltage of 30 kV with a current of 15 mA and the process parameters were set as follows: 2 θ angle range of 3°- 40°, step size of 0.020° (2 θ) and scan speed of 2°/min.

9.3 Fourier transform infra-red (FT-IR) spectroscopy

The samples were measured in a FT-IR spectrometer (Thermo Scientific model Nicolet iS10, USA) using Attenuated Total Reflectance (ATR) technique. The samples were analyzed at room temperature and the data were recorded in the range of 400–4000 cm^{-1}.

10. Preparation of niosome

Niosome was prepared by thin-film hydration method (137). The niosome formulations were composed of non-ionic surfactant, cholesterol, and membrane stabilizer/charged inducer at the mole ratio of 47.5: 47.5: 5. This ratio was optimized during blank niosome preparations that shown to be its relatively good physicochemical characteristics. The total lipid composition was prepared at 100 μM in 5 ml of hydration medium. The surfactants used in this study were Span® 60 and Brij® 76. Solulan® C24 (SC24) was used as a steric stabilizer. Stearylamine (STA) and dicetylphosphate (DCP) were used to give electrostatic stabilization of vesicles as well as positive and negative charge, respectively. Briefly, accurately weighed amount of non-ionic surfactant, cholesterol and membrane stabilizer/charge inducer were dissolved in 10 ml of chloroform in 1L round bottom flask. The lipid mixture was slowly evaporated under reduced pressure at 40°C using a rotary evaporator (BUCHI Rotavapor R-200, Switzerland) with a constant speed of rotation. The flask was partially immersed in a water bath and evaporated until a dried thin film appeared on the inner wall of the flask. Then, it was kept in a desiccator under vacuum for 2 h to ensure total removal of trace solvents. After that, dried lipid film was hydrated with 5 mL of phosphate buffer saline (pH 7.4) containing FOS, EDTA and Na-MS with and without γCD. The hydration of dried film was carried out by rotating the flask in a water bath at 60°C for 30 min using a rotavapor under normal pressure. The size reduction was made by sonicating in an ultrasonic bath (GT sonic, China) at 60°C for 30 min. In order to complete annealing and partition of the drug between the lipid bilayer and the aqueous phase, the formulation was left overnight at

room temperature and then, stored at 4°C until subjected to analysis. The compositions of niosome formulae are shown in Table 5.

Table 5 Compositions of FOS loaded niosomal formulations

Formulation [a]	F1	F2	F3	F4	F5	F6	F7	F8	F9	F10	F11	F12
Ingredients in organic phase (μM) [b]												
Span® 60	47.5	47.5	47.5	47.5	47.5	47.5	-	-	-	-	-	-
Brij®76	-	-	-	-	-	-	47.5	47.5	47.5	47.5	47.5	47.5
Cholesterol	47.5	47.5	47.5	47.5	47.5	47.5	47.5	47.5	47.5	47.5	47.5	47.5
SC24	5	-	-	5	-	-	5	-	-	5	-	-
DCP	-	5	-	-	5	-	-	5	-	-	5	-
STA	-	-	5	-	-	5	-	-	5	-	-	5
Ingredients in aqueous phase (% w/v) [c]												
FOS	1	1	1	1	1	1	1	1	1	1	1	1
γCD	-	-	-	5	5	5	-	-	-	5	5	5

[a] SC24, Solulan®C24; DCP, dicetylphosphate; STA, stearylamine; FOS, fosinopril sodium

[b] solubilized in 10 ml of chloroform

[c] solubilized in 5 ml of phosphate buffer saline pH 7.4 containing 0.1% (w/v) EDTA and 0.1% (w/v) sodium metabisulfite

จุฬาลงกรณ์มหาวิทยาลัย
Chulalongkorn University

11. Physicochemical and chemical characterizations

11.1 Appearance, microscopic observation and pH, viscosity and osmolality determination

The niosomal formulations containing FOS were subjected to visual inspection. The polarized light microscope (Nikon Eclipse E200, Japan) was used to verify the existence of vesicular bilayer in niosomal preparations (138). All niosome formulation containing FOS were subjected to analysis. The polarized light photomicrographs were recorded by mean of a fitted digital camera (Canon EOS 700D, Japan). The pH

values of all formulations were measured with pH meter (Mettler Toledo, Seven Compact, Germany) at 25°C. The viscosity was determined by viscometer (Sine-wave Vibro SV-10, Japan) using the Tuning-fork vibration method with frequency of 30 Hz at 25°C and 34°C. The osmolality was determined by osmometer (Gonotec, OSMOMAT 3000 basic, Germany) at room temperature using freezing point depression principle. All measurements were determined in triplicate.

11.2 Particle size and size distribution, and zeta potential

The particle size and size distribution, and zeta potential of FOS loaded niosome formulations were measured by dynamic light scattering (DLS) technique (Zetasizer ^{TM} Nano ZS with software version 7.11, Malvern, UK). The sample was put in a cuvette and placed in the instrument. The measurements were carried out at a scattering angle of 180° and a temperature of 25°C. The particle size distribution was expressed as polydispersity (PDI). The particle size, size distribution and zeta potential were automatically calculated and analyzed by the software included within the system. Each measurement was performed in triplicate.

จุฬาลงกรณ์มหาวิทยาลัย
Chulalongkorn University

11.3 Determination of drug content and entrapment efficiency(EE)

Total drug content in niosomal preparation was determined by dissolving 100 µL of sample in 10 mL of methanol : water (50:50 v/v). After proper dilution, the solution was filtered through 0.45 µm nylon filter and analyzed by HPLC.

For the determination of the percentage of EE (%EE), the sample was ultra-centrifuged (HITACHI CP100NX, Japan) at 18,000 rpm at 4°C for 1 h. Then, the content of unentrapped drug in the supernatant was

diluted with methanol : water (50:50 v/v) and quantified by HPLC. All samples were done in triplicate. The %EE was calculated as Eq. 4 (139):

$$\%EE = \frac{(Dt-Ds)}{Dt} \times 100 \qquad \text{Eq.4}$$

Where Dt is total drug content and Ds is drug content in supernatant.

11.4 Transmission electron microscopy (TEM) analysis

The morphological examination of FOS loaded niosomes with or without CD were performed by TEM technique. Initially, the sample was placed on a formvar-coated grid. After blotting the grid with a filter paper, the grid was transferred onto a drop of negative stain. Aqueous 1% phosphotungstic acid solution was used as a negative stain. The sample was air dried at room temperature and finally the samples was examined by TEM (Model JEM-2100F, JEOL, USA).

12. *In-vitro* release study

จุฬาลงกรณ์มหาวิทยาลัย
Chulalongkorn University

The *in-vitro* release study was performed by using modified Franz diffusion cell apparatus consisting of donor and receptor chambers (NK laboratories Co., Ltd, Bangkok, Thailand). These two chambers were separated by a semipermeable membrane (MWCO 12000-14000 Da). The membrane was presoaked overnight in the receptor phase that consisted of phosphate buffer saline (pH 7.4). The receptor phase was degassed to remove dissolved air before it was placed in the receptor chamber. The sample (1.5 mL) of each niosomal formulation was placed into the donor chamber. The receptor phase was continuously stirred at 150 rpm throughout the experiment and controlled temperature at 34 ± 1^{o}C by

thermostated circulating bath (GRANT W6, England). A 150 μL aliquot of the receptor medium was withdrawn at time interval and replaced immediately with an equal volume of fresh receptor phase. The FOS content in the receptor medium was determined by HPLC and the amount of cumulative drug release was calculated. Each formulation was done in triplicate.

13. *Ex-vivo* permeation study

The *ex-vivo* permeation study was performed across cornea and sclera of porcine eyes obtained within 4 h after the death of pigs from slaughterhouse. In this study, cornea and sclera were disserted from porcine eyes and replaced the semipermeable cellophane membrane as previously described in the *in-vitro* release study. The selected FOS loaded niosomal formulations in the presence and absence of γCD, and aqueous solution of FOS/γCD complex used as a control were done at least in triplicate and the FOS content in the receptor phase at interval time was determined by HPLC. The steady state flux was calculated as the slope of linear section of the amount of cumulative drug release (q) versus time (t) profiles, and the apparent permeability coefficient (P_{app}) was calculated from the flux (J) according to the Eq.5:

$$J = \frac{dq}{A \cdot dt} = P_{app} \cdot C_d \qquad \text{Eq.5}$$

where A is the surface area of the mounted membrane (1.7 cm^2) and C_d is the initial concentration of the drug in the donor chamber.

14. Physical and chemical stability studies

To investigate the effect of either niosome platform or CD inclusion complex or their combination on the physical and chemical stability of FOS in aqueous solutions, selected optimal FOS loaded niosomal formulations (in the presence and absence of γCD) including aqueous solution of FOS/γCD complex were evaluated by the on-going stability program following International Conference on Harmonisation (ICH) guidelines (140, 141). The samples were stored in tightly closed glass vials at 4°C, long-term condition (30±2 °C, 75±5 % RH) and accelerated condition (40±2 °C, 75±5 % RH). Physical appearance was assessed and formulations were analyzed with respect to pH, particle size and size distribution, zeta potential and the drug content at time interval of 0, 1, 3 and 6 months.

15. Statistical analysis

All quantitative data were presented as means ± standard deviation (S.D.). The data were statistically calculated using one-way ANOVA (SPSS software version 16.0) with a Bonferroni's post-hoc test. The $p<0.05$ was considered as statistically significant.

จุฬาลงกรณ์มหาวิทยาลัย
Chulalongkorn University

CHAPTER IV
RESULTS AND DISCUSSION

1. Stoichiometry determination by Job's Plot method

According to the Job's Plot method of continuous variation, the maximum concentration of the inclusion complex was presented where the molar ratio R corresponds to the complexation stoichiometry. In this study, the maximum absorbance of all three drugs i.e., QUI, FOS and CAP with three different parent CDs (αCD, βCD, γCD) were observed for R=0.5 (Figure 6), which indicated that the drugs formed inclusion complexes with tested CDs in the stoichiometric ratio of 1:1.

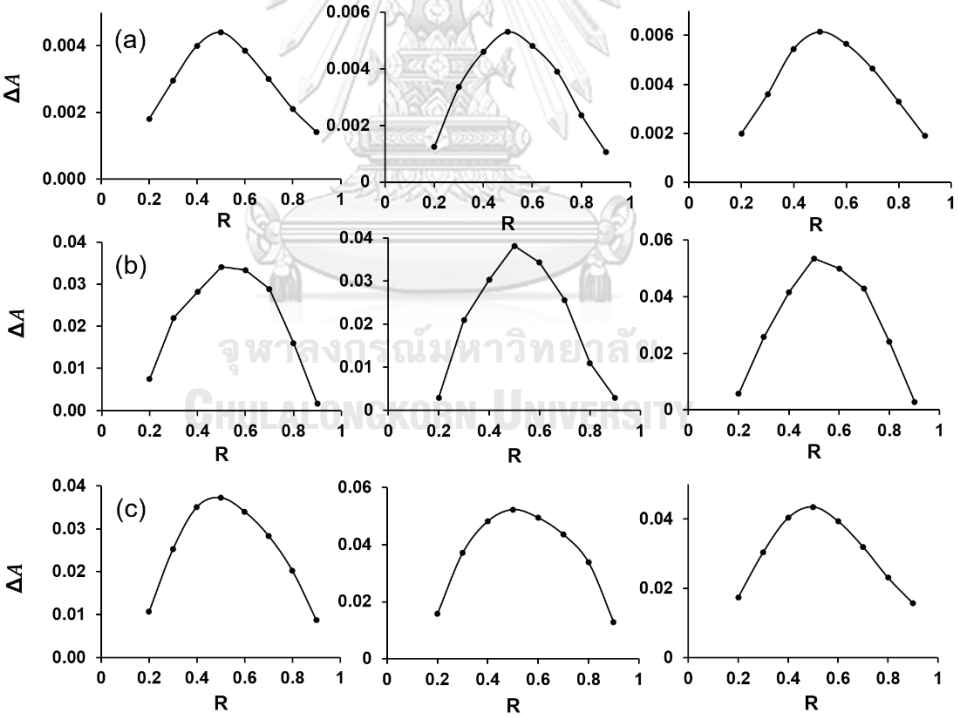

Figure 6 Stoichiometric determinations of (a) quinapril (b) fosinopril sodium (c) captopril; αCD (left), βCD (middle) and γCD (right). Data represented means of three determinations.

These results were in consistent with previous investigations. Li et al. (2002) reported that 1:1 inclusion complex of QUI with βCD as an optimum stoichiometry (104). The stoichiometry of inclusion complex of FOS with βCD was reported as 1:1 in aqueous solution (142). Ikeda et al. (2002) revealed that the formation of CAP with αCD and βCD in aqueous solutions were observed as 1:1 inclusion complexes (143). However, none of studies have been reported regarding to the complex formation of γCD for all these three drugs. In this study, it was found that all three ACE inhibitors i.e., QUI, FOS and CAP were formed 1:1 inclusion complexes with all natural CDs. Therefore, it was concluded that even larger γCD cavity, the stoichiometry of drug:CD remained 1:1 of inclusion complex.

2. Stability constant determination

It was observed that a good linear relationship (R^2= 0.9855 - 0.9965) was obtained when ΔA^{-1} was plotted against $[CD]^{-1}$, which confirmed that the stoichiometric ratio of 1:1 between all tested drugs and CDs inclusion complexes. The stability constant (K_s) value was determined to compare the affinity of drugs with different CDs. In correlation with Benesi-Hildebrand's model, $1/([Drug]\cdot K_s\cdot\Delta\varepsilon)$ was regarded as the slope, and $1/([Drug]\cdot\Delta\varepsilon)$ as the intercept, from which K_s value (i.e. $K_{1:1}$ in these cases) was determined from dividing the intercept by the slope. The CD ranking order for $K_{1:1}$ of all three drugs was as follows: αCD < βCD < γCD (Table 6). In comparison of the affinity of drugs to CD cavities, FOS showed the highest $K_{1:1}$ value for each type of CD especially FOS/γCD inclusion complex gave the greatest complexation with $K_{1:1}$ value of 650.1. The stability constant value of drug/CD complex plays an important role in

determining the extent of protection of drug against various degradations (114, 115). In this study, γCD indicated more potential as a stabilizer which was almost two times greater than βCD and three times of αCD. Based on the stability constant results, FOS was selected for further studies.

Table 6 Stability constant ($K_{1:1}$) of the drug/CD complexes in ultrapure water (mean values, n=3)

Drug	Stability constant [($K_{1:1}$), M^{-1}]		
	αCD	βCD	γCD
Quinapril	191.1	294.4	357.2
Fosinopril	244.2	389.7	650.1
Captopril	174.6	218.7	262.0

3. Kinetic degradation study

The effect of CD type on kinetic degradation of FOS was further investigated. Figure 7 displays log% FOS remained in aqueous solutions with and without CD against time after storage at 25°C and 40°C. As expected, FOS content decreased with increasing time interval especially at the temperature storage condition of 40°C. It indicated the overall degradation of FOS in these aqueous solutions followed first order kinetics (R^2 = 0.9532 - 0.9897).

จุฬาลงกรณ์มหาวิทยาลัย
Chulalongkorn University

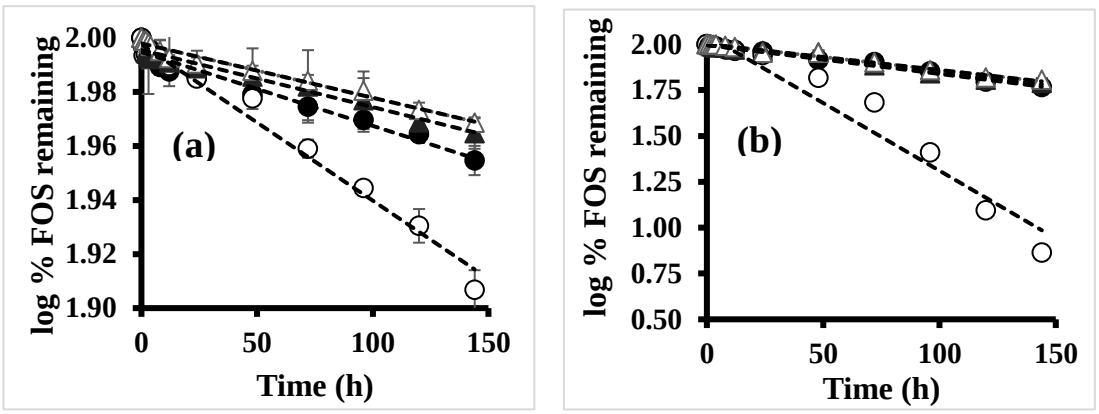

Figure 7 The first-order plots for degradation of FOS alone or with CDs in aqueous solution (n=3, mean±S.D.); (a) at 25°C (b) at 40°C; (●) FOS alone; (○) αCD; (▲) βCD; (△) γCD. The error bars are smaller than the symbol size at 40°C.

The degradation rate constant (*k*) value was calculated from the slope obtained from first-order plot which shown in Table 7. Surprisingly, it was found that the degradation rate of FOS in the presence of αCD was higher than that of pure FOS solution. It has been evidenced that FOS has surface active property that trends to be self-association in aqueous medium. This behavior is directly responsible for concentration dependent stability of FOS in aqueous solution (68). Therefore, it was assumed that αCD may disrupt the self-aggregation of FOS molecules consequently to accelerate the hydrolysis reaction rate of FOS in aqueous solution. The effect of CD complexation on acceleration of drug degradation was also previously reported (34, 101, 106-108). However, both FOS/βCD and FOS/γCD complexes showed relatively lower degradation rate. Bratu et al. (2009) revealed that propanoyloxy-propoxy fraction of FOS was resided within βCD cavity whereas the phenyl butyl part was above the wider rim and the 4-cyclohexyl-2-carboxyl-pyrrolidine part was above the narrower

rim (144). This showed that the larger cavity sizes of both βCD and γCD could be able to encapsulate and protect FOS molecule from hydrolytic degradation, and resulting in a slower rate of degradation. It was observed that the least *k* value was exhibited with FOS/γCD complexes at both storage temperature conditions i.e., 25°C and 40°C. This observation confirmed the drug degradation could be protected that correlated with the most relatively stable FOS/γCD complexes (i.e., high $K_{1:1}$).

Table 7 Degradation rate constant (k) of FOS in pure water or in CD complexing media (mean values, n=3)

	k (h^{-1})	
	25°C	40°C
pure FOS solution	6.2871×10^{-4}	3.6226×10^{-3}
FOS/αCD solution	1.3288×10^{-3}	1.7005×10^{-2}
FOS/βCD solution	4.8593×10^{-4}	3.4153×10^{-3}
FOS/γCD solution	4.6290×10^{-4}	3.2541×10^{-3}

จุฬาลงกรณ์มหาวิทยาลัย
Chulalongkorn University

4. Effect of CD on thermal stability of FOS

The effect of γCD on thermal stability of FOS was determined by autoclaving and sonicating methods. The percent of FOS remaining in pure water or 5% (w/v) aqueous γCD solution after one to three heating cycles are shown in Table 8.

After three heating cycles, it was observed that FOS was totally degraded in pure water by autoclaving whereas 36.77% was remaining by sonication method. FOS is an ester prodrug, and hydrolysis degradation was accelerated as temperature increased (145). Thermal stability of FOS

was improved by complexing with γCD in both heating methods (p<0.05) but more obviously through sonication method. It demonstrated that FOS in aqueous solutions without and with γCD could not withstand at high temperature and not feasible to conduct the terminal sterilization by autoclaving.

Table 8 The percentage of FOS remaining in pure water or 5% (w/v) aqueous γCD solution after one to three heating cycles by autoclaving or sonication in ultrasonic bath (n=3, mean±S.D.)

Thermal cycles	% Fosinopril remaining	
	pure water	5% (w/v) aqueous γCD solution
Autoclaving [a]		
cycle 1	12.77±0.36	22.62±0.49 [c]
cycle 2	0.00±0.00	5.95±0.42 [c]
cycle 3	0.00±0.00	5.43±0.78 [c]
Sonication [b]		
cycle 1	90.48±0.59	95.93±0.79 [c]
cycle 2	77.70±0.88	90.55±0.19 [c]
cycle 3	36.77±0.81	88.72±0.54 [c]

[a] each cycle consists of 121°C for 20 min
[b] each cycle consists of 60°C for 30 min
[c] p<0.05 was considered statistically significant difference when comparing to pure water in each cycle

Although complexation with γCD could not provide a complete protection of FOS hydrolysis through the heating process, it was relatively stable by sonication method (60°C for 30 min). However, the percent loss of FOS in the presence of γCD after one to three heating cycles was

จุฬาลงกรณ์มหาวิทยาลัย
Chulalongkorn University

statistically significance (p<0.05) and thus, thermal stability was further investigated by the addition of antioxidants.

5. Effect of antioxidants on thermal stability of FOS

According to the thermal stability data, the percent loss of FOS in the presence of γCD was still higher after three sonication cycles. The literature has been reported that FOS was degraded in two distinct pathways by metal ions mediated degradation or hydrolysis degradation (28). Trace metal ions that can arise from the bulk drug, formulation excipients or glass containers, and act as degradation catalysts in the formation of highly reactive free radicals, especially in the presence of oxygen (146). EDTA is the most commonly used chelating agent which form a very stable complexes with metal ions that catalyze free radical initiation (146). The other one, Na-MS is one of the regulatory approved antioxidants for aqueous system. Due to its potent oxygen scavenging action, it is widely used in liquid ophthalmic products (146). The literatures have been reported antioxidant action of Na-MS is usually aided in the presence of chelating agents (146, 147). Therefore, effect of antioxidants i.e. EDTA or Na-MS individual and combination thereof in aqueous solutions containing FOS/γCD on the thermal stability of FOS were further determined.

จุฬาลงกรณ์มหาวิทยาลัย
CHULALONGKORN UNIVERSITY

After three cycles of sonication, it was seen that the addition of only 0.1% Na-MS could not provide sufficient thermal stability. However, the degradation of FOS was found less than 2% when incorporating 0.1% (w/v) EDTA individually or in combination with 0.1% (w/v) Na-MS into 5% (w/v) γCD solution (p>0.05) (Table 9). EDTA plays the role in enhancing thermal stability of FOS possible through metal chelation or via

antioxidant in aqueous solution. The slightly synergist effect was found in the combination of these two antioxidants and the percent loss of FOS in each cycle of sonication was insignificantly difference (p>0.05). There were evidenced that EDTA promoted the effect of Na-MS in retarding oxidation reaction (147, 148). Therefore, the combined use of EDTA and Na-MS was considered to be antioxidants for further studies.

Table 9 The percentage of FOS remaining in 5% (w/v) aqueous γCD solution with antioxidants after one to three heating cycles by sonication in ultrasonic bath at 60°C for 30 min (n=3, mean±S.D.)

Thermal cycle	% Fosinopril remaining in 5% (w/v) aqueous γCD solution in the presence of antioxidants		
sonication [a]	0.1% EDTA	0.1% Na-MS	0.1% EDTA 0.1% Na-MS
cycle 1	100.34±0.77	97.94±0.69	99.52±0.63
cycle 2	99.91±1.04	99.50±0.67	100.16±0.77
cycle 3	98.42±0.79	96.58±0.71	98.85±0.60

[a] each cycle consists of 60°C for 30 min

จุฬาลงกรณ์มหาวิทยาลัย
Chulalongkorn University

6.Characterization of FOS/γCD inclusion complex

6.1 Solution-state characterization

6.1.1 ^{1}H-NMR spectroscopy

The observation brought about by ^{1}H-NMR spectroscopy could be used to establish direct evidence of the guest into the CD cavity. The change in chemical shifts of FOS alone and in the presence of γCD are

shown in Table 10. It is well- known that H-3 and H-5 protons of CDs are located in the inner cavity of CDs and prominent chemical shifts of H-3 and H-5 are major factors for possible complex formations of drug and CDs (89). The result showed that ^{1}H signals of inner protons, H-3 and H-5 of γCD showed upfield shifts of -0.043 and -0.109 ppm, respectively. According to the literature, the upfield shifts occur because of anisotropic magnetic effect induced by the presence of aromatic ring of guest molecule within the CD cavity (149). It was observed that Δδ* values of H-5 of γCD was significantly higher than that of H-3. Therefore, it can be concluded that FOS was deeply embedded into γCD cavity and exhibited the stable inclusion complex (150). Moreover, upfield shift of H-1 and downfield shift of H-6 were observed whereas there was only negligible chemical shift was found at H-2 and H-4 protons. It was revealed that the moieties of FOS molecule interacted considerably with both primary and secondary hydroxyl rims of γCD and no interaction with outer surface of γCD.

Regarding with Δδ* of FOS molecule in γCD complex, upfield and downfield shifts of CH_3-14, 14′ and CH_3-17 were found, respectively. These results suggested that the 2-methyl 1-propanoyloxypropoxy part of FOS was also well fitted into the inner cavity of γCD. According to the above ^{1}H-NMR observations, it can be concluded that FOS was deeply embedded into γCD cavity and exhibited the stable inclusion complex (150).

จุฬาลงกรณ์มหาวิทยาลัย
Chulalongkorn University

Table 10 [1]H-NMR chemical shifts (ppm) of FOS alone and in the presence of γCD

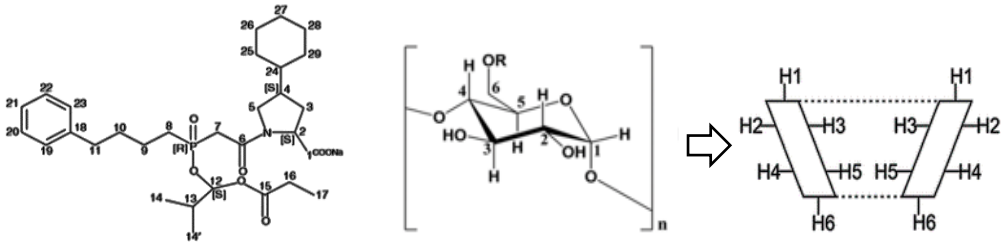

Fosinopril sodium

Cyclodextrin
γCD, n=8, R=H

^{1}H	δ_{free}	$\delta_{complex}$	$\Delta\delta^*=(\delta_{complex}-\delta_{free})$
FOS			
H-20,22	7.204	7.211	+0.007
H-19,23	7.138	7.122	-0.016
H-21	7.096	7.104	+0.008
H-14,14′	0.744	0.714	-0.030
H-16	2.312	2.334	+0.022
H-17	0.980	0.998	+0.018
γCD			
H-1	4.984	4.972	-0.012
H-2	3.528	3.532	+0.004
H-3	3.808	3.765	-0.043
H-4	3.463	3.466	+0.003
H-5	3.744	3.635	-0.109
H-6	3.725	3.740	+0.015

จุฬาลงกรณ์มหาวิทยาลัย
Chulalongkorn University

6.1.2 Rotating Frame Overhauser Enhancement Spectroscopy (ROESY)

To clearly establish the inclusion structure of FOS in γCD cavity, ROESY experiment was performed. As shown in Figure 8, intermolecular

ROE cross-peaks were observed between protons of aromatic moiety of FOS molecule (H-20, H-22 and H-19, H-23, H-21) and internal protons of γCD (H-3 and H-5). Thus, it was confirmed that aromatic ring was inserted into host γCD cavity. The existence of ROE cross-peaks between the protons of two different molecules in 2D ^{1}H-NMR spectrum indicated that the presence of interaction between two molecules i.e., inclusion complex formation (151). As both internal protons of γCD cavity showed cross peaks with protons of aromatic moiety, it was suggested that the penetration of aromatic ring was possibly from wider (H-3) side as well as narrower rim (H-5) side of γCD (152).

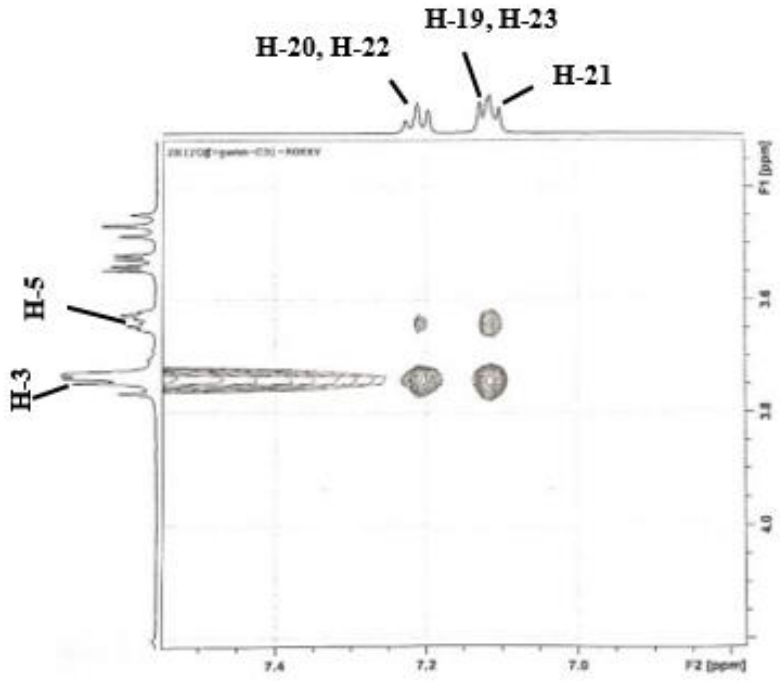

Figure 8 Partial counter plot of 500 MHz, 2D ROESY spectrum of 1:1 FOS/γCD complex in D_2O, showing cross peaks of aromatic protons of FOS with inner protons of γCD cavity

6.2 Molecular docking study

A combination of experimental and computational methods is generally acceptable for the structure assignment of drug/CD inclusion complexes. The possible binding mode for inclusion complex formation of FOS and γCD was determined computationally by molecular docking approach. The overview and side view geometries for aromatic ring insertion are shown in Figures 9a and 9b.

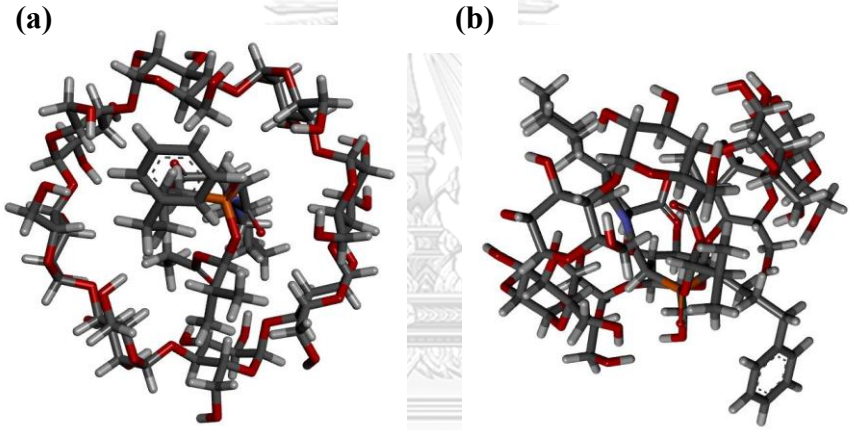

Figure 9 Geometry of inclusion complex of FOS with γCD through the insertion of aromatic ring of FOS from secondary hydroxyl rim of γCD (a) overview, (b) side view. Grey backbone represents FOS moiety whereas grey with red backbone represents γCD moiety.

The docking analysis revealed that FOS could form possible inclusion complexes with γCD through its aromatic ring insertion via the secondary hydroxyl rim of γCD by CDOCKER interaction energy of -45.3 kcal/mol. It showed that phenyl butyl part of FOS was located above the narrower rim while propanoyloxy-propoxy portion was inside the cavity and 4-cyclohexyl-2-carboxyl-pyrrolidine part was protruded above

the wider rim γCD. Therefore, computerized favorable complex obtained by molecular docking study was in good correlation with the inclusion mode predicted through experimental ^{1}HNMR and 2D ROESY data.

6.3 Solid-state characterization

6.3.1 DSC

DSC thermogram of FOS presented a sharp endothermic peak at 194.3°C which corresponded to its the melting point (Figure 10a) (144). The thermal profile of γCD exhibited a broad endothermal peak at 96.6°C due to dehydration associated with the loss of water from solid γCD (Figure 10b) (153).

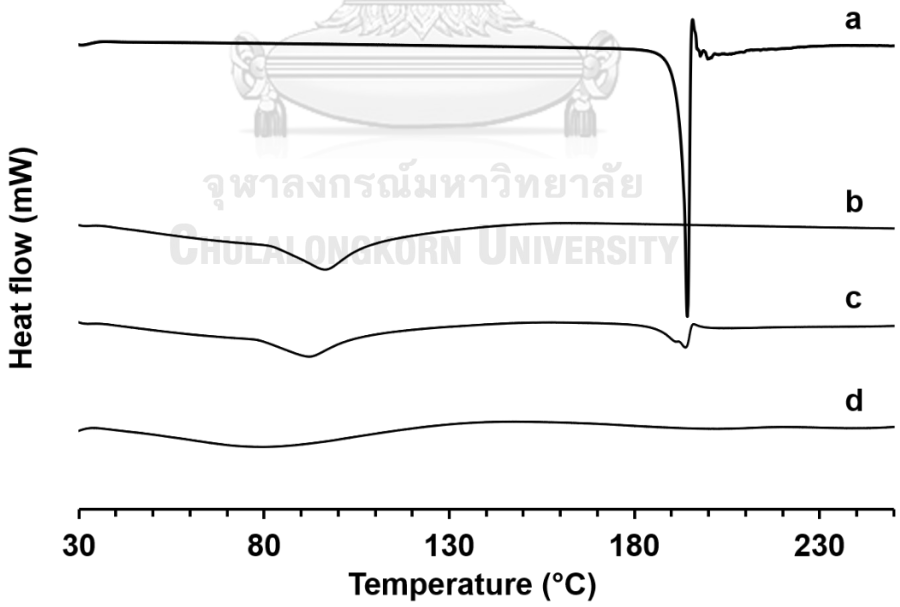

จุฬาลงกรณ์มหาวิทยาลัย
Chulalongkorn University

Figure 10 DSC thermograms of (a) pure FOS, (b) pure γCD, (c) PM FOS/γCD, (d) FD FOS/γCD

In PM sample, the endothermic peak of FOS was changed into a broad peak and slightly shifted to a lower temperature, at 193.8°C. This might be due to a weak interaction between FOS and γCD during blending or sample heating process of DSC scanning. However, in the case of FD sample of FOS/γCD, the broad and shifted of dehydration endotherm peak of γCD, as well as a disappearance of the melting peak of FOS was observed. The loss of endothermal melting peak of FOS confirmed the possibility of inclusion complex formation.

6.3.2 PXRD

PXRD spectra of pure FOS, γCD as well as PM and FD of FOS/γCD prepared by 1:1 molar ratio are shown in Figure 11. The crystalline behavior of FOS was highlighted by several intense peaks at various diffraction angles (2θ) of 4.64, 5.06, 6.14, 7.90, 10.14, 12.26, 13.86, 15.12, 16.64, 18.64, 19.84, 20.40, 21.22, 22.76 and 23.44° (Figure 11a) (142). The γCD also represented the characteristic peaks at 5.0, 10.1, 12.2, 13.8, 15.3, 15.9, 16.3, 16.8, 18.7, 20.3, 21.6, 22.8 and 23.3° that obtained from its crystalline nature (Figure 11b) (154). Only a simple overlapping of individual patterns was observed in PM system and the sharp crystalline peaks of FOS were still detected (Figure 11c).

In case of FD sample, the corresponding FOS peaks were completely disappeared and displayed only the halo pattern (Figure 11d). This was possibly due to the conversion of amorphous state and/or molecular encapsulation of FOS into γCD cavity.

จุฬาลงกรณ์มหาวิทยาลัย
Chulalongkorn University

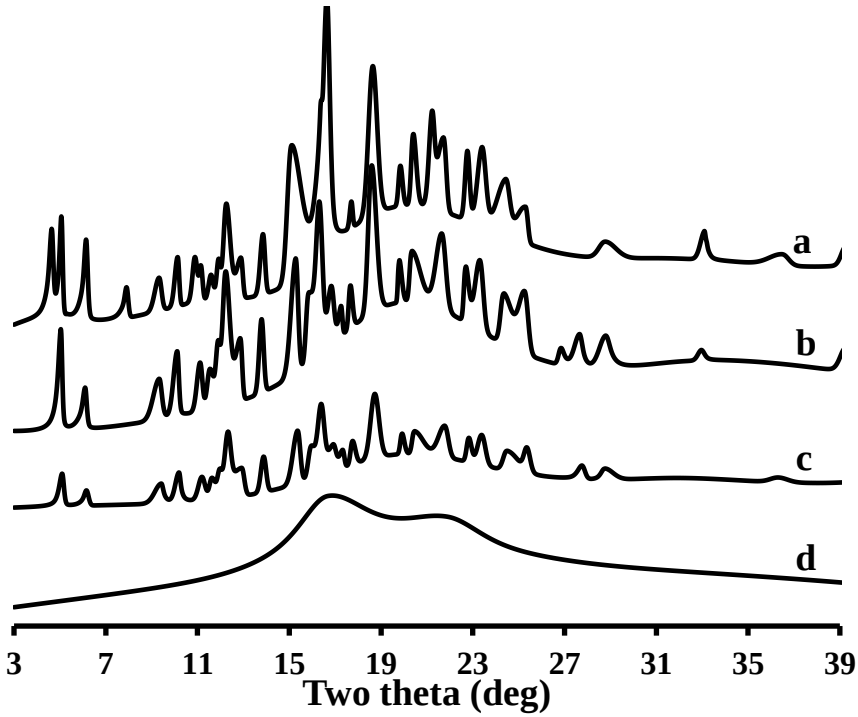

Figure 11 PXRD spectra of (a) pure FOS, (b) pure γCD, (c) PM FOS/γCD, (d) FD FOS/γCD

6.3.3 FT-IR spectroscopy

FT-IR spectroscopy was applied to verify the presence of interaction between CD and guest molecules by observing the changes or shifts in absorption spectrum. Figure 12 displays the FT-IR spectra of pure FOS, γCD, their PM and FD samples. The FT-IR spectrum of pure FOS was characterized by intense absorption peaks of C=O stretching vibration at 1759 cm^{-1}, 1600 cm^{-1} and 1620 cm^{-1} due to the presence of ester, carbonyl and amide groups, respectively. The presence of proline ring and phenyl ring were proved by C-N stretching vibration at 1451 cm^{-1} and weak C_{ar}-H stretching vibration from 3000-3150 cm^{-1} region, respectively (Figure 12a) (142). The FT-IR spectrum of γCD was characterized by broad absorption band at 3283 cm^{-1} due to symmetric and asymmetric O-H

stretching vibration as well as at 2927 cm^{-1} by C-H stretching mode as shown in Figure 12b (153).

In PM, the prominent characteristic peaks of FOS i.e., 1759 cm^{-1}, 1600 cm^{-1} and 1620 cm^{-1} were still presented. In addition, C-N stretching vibration at 1451 cm^{-1} and weak C_{ar} -H stretching vibration were also found. It can be concluded that there was less interaction of FOS and γCD, and only simple superimposition of individual components were formed in PM (Figure 12c).

In the case of FD sample, the intense absorption peaks of C=O stretching vibration of ester bond at 1759 cm^{-1} was shifted to 1743 cm^{-1}. The two sharp peaks at 1600 cm^{-1} and 1620 cm^{-1} correspond to carbonyl and amide groups were disappeared and showed only a broad peak at 1604-1611 cm^{-1} (Figure 12d). These results suggested that there were some interactions of functional groups of FOS and γCD during the inclusion complex formation. Likewise, the weak C_{ar} -H stretching vibrations were also disappeared in FD sample which indicated that the existence of interaction between aromatic ring of FOS molecule and γCD. In addition, the FD spectrum of FOS/γCD exhibited that the band of O-H stretching vibration was shifted from 3283 cm^{-1} to 3390 cm^{-1}. These results provided the existence of interactions between mainly aromatic ring and phosphinate ester group of FOS and γCD binary complexation (142).

จุฬาลงกรณ์มหาวิทยาลัย
Chulalongkorn University

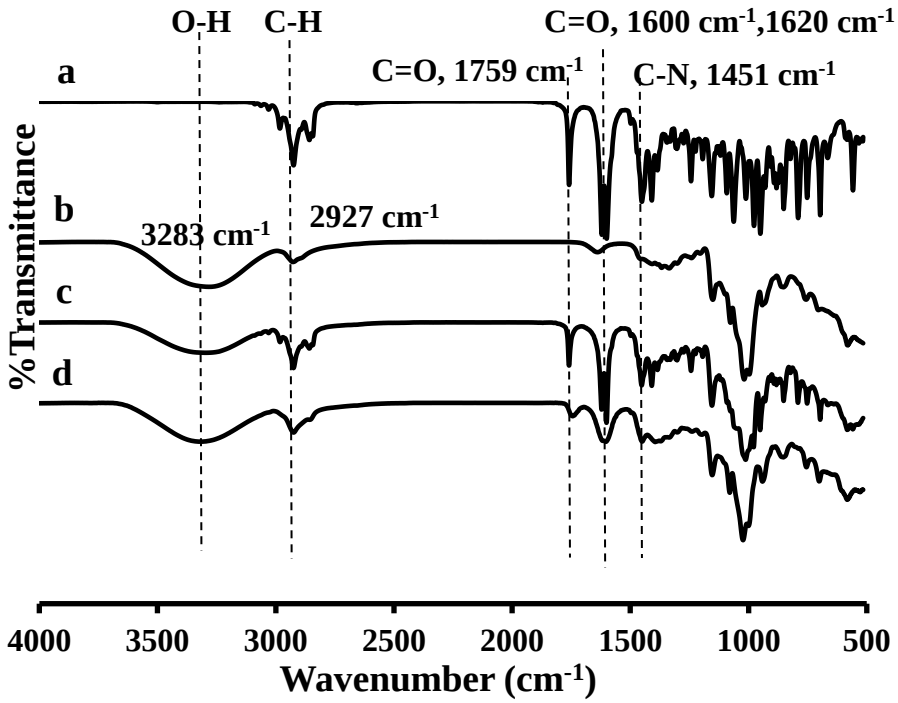

Figure 12 FT-IR spectra of (a) pure FOS, (b) pure γCD, (c) PM FOS/γCD, (d) FD FOS/γCD

According to the solution and solid-state characterizations, the proposed conformations of 1:1 FOS/γCD complex are shown in Figure 13. It demonstrated that γCD cavity was occupied by the aromatic ring (Figure 13a) or 2-methyl-1-propanoyloxypropoxy part of FOS (Figure 13b). The significant shift of Δδ* at H-5 of γCD revealed that FOS was deeply embedded into γCD cavity, and the exhibition of stable inclusion complex could be provided relatively protection of FOS molecule from hydrolytic degradation.

จุฬาลงกรณ์มหาวิทยาลัย
Chulalongkorn University

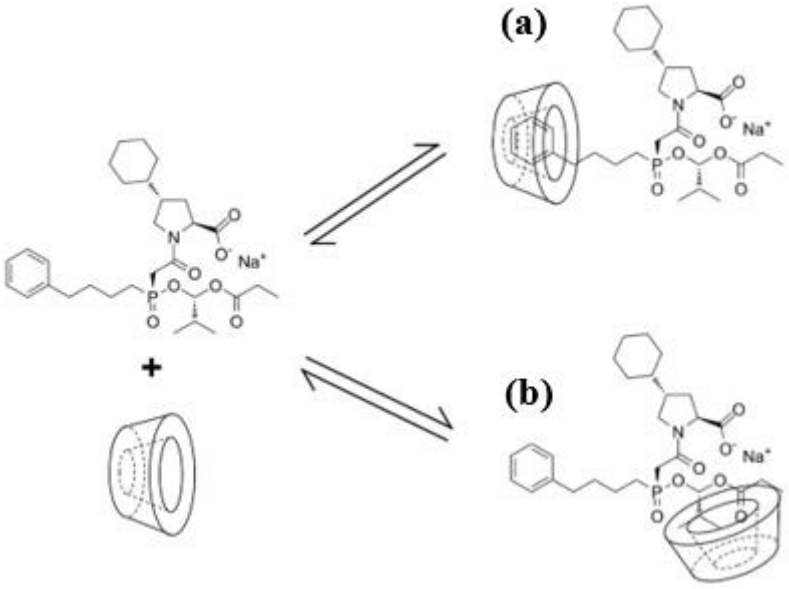

Figure 13 The proposed conformations of 1:1 FOS/γCD inclusion complex

7.Physicochemical and chemical characterization of niosomal formulations containing fosinopril

7.1 Appearance, microscopic images, pH, viscosity, and osmolality

จุฬาลงกรณ์มหาวิทยาลัย
Chulalongkorn University

The FOS loaded with Span® 60 (F1-F3) showed opalescent appearance whereas it was white translucent obtained with niosomes containing Brij® 76 (F7-F9). The turbidity was increased and a milky-white suspension were obtained by the addition of γCD (F4-F6 and F10-F12) (Figure 14). Although, all niosomal preparations were ultimately settled after 48 h, they were eased of re-dispersion with gentle agitation to obtain a homogenous suspension.

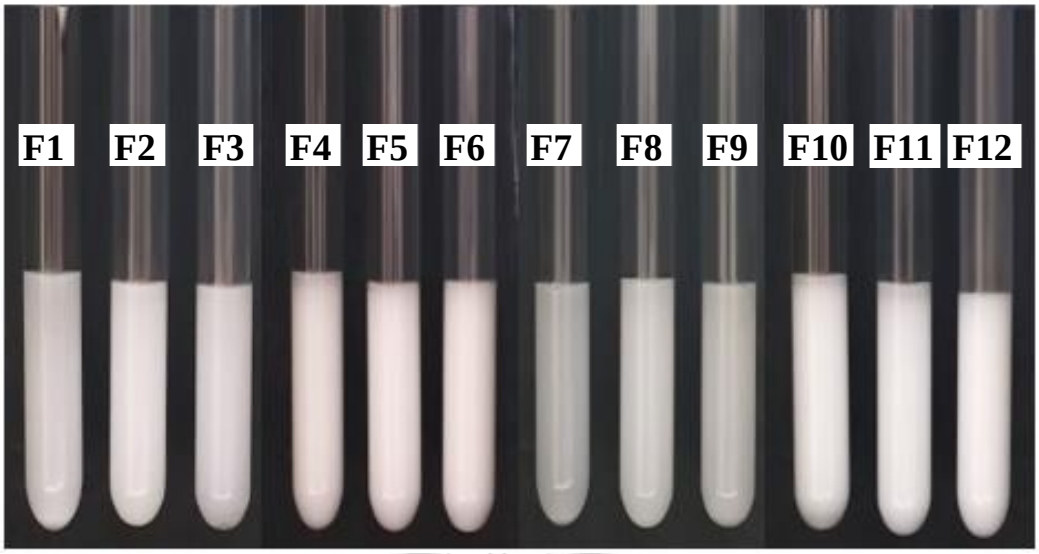

Figure 14 The appearance of FOS loaded Span® 60 and Brij® 76 niosomes in the presence and absence of γCD

The birefringence of the lamellar structure has been used to identify niosomal structure as well as other related bilayers (155). Under polarized light microscope, niosome was successfully formed in all formulations as shown in Figures 15 and 16. It was noticed that aggregation or fusion of vesicle was found in formulations with positive charged stabilizer, STA (F3, F6, F9 and F12). Some of them displayed rupture of vesicles. Aggregation was attributed due to the shielding of the vesicle surface charge by ions in solution and thereby reducing the electrostatic repulsion (156).

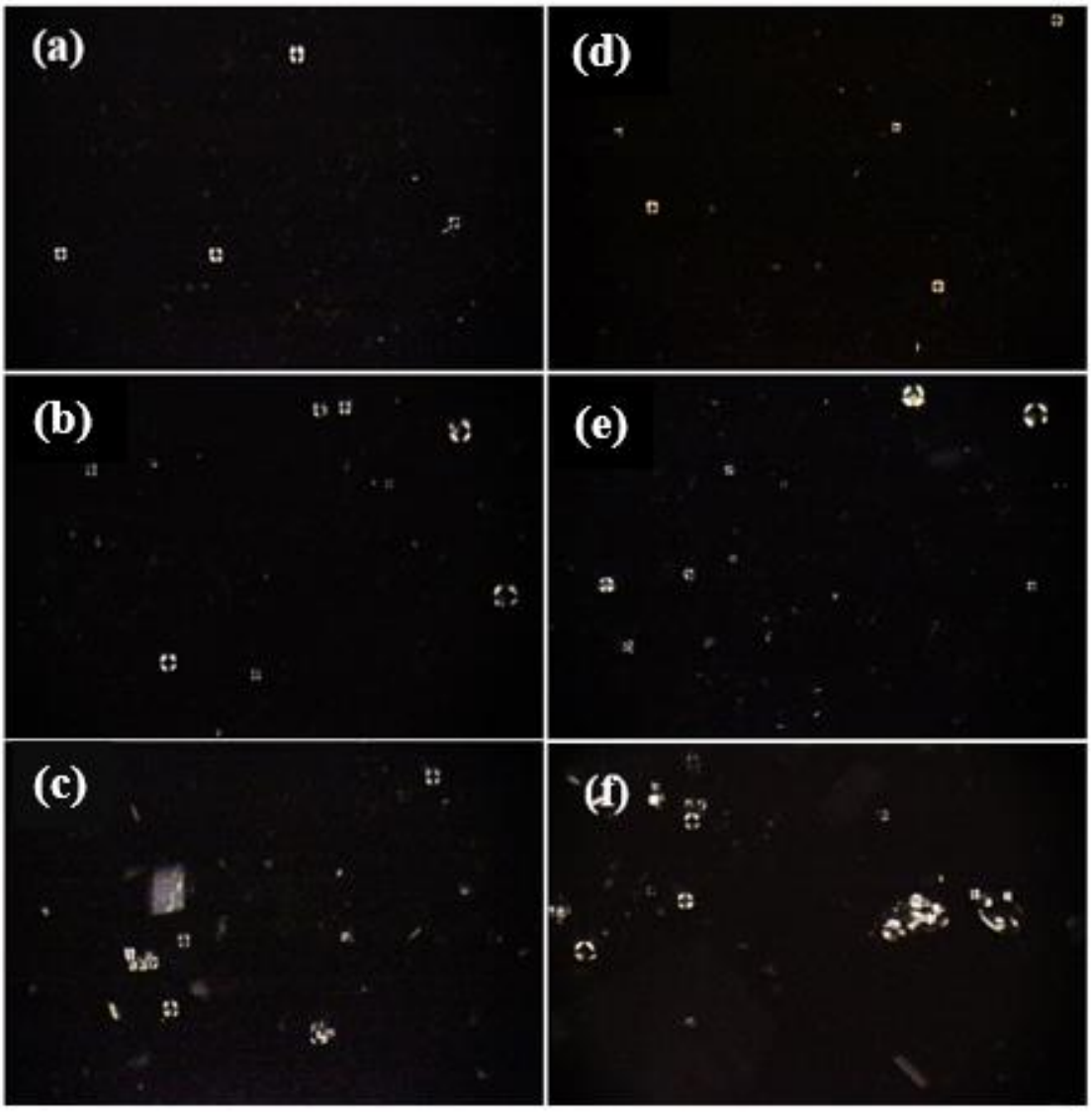

CHULALONGKORN UNIVERSITY

Figure 15 Polarized light microscopic images of FOS loaded niosomal formulations in the presence of Span® 60 surfactant with or without 5% γCD; (a) F1; (b) F2; (c) F3; (d) F4; (e) F5 ; (f) F6 (Magnification of 10×40)

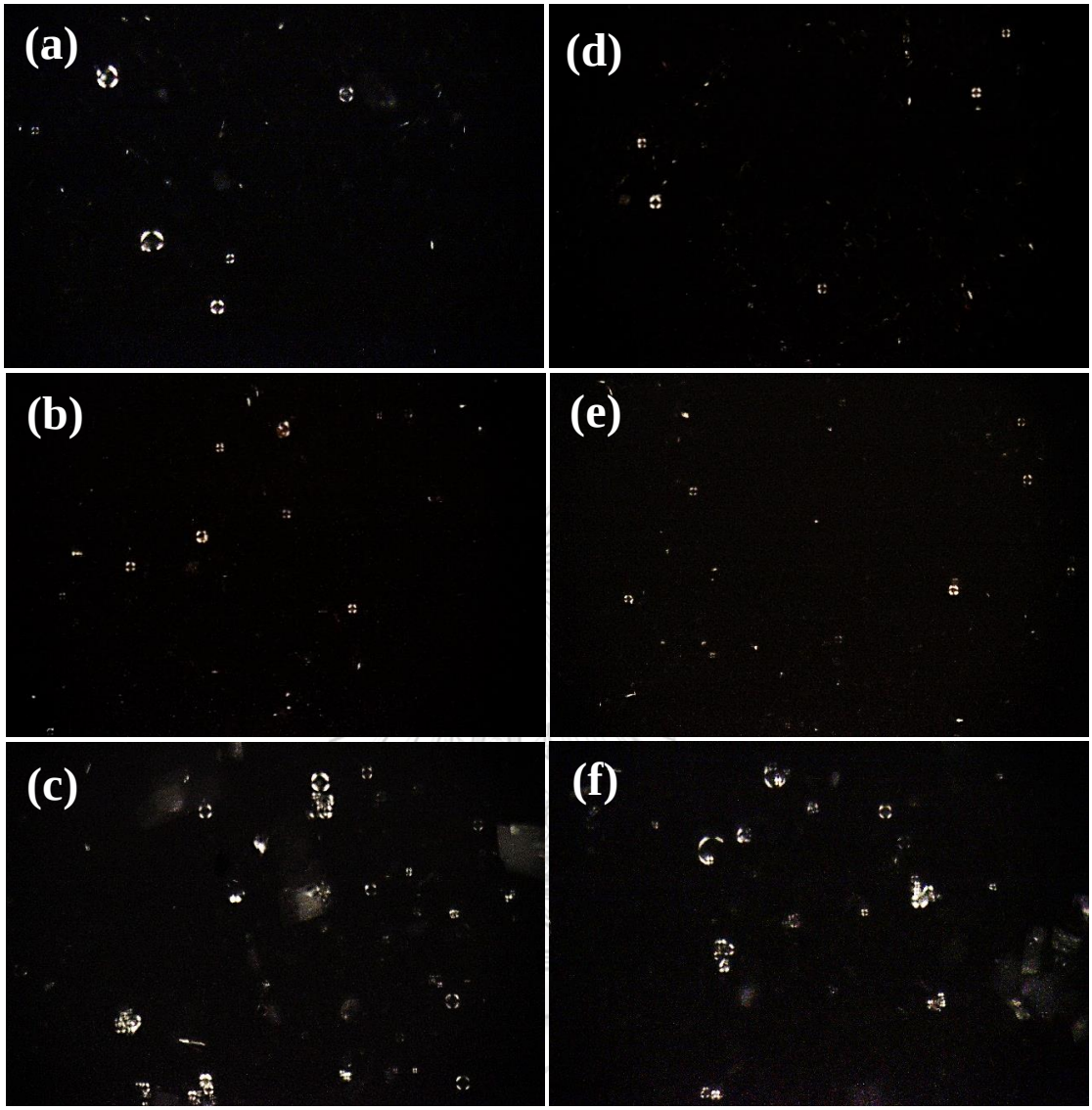

CHULALONGKORN UNIVERSITY

Figure 16 Polarized light microscopic images of FOS loaded niosomal formulations in the presence of Brij®76 surfactant with or without 5% γCD; (a) F7; (b) F8; (c) F9; (d) F10; (e) F11; (f) F12 (Magnification of 10×40)

Table 11 shows pH value, viscosity and osmolality of each formulation. The pH values of all formulations were in the range of 6.7-7.2 which was acceptable and very closed or within the ideal pH for the eye drop i.e., 7.2 ± 0.2 (157). The slightly lower in pH values were found by

the addition of γCD but not significant ($p>0.05$). The viscosity of all niosomal preparations were in the range of 1- 2 mPa.s. Although the optimal viscosity for ophthalmic preparation is generally considered in the range of 15-25 mPa.s, the low viscosity preparations will not affect the vision and unlikely cause any lacrimation or blurredness (158). The viscosity measured at 34°C was slightly lower than that measured at 25°C. As expected, the increasing the temperature resulted in decreasing viscosity (159). All formulations were slightly hypertonic and beyond the acceptable values (within 260-330 mOsm/kg). Due to osmotic property of CDs, osmolality was found to be higher in preparations containing γCD. However, hypertonic eye drops are better tolerated than hypotonic eye drops and also a short-term discomfort due to dilution with lachrymal fluid takes place rapidly after administration (160).

7.2 Particle size and size distribution, and zeta potential

The particle size and size distribution of supernatant niosomal suspensions measured by DLS technique are shown in Table 12. It demonstrated that all niosomal preparations showed the characteristic of size with bimodal or trimodal size populations based on the intensity distribution. The average particle size was found in the range of 190-270 nm. The PDI values were found between 0.1 and 0.5. This indicated that the particle size was distributed uniformity with a narrow size distribution (PDI<0.7) (161). In most cases, the size of niosomes with Span®60 (HLB 4.7) were larger than those of Brij® 76 (HLB 12.4). It is generally well-known that vesicle size is directly dependent on HLB value of surfactant used where the higher HLB gives the larger size of vesicle (162-165). However, there are several studies which inversely reported that

จุฬาลงกรณ์มหาวิทยาลัย
Chulalongkorn University

the lower HLB value gave vesicle with a larger size (166-168). The discrepancy is probably due to different preparation methods, different physiochemical properties of loaded drugs and the effect of membrane additives.

Table 11 pH value, osmolality and viscosity of the formulations (n=3, mean±S.D.)

Formulations	pH	Osmolality (mOsm/kg)	Viscosity (mPa.s)	
			25±1°C	34±1°C
F1	7.02 ±0.05	358±5	1.48±0.01	1.18±0.01
F2	6.73 ±0.04	364±6	1.81±0.02	1.30±0.01
F3	7.26 ±0.03	366±8	1.38±0.02	1.12±0.01
F4	6.83 ±0.03	372±5	1.76±0.02	1.50±0.01
F5	6.70 ±0.03	374±6	1.98±0.02	1.72±0.02
F6	6.75 ±0.01	382±5	1.75±0.01	1.52±0.01
F7	6.91 ±0.01	346±6	1.43±0.01	1.21±0.01
F8	6.95 ±0.01	354±8	1.64±0.02	1.34±0.01
F9	7.22 ±0.03	359±10	1.41±0.01	1.15±0.01
F10	6.87 ±0.02	364±8	1.68±0.02	1.34±0.02
F11	6.78 ±0.08	378±3	1.86±0.01	1.56±0.01
F12	6.86 ±0.05	379±9	1.65±0.02	1.38±0.01

The addition of membrane charge was found to have an influence on particle size (Table 12). It was seen that incorporation of DCP into Span®60 niosome (F2) produced relatively larger average particle sizes than those of STA followed by SC24 (F3 and F1, respectively). It could be explained by the similar charge of DCP, Span®60 and cholesterol head groups that cause electrostatic repulsion between them, decreasing membrane curvature, and therefore increased in particle size (169). Generally,

inclusion of charged molecules into bilayers increase the size of the vesicles in contrast to uncharged one. The presence of a net charge, whether negative or positive increases water uptake into the lipid bilayer. Such hydration led to increase membrane thickness and consequently, increase the vesicle size (40). The effect of STA on vesicle size was moderate relative to DCP, although the overall result was increased in size compared to SC24. In contrast, in case of Brij®76, vesicle size was found in the trend of SC24>STA>DCP. This might be due to difference in accommodating ability of surfactants to the membrane additives. The incorporation of SC24 in hydrophilic Brij®76 surfactant lead to increase in the membrane permeability and interstitial spaces between the bilayer membranes by its bulky structures with long and highly hydrophilic poly-24-oxyethylene chains, resulting in increased in size (170). The smaller in vesicle size of Brij®76/DCP niosome was possibly due to interaction of their hydrophilic groups through hydrogen bonding. Incorporation of Brij®76, higher HLB enhanced hydrogen bonding, led to an increase the curvature of the bilayer and resulted in reduction of vesicle size (171, 172).

จุฬาลงกรณ์มหาวิทยาลัย
Chulalongkorn University

Comparing to the formulations with or without γCD, in most cases, it was seen that the preparations containing γCD displayed significantly smaller mean particle size than those of the corresponding pure FOS loaded niosomes (p<0.05). According to the literature, CDs form hydrophobic interactions with hydrophobic tail as well as hydrogen bonding with polar head group of non-ionic surfactants (173). The complexation of CD with hydrophobic tails of surfactants resulted in lower packing density of incorporated surfactant and decreased membrane thickness (174). The adsorption of CD on niosome surface also decreased in vesicle size. This was due to interacting of CD with polar head groups of surfactant through

hydrogen bonding, which lead to increase the area of polar head groups at the interphase as well as altered the radius of curvature (175).

Zeta-potential of all niosomal formulations were found to be negative values (Table 12). This might be due to free hydroxyl groups present in cholesterol and surfactant molecule (176). Because of contribution of negative charge due to ionization of the acidic ($-HPO_4$) group by DCP, it gave a higher negative zeta potential value. The resultant electrostatic repulsion was likely to account for reducing the tendency of niosome aggregation. Conversely, STA introduced a positive charge via the protonation of basic-NH_2 group which adsorbed on the surface of niosome and exhibited lower negative zeta potential value through charge neutralization than the uncharged one i.e., SC24 (177). SC24 has no net charge and does not provide the additional ions into dispersion medium. It enhances membrane physical stability by providing steric stabilization (39). The higher negative zeta potential obtained by the addition of DCP could be of great importance to increase the stability and keeping niosomal suspension from coalescence and aggregation during storage.

จุฬาลงกรณ์มหาวิทยาลัย
Chulalongkorn University

Regarding the niosomal formulations in the presence of γCD, the lower zeta potential values were observed than that of corresponding non-CD based niosomes. This was due to CD obscured or acted as a shell on the surface charge of niosome by hydrogen bonds formation between hydrophilic head group of surfactants with hydroxy groups on the exterior of CD (174, 175, 178, 179).

Table 12 Mean particle size, size distribution and zeta potential of the formulations (n=3, mean±SD)

Formulation	Particle size (d.nm) (% intensity Area)	Z-average (d.nm)	Size distribution (PDI)	Zeta Potential (mV)
F1	188.5±14.7 (83.4) 768.7±41.3 (11.1) 5253.0±51.2 (5.5)	245.1±5.02	0.46±0.03	-32.70±1.64
F2	236.6±2.1(96.1) 5426.0±8.7 (3.9)	262.4±5.00	0.45±0.01	-37.70±1.15
F3	222.8±4.1 (95.6) 5160.0±24.6 (4.4)	250.4±6.31	0.35±0.03	-15.43±1.46
F4	201.9±10 (73.8) 4705.0±68.8(19.7) 11.7±1.5 (6.5)	198.0±4.50[a]	0.52±0.01	-20.27±0.67
F5	244.7±2.6 (95.1) 5296.7±11.6 (4.9)	246.8±3.71[a]	0.42±0.01	-27.17±1.63
F6	231.9±0.5 (94.3) 4844.7±17.9 (5.7)	229.1±5.16[a]	0.36±0.06	-13.40±1.91
F7	229.8±3.8 (95.5) 5370.3±26.8 (4.5)	257.2±4.29	0.32±0.01	-24.30±2.01
F8	209.7±1.5 (86.7) 3197.3±13.1 (13.3)	212.0±0.72	0.36±0.03	-34.97±0.35
F9	217.9±2.8 (83.9) 3579.7±17.6 (16.1)	214.8±4.01	0.37±0.02	-7.41±0.40
F10	257.7±4.0 (93.2) 4914.0±16.1(6.8)	246.0±0.96[a]	0.11±0.02	-21.20±1.04
F11	220.3±2.5 (85.7) 3744.0±7.2 (9.6) 1380.3±5.0 (4.7)	200.0±1.87[a]	0.32±0.01	-23.73±1.97
F12	229.5±1.0 (93.2) 5115.0±55.7 (6.8)	211.6±1.52	0.34±0.05	-6.94±0.43

[a] $p<0.05$ was considered statistically significant difference when comparing to the respective formulation in the absence of γCD

7.3 Total drug content and percent entrapment efficiency (% EE)

The total drug content and % EE of FOS niosomal preparations are shown in Table 13. The % EE of all preparations were found in the range of 7-34 %. It is well known that lipophilic drugs are preferentially up taken by niosome compared to hydrophilic ones due to higher partitioning through the lipid phase of the vesicles (180). The literatures revealed that the low %EE was also related to the other factors, surfactant/lipid level, the concentration of the drug molecules and membrane additives, and the interaction of encapsulated drug with niosomal membrane (170, 181).

In all cases, %EE values of 21-35% were obtained in niosomes prepared using Span® 60 (F1, F2, F4 and F5) which were relatively superior to those prepared with Brij® 76. This might be due to lower HLB value of Span®60 (HLB 4.7) in contrast to Brij® 76 (HLB 12.4). When the HLB value is greater than 10, it is necessary to increase the amount of cholesterol to be added in order to compensate for the larger head groups (181). There was reported that entrapment of minoxidil was increased in the presence of higher cholesterol content in Brij® 76 niosomes (171). In addition, Span®60 has a higher transition temperature (Tc) i.e., 53°C when compared with Brij® 76 (34°C) (171). The surfactant with higher Tc usually forms less leaky vesicles and thus, resulting higher drug entrapment of water-soluble solutes (45, 163).

Regarding to the effect of stabilizer on %EE, it was found in the trend of DCP>SC24>STA. The presence of double hydrocarbon chains in DCP imparted a more packing of the bilayer membrane and resulting the higher %EE (170). Due to the presence of highly hydrophilic poly-24-oxyethylene chains of SC24, the membrane is more flexible and permeable. On the other hand, the leakage of the drug molecule is more

favorable and thus decreases % EE (170). The lowest %EE by STA could be explained by electrostatic induced chain tilt which subsequently changes in the lateral packing of the bilayers (182). This result was in accordance with the observation of rupture of vesicle by aggregation and fusion of vesicles under polarized light microscope.

Table 13 Total drug content and entrapment efficiency of niosomal formulations (n=3, mean±S.D.)

Formulation	Total Drug Content (%)	%EE
F1	93.93±0.15	21.34±0.42
F2	92.96±0.06	28.68±0.77
F3	94.66±0.05	9.20±0.30
F4	95.11±0.14	25.99±0.78
F5	95.65±0.12	34.43±0.80
F6	93.66±0.07	11.30±0.85
F7	97.15±0.03	10.70±0.27
F8	91.10±0.06	12.94±0.57
F9	91.06±0.08	7.73±0.97
F10	94.82±0.04	12.58±0.85
F11	96.62±0.23	14.02±0.10
F12	96.62±0.09	8.09±0.80

จุฬาลงกรณ์มหาวิทยาลัย
Chulalongkorn University

According to our based of knowledge, there are few studies have been reported CD inclusion complex in niosome vesicles (122, 125-128, 175, 183). Our resulted data have shown that %EE of FOS was increased when incorporated in the form of FOS/γCD complex into niosomal preparations. This finding was in agreement with the previous reports (123,

127). The higher % EE in niosome containing γCD might be due to the fact that CD forms hydrogen bonding interaction with polar head group of non-ionic surfactants. The stronger hydrogen binding intensity, the greater % EE was obtained (173, 184). Moreover, complexation of free CD with hydrophobic tails of surfactants creates a more internal aqueous space by decreasing membrane thickness (174, 175). Due to the lower %EE of Brij® 76 niosomes (F7, F8, F10 and F11) and the evidence of the particle aggregation with the lowest %EE among the groups in niosomes using STA as stabilizer (F3, F6, F9 and F12), these formulations were excluded for further studies.

8. Transmission electron microscopy (TEM)

The TEM micrographs of selected niosomal preparations (i.e., Span® niosomes) are shown in Figure 17. It demonstrated that the vesicles were well identified and presented in a nearly spherical shape. TEM images of niosomal formulations in the presence of γCD showed lesser the particle size which was agreed with those determined by DLS measurement (Table 12). It was observed that the small white spots distributed in niosome stabilized by SC24 in the presence and absence of γCD (Figures 17a and 17c). The previous literature reported that the more blackish staining, the more lipophilic portion of niosome where a distinct, large internal aqueous phase represented as a light staining (185). Interestingly, in case of DCP in the presence of γCD, the larger internal aqueous core was detected (Figure 17d) when compared to the one without γCD (Figure 17b). The wider in hydrophilic core of niosome, the more capacity that can accommodate both hydrophilic drug and water-soluble drug/CD complexes. Therefore, TEM

จุฬาลงกรณ์มหาวิทยาลัย
Chulalongkorn University

micrographs showed a good correlation with the higher %EE of FOS loaded Span® 60/DCP niosome containing γCD (Table 13).

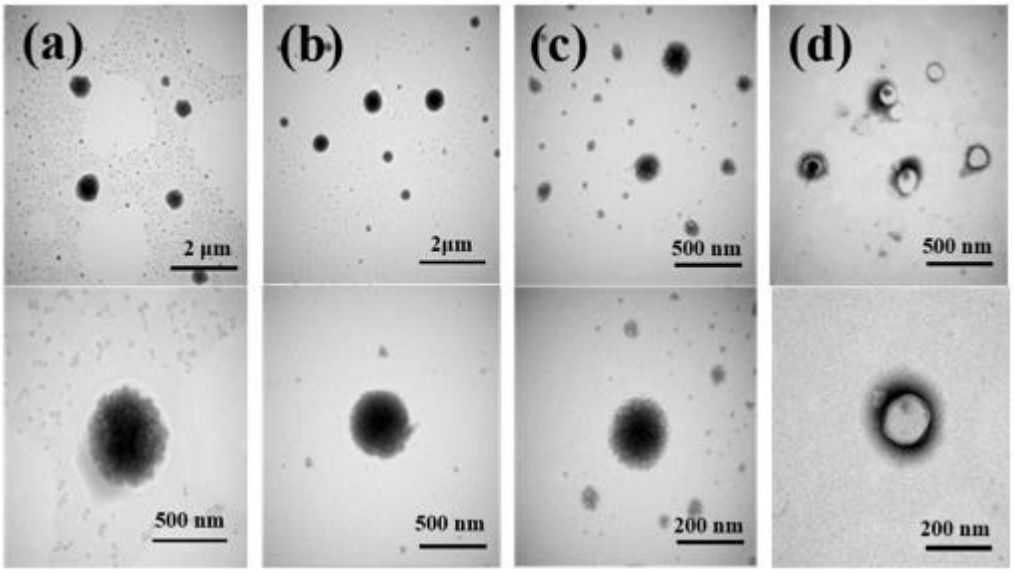

Figure 17 TEM micrographs of FOS loaded niosomes (a) F1, (b) F2, (c) F4 and (d) F5

จุฬาลงกรณ์มหาวิทยาลัย
Chulalongkorn University

9. *In-vitro* release study

The *in-vitro* release profiles of selected niosomal formulations are shown in Figure 18. It was noticed that more controlled release manner was obtained from FOS loaded niosomes stabilized by DCP (F2 and F5) than those of stabilized by SC24 (F1 and F4). Due to the parallel alignment of double hydrocarbon chains of DCP to the hydrocarbon chains of Span®60 as well as its parallel orientation of polar phosphate groups to the polar heads the of Span®60, DCP provided more packing and filling in any irregularities through the bilayer membrane (170). Such enhancement in the packing properties could render less membrane permeability to the entrapped water-soluble molecules and the drug release was retarded (170).

In contrast to the niosomal formulation containing nonionic SC24 (F1 and F4), the bilayer structure upon hydration of the film would be looser and more flexible. This was due to the presence of bulky structures with long and highly hydrophilic poly-24-oxyethylene chains of SC24, which could increase the membrane permeability to the water-soluble solutes resulted in faster drug release (170).

In both cases, FOS/γCD complexes entrapped niosomal formulations showed slower release rate than those of only FOS loaded niosomes. Similar result has been reported with methotrexate where niosome with drug/βCD inclusion complexes produced relatively slower release pattern of the entrapped drug compared to both free drug incorporated niosome and drug/CD complex preparation (123). Sheena et al. (1997) compared the release profiles of pilocarpine/βCD loaded and non-CD based niosomal preparations. The result revealed that βCD-based niosomal formulations showed slower and sustained release than that of conventional niosome (127). However, the opposite finding was also reported in the previous study (128). This might be as the consequence of differences in niosome preparation, nature of drug molecule, the binding affinity of drug/CD complex, and release pattern of drug molecule i.e., exist directly as a free drug from the inner aqueous phase to the lipid bilayers or firstly in the form of drug/CD complexes to the lipid bilayers and then released as a free drug (186).

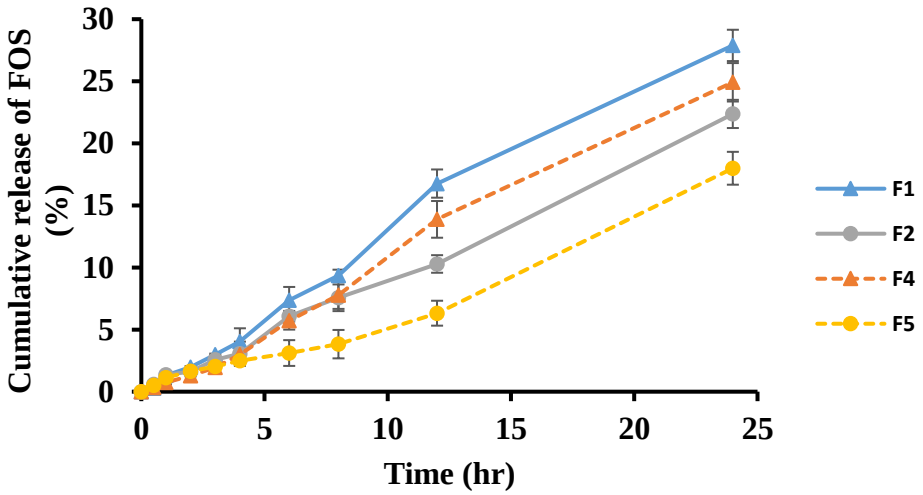

Figure 18 The release profiles of FOS niosomal preparations and FOS/γCD loaded niosomal preparation through semipermeable membrane with MWCO 12000-14000 Da (n=3, mean±S.D.)

Twenty-four hours control is an important issue in evaluating IOP reduction of glaucoma patients (187). The more controlled release action of FOS niosomal preparation is greater beneficial for targeted glaucoma treatment. Therefore, the optimum formulations i.e., F2 and F5 were selected for further *ex-vivo* permeation and stability studies.

จุฬาลงกรณ์มหาวิทยาลัย
CHULALONGKORN UNIVERSITY

10. *Ex-vivo* permeation study

The flux and apparent permeation coefficient (P_{app}) values of FOS loaded Span®/DCP niosomal preparations in the presence and absence of γCD including aqueous solution containing FOS/γCD complex are displayed in Table 14. It was noticed that P_{app} through sclera was higher than the cornea in all tested preparations. This might be due to the loose structural matrix and less complicated tissue layer of sclera (188, 189). According to the literature, the permeability of sclera is approximately 10

times greater than the cornea (190). It is an alternative pathway to deliver the drug in both anterior and posterior segment of the eye. Loch et al. (2012) showed that the higher P_{app} values of ciprofloxacin, timolol and lidocaine for sclera than those for cornea (191). Ahmed and Patton (1985) also revealed that intraocular penetration of a large molecule weight, insulin across the sclera was higher than through the cornea (192).

In both cases of cornea and sclera, the flux and P_{app} values of FOS from niosomal preparations was significantly lower than FOS/γCD complex preparation ($p<0.05$) (Table 14). As expected, the FOS loaded niosomes exhibited more controlled drug release manner than that of FOS/γCD complex preparation because free drug or drug/CD inclusion complex had to be diffused from inner aqueous core of niosome through the lipid bilayer and then permeated through the membrane (193). It was supported and confirmed that FOS molecules in both free and inclusion complex forms were deposited into the inner core of niosomes. Regarding to the effect of CD incorporated into niosomal formulation, it was found that both flux and P_{app} of γCD loaded niosome (F5) was lower than those of without CD (F2). Again, it was emphasized that most of FOS molecules were included in γCD cavity as inclusion complexes and were localized in the inner core of niosome (i.e., high %EE). In addition, CD forms a strong hydrogen bonding interaction with polar head group of non-ionic surfactants resulted lower in flux and P_{app} values of FOS loaded niosome containing γCD.

Table 14 The flux and apparent permeation coefficient (P_{app}) of FOS loaded niosomal preparation in the presence and absence of γCD, and aqueous FOS/γCD complex solution, through porcine cornea or sclera (n=4, ± S.D.)

Formulations	Cornea		Sclera	
	Flux ± S.D. ($\mu g h^{-1} cm^{-2}$)	P_{app} ± S.D. ($\times 10^{-6}$ cms^{-1})	Flux ± S.D. ($\mu g h^{-1} cm^{-2}$)	P_{app} ± S.D. ($\times 10^{-6}$ cms^{-1})
F2	31.086±6.32	0.920±0.18	40.066±40.35	1.155±0.11
F5	22.843±7.95	0.635±0.21	33.092±2.38	0.927±0.08
FOS/γCD complex	62.794±6.23[a]	1.870±0.18[a]	86.762±5.25[a]	2.583±0.16[a]

[a]Statistically significant difference when compared with the niosomal formulations, F2 and F5 ($p<0.05$)

11. Physical and chemical stability studies of FOS

In order to evaluate the stability of FOS in niosomal vesicles, the appearance, pH, particle size and size distribution, zeta potential and percent drug content were used as the parameters for determination. In this study, two selected formulations i.e., F2 and F5 were evaluated and aqueous solution of FOS/γCD complex was used as a control. The criteria that chosen these two optimal formulations was based on higher %EE and zeta potential values including exhibited the controlled release behavior. The physical stability i.e., pH, mean particle size and size distribution, and zeta potential of FOS after storage of 4°C, long-term condition (30±2 °C, 75±5 % RH) and accelerated condition (40±2 °C, 75±5 % RH) at various time intervals are shown in Tables 15, 16 and 17, respectively.

จุฬาลงกรณ์มหาวิทยาลัย
Chulalongkorn University

In the case of aqueous solution of FOS/γCD complex, no change in physical appearance was found at 4°C but the drug was precipitated at 30°C and 40°C. The pH value was slightly decreased at 4°C but more obvious at higher temperatures. The particle size was significantly increased at all storage condition and PDI values were out of specification at 30°C and 40°C. The zeta potential values were also decreased in all conditions and significantly decreased of it at storage condition of 40°C. It was concluded that FOS in the complexing medium had low physical stability especially the particle size growth upon storage for 6 months.

After the storage of 6 months at 4°C, both niosomal formulations tested maintain physically stable i.e., no change in appearance and re-dispersion could be easily done by gentle swirling to form a homogenous suspension. The slightly decreased in pH was found but not significant ($p<0.05$). However, at higher storage temperatures of 30°C and 40°C, a significant reduction in pH was detected (Table 15). This might be due to a progressive increase in hydrolysis of fatty acid in niosome with increasing temperature (194). Regarding with vesicle sizes and size distribution, both F2 and F5 had no appreciable changes at 4°C which indicated a good physical stability of these systems at that storage temperature. As expected, the larger difference of these parameters was observed at higher temperatures of 30°C and 40°C. The particle size was exponentially increased and the PDI values were out of specification at 30°C and 40°C (PDI> 0.7) over the 6-month period (Table 16). This might be due to higher mobility of the bilayer at room temperature or higher. The aggregation or fusion of vesicles are generally occurred as molecular mobility increases and transform to the larger ones (195, 196). The decreasing in zeta potential values were found in all storage conditions but

จุฬาลงกรณ์มหาวิทยาลัย
Chulalongkorn University

more significantly at higher temperatures (Table 17). This lower zeta potential was directly correlated to lower electrostatic repulsion and as the result, aggregation or fusion of vesicles resulting in increased in particle size.

According to the 6-month chemical stability data (Table 18), the drug content was significantly decreased in aqueous solution consisted of FOS/γCD complex which represented 51%, 8% and 3% at 4°C, 30°C and 40°C, respectively. It was noticed that FOS could not withstand in aqueous solution containing γCD. On the other hand, the CD inclusion complex was not sufficient to enhance the chemical stability of FOS. We have found that the niosomal preparations revealed greater in chemical stability than non-niosomal preparation i.e., aqueous solution containing FOS/γCD complex at all storage conditions. Regarding to the effect of CD on the chemical stability of drug, F5 showed relatively more stable than F2 at all storage temperatures. After storage of 6 months, F2 remained 88% and F5 remained 92% at 4°C, whereas at 30°C, it was remained 17% and 23%, respectively. However, the drug content was left only 7% for F2 and 10% for F5 at 40°C. It was revealed that incorporation of γCD as FOS/γCD complex into niosome showed relatively more stable than into that of without CD.

จุฬาลงกรณ์มหาวิทยาลัย
CHULALONGKORN UNIVERSITY

Table 15 pH values of FOS niosomal preparation and FOS/γCD complex storage at 4°C, 30±2 °C (75±5% RH) and 40±2 °C (75±5% RH) for 0, 1,3 and 6 months (n=3, mean±S.D.)

Formulation	pH values			
4°C	0 Month	1 Month	3 Month	6 Month
F2	6.82±0.02	6.76±0.02	6.71±0.04	6.63±0.02
F5	6.72±0.02	6.68±0.01	6.63±0.02	6.52±0.04
FOS/γCD complex	7.41±0.01	7.32±0.02	7.10±0.02	6.78±0.05
30°C				
F2	6.82±0.02	6.57±0.03	6.32±0.11	4.39±0.03
F5	6.72±0.02	6.53±0.03	5.53±0.03	4.58±0.03
FOS/γCD complex	7.41±0.01	5.60±0.02	5.34±0.06	4.70±0.01
40°C				
F2	6.82±0.02	5.88±0.04	4.42±0.09	4.23±0.10
F5	6.72±0.02	5.56±0.03	4.64±0.01	4.39±0.04
FOS/γCD complex	7.41±0.01	5.11±0.04	4.89±0.01	4.49±0.04

จุฬาลงกรณ์มหาวิทยาลัย
Chulalongkorn University

Table 16 The average particle size and size distribution (PDI) of FOS niosomal preparation and FOS/γCD complex storage at 4°C, 30±2 °C (75±5% RH) and 40±2 °C (75±5% RH) for 0, 1, 3 and 6 months (n=3, mean±S.D.)

Formulation	Average particle size (nm) and size distribution (PDI)			
4°C	0 Month	1 Month	3 Month	6 Month
Average particle size				
F2	275.10±48.20	281.20±7.40	306.80±8.85	435.67±19.48
F5	241.70±34.40	258.03±8.80	266.45±22.86	421.47±10.34
FOS/γCD complex	243.60±45.60	282.00±26.20	768.35±134.22	2330.75±296.58
Size distribution (PDI)				
F2	0.44±0.02	0.44±0.01	0.55±0.07	0.64±0.03
F5	0.18±0.01	0.24±0.03	0.42±0.05	0.59±0.02
FOS/γCD complex	0.51±0.01	0.51±0.07	0.53±0.06	0.55±0.01
30°C				
Average particle size				
F2	275.10±48.20	293.30±27.10	391.40±7.69	911.85±43.73
F5	241.70±34.40	254.70±10.10	309.57±13.63	452.27±26.40
FOS/γCD complex	243.60±45.60	1019.40±179.3	1023.20±65.15	3244.75±216.10
Size distribution (PDI)				
F2	0.44±0.02	0.45±0.10	0.52±0.02	0.71±0.08
F5	0.18±0.01	0.29±0.10	0.53±0.07	0.74±0.10
FOS/γCD complex	0.51±0.01	0.59±0.01	0.75±0.05	0.78±0.16

จุฬาลงกรณ์มหาวิทยาลัย
Chulalongkorn University

Table 16 The average particle size and size distribution (PDI) of FOS niosomal preparation and FOS/γCD complex storage at 4°C, 30±2 °C (75±5% RH) and 40±2 °C (75±5% RH) for 0, 1, 3 and 6 months (n=3, mean±S.D.) (Con't)

Formulation	Average particle size (nm) and size distribution (PDI)			
40°C	0 Month	1 Month	3 Month	6 Month
Average particle size				
F2	275.10±48.20	296.20±7.40	380.80±14.07	1895.00±511.53
F5	241.70±34.40	277.80±10.40	360.10±47.86	1071.10±140.27
FOS/γCD complex	243.60±45.60	1607.20±285.10	1846.70±91.79	3942.70±420.90
Size distribution (PDI)				
F2	0.44±0.02	0.48±0.10	0.73±0.01	1.00±0.00
F5	0.18±0.01	0.33±0.10	0.53±0.09	0.95±0.05
FOS/γCD complex	0.51±0.01	0.79±0.10	0.88±0.08	0.97±0.24

จุฬาลงกรณ์มหาวิทยาลัย
Chulalongkorn University

Table 17 The average zeta potential values (ZP) of FOS niosomal preparation and FOS/γCD complex storage at 4°C, 30±2 °C (75±5% RH) and 40±2 °C (75±5% RH) for 0, 1, 3 and 6 months (n=3, mean±S.D.)

Formulation	Average zeta potential value (mV)			
4°C	0 Month	1 Month	3 Month	6 Month
F2	-35.15±1.48	-35.14±1.89	-35.09±0.09	-34.92±2.15
F5	-25.83±0.87	-25.35±0.06	-25.22±1.65	-25.12±1.65
FOS/γCD complex	-11.13±0.62	-10.87±0.46	-10.74±0.47	-10.45±0.47
30°C				
F2	-35.15±1.48	-35.10±1.75	-35.07±1.11	-32.63±1.19
F5	-25.83±0.87	-25.23±0.89	-25.17±1.34	-21.53±0.88
FOS/γCD complex	-11.13±0.62	-10.97±0.66	-10.73±0.14	-9.53±0.14
40°C				
F2	-35.15±1.48	-27.77±0.85	-25.97±1.30	-23.87±1.89
F5	-25.83±0.87	-23.80±1.56	-22.45±0.52	-19.95±0.71
FOS/γCD complex	-11.13±0.62	-9.50±0.56	-8.35±0.50	-8.02±0.86

จุฬาลงกรณ์มหาวิทยาลัย
Chulalongkorn University

Table 18 Total FOS content (%) of FOS niosomal preparation and FOS/γCD complex storage at 4°C, 30±2 °C (75±5% RH) and 40±2 °C (75±5% RH) for 0, 1, 3 and 6 months (n=3, mean±S.D.)

Time (month)	Formulations		
	F2	F5	FOS/γCD complex
4°C			
0 Month	100.00±0.00	100.00±0.00	100.00±0.00
1 Month	97.95±0.70	98.44±0.64	81.09±0.92
3 Month	93.72±0.73	95.21±0.39	73.84±0.68
6 Month	88.33±0.54	92.75±0.83	51.10±1.18
30±2°C (75±5% RH)			
0 Month	100.00±0.00	100.00±0.00	100.00±0.00
1 Month	93.32±0.53	95.13±0.86	28.72±0.30
3 Month	83.40±0.78	87.37±0.57	20.94±0.73
6 Month	17.17±0.59	23.67±0.57	8.49±0.70
40±2°C (75±5% RH)			
0 Month	100.00±0.00	100.00±0.00	100.00±0.00
1 Month	46.09±0.88	56.34±0.82	19.95±0.60
3 Month	27.88±0.71	36.70±1.08	12.26±0.36
6 Month	7.75±0.83	10.68±1.06	3.59±0.70

จุฬาลงกรณ์มหาวิทยาลัย
Chulalongkorn University

In fact, both niosomal formulations (in the presence and absence of γCD) were chemically stable at least 3 months under the refrigerated condition of 4°C. It was clearly concluded that the CD inclusion complex could not provide sufficient physical and chemical stability of FOS in an aqueous solution. The nanoparticulate system, niosomal formulation was more beneficial to protect FOS degradation especially in case of FOS/γCD complex incorporated and deposited in the inner core of niosome.

From the overall resulted data, the proposed drawing of FOS loaded niosomes are shown in Figure 19. Niosomal platforms could prevent the chemically unstable drug by entrapping the drug molecules inner the aqueous core. Additionally, the effect of γCD inclusion complex formation is the predominant factor to provide higher %EE of FOS in niosomal formulation which prevents the drug degradation via hydrolysis consequently enhance the chemical stability of FOS in aqueous solution.

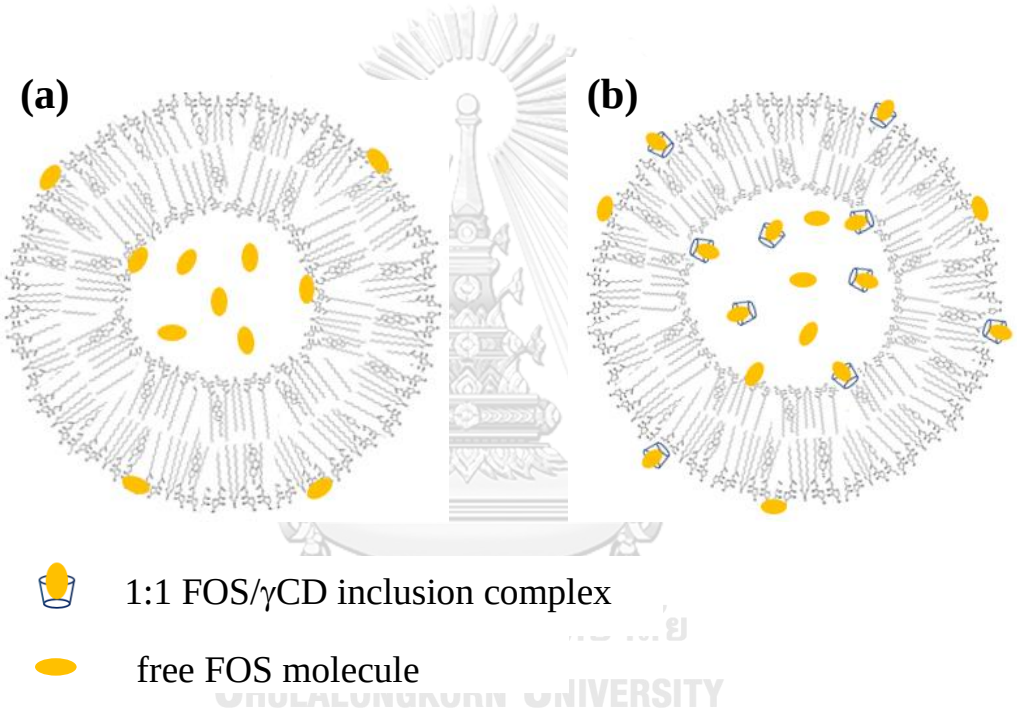

Figure 19 The proposed drawing of (a) FOS loaded niosomes and (b) FOS/γCD loaded niosome

CHAPTER V
CONCLUSIONS

In this study, three ACE inhibitors i.e., captopril, quinapril and fosinopril (FOS) were used to determine the inclusion complexes formation with parent CDs i.e., αCD, βCD and γCD. All tested CDs represented 1:1 stoichiometry inclusion complex with individual drugs and FOS/γCD inclusion complex exhibited the highest stability constant. The kinetic degradation study confirmed that FOS showed the lowest degradation rate through the formation of γCD inclusion complexes. Thermal stability data revealed that FOS was relatively stable via sonication method in the presence of γCD and enhanced its stability by addition of antioxidants. The inclusion complex formation of FOS/γCD was further examined by molecular docking, solution-state (^{1}H-NMR and 2D ^{1}H-NMR) and solid-state (DSC, PXRD, FT-IR). All of these characterization results confirmed that true inclusion complex between FOS and γCD was formed, and these supported the ability of γCD to enhance the chemical stability of FOS in aqueous solution.

จุฬาลงกรณ์มหาวิทยาลัย
Chulalongkorn University

In order to enhance the chemical stability of FOS in aqueous solution, niosomal formulations were developed. The niosome was prepared by using non-ionic surfactant, cholesterol and membrane stabilizer/charged inducer at the mole ratio of 47.5: 47.5: 5. Thin-film hydration method was performed with the total lipid concentration of 100 μM in 5 ml hydration medium. The surfactants used in this study were Span® 60 and Brij® 76. Solulan® C24 (SC24) was used as a steric stabilizer. Stearylamine (STA) and dicetylphosphate (DCP) were used to give electrostatic stabilization of vesicles as well as positive and negative

charge, respectively. The effects of CD, surfactant type and membrane stabilizer/charged inducers on physiochemical and chemical properties of niosome were characterized. The pH values of all formulations were within the acceptable range. The low viscosity was found in all preparations. The slightly hypertonic solution was found especially in niosomal preparations containing γCD. The average particle size was detected in nanometer range and PDI values were within the acceptable range. The entrapment efficiency (%EE) was found higher in niosome composed of Span®60/SC24 and Span®60/ DCP, with respective γCD incorporated niosome. The *in-vitro* release study revealed that the formulations with higher %EE, a slower drug release was obtained. Based on %EE, zeta potential value and *in-vitro* release profile, Span®60 /DCP niosomal formulations in the presence and absence of γCD were selected for *ex-vivo* permeation study and further physical and chemical stability studies. The slow permeation rate of FOS through excised porcine cornea and sclera was obtained in the niosomal formulation containing γCD. The chemical stability of FOS in the formation of γCD inclusion complex could not withstand in aqueous solution. Niosomal preparations could protect FOS degradation and exhibited physical and chemical stability for at least three months at 4ºC. The optimum formulation to enhance the chemical stability of FOS consisted of FOS/γCD complex loaded niosome. Our studies successfully investigated the preformulation and ophthalmic formulation development of FOS. However, to demonstrate a clinically viable formulation, the *in vitro* cytotoxicity, irritation test and *in vivo* pharmacokinetic in rabbit eye were considered for future perspective studies.

จุฬาลงกรณ์มหาวิทยาลัย
CHULALONGKORN UNIVERSITY

REFERENCES

จุฬาลงกรณ์มหาวิทยาลัย
Chulalongkorn University

1. Sugrue MF. The pharmacology of antiglaucoma drugs. Pharmacology & Therapeutics. 1989;43(1):91-138.

2. Alward WLM. Medical management of glaucoma. New England Journal of Medicine. 1998;339(18):1298-307.

3. Quigley HA, Broman AT. The number of people with glaucoma worldwide in 2010 and 2020. British Journal of Ophthalmology. 2006;90(3):262.

4. Gupta P, Zhao D, Guallar E, Ko F, Boland MV, Friedman DS. Prevalence of glaucoma in the United States: The 2005-2008 national health and nutrition examination survey. Investigative Ophthalmology & Visual Science. 2016;57(6):2905-13.

5. Davson H. Aqueous humour and the intraocular pressure. Physiology of the eye. 4th ed. New York :Academic press; 1980. p.9-81.

6. Leske MC. Open-angle glaucoma—an epidemiologic overview. Ophthalmic epidemiology. 2007;14(4):166-72.

7. Bill A, Phillips CI. Uveoscleral drainage of aqueous humour in human eyes. Experimental Eye Research. 1971;12(3):275-81.

8. Quigley HA. Glaucoma. Lancet. 2011;377(9774):1367-77.

9. Lotti VJ, Pawlowski N. Prostaglandins mediate the ocular hypotensive action of the angiotensin converting enzyme inhibitor MK-422 (enalaprilat) in african green monkeys. Journal of Ocular Pharmacology and Therapeutics. 1990;6(1):1-7.

10. Santos RA, Brosnihan KB, Jacobsen DW, DiCorleto PE, Ferrario CM. Production of angiotensin-(1-7) by human vascular endothelium. Hypertension. 1992;19(2 Suppl): II56-61.

11. Campbell DJ, Kladis A, Duncan AM. Effects of converting enzyme inhibitors on angiotensin and bradykinin peptides. Hypertension. 1994;23(4):439-49.

12. Li P, Chappell MC, Ferrario CM, Brosnihan KB. Angiotensin-(1–7) augments bradykinin-induced vasodilation by competing with ACE and releasing nitric oxide. Hypertension. 1997;29(1):394-8.

จุฬาลงกรณ์มหาวิทยาลัย
CHULALONGKORN UNIVERSITY

13. Jaiswal N, Diz DI, Chappell MC, Khosla MC, Ferrario CM. Stimulation of endothelial cell prostaglandin production by angiotensin peptides. Characterization of receptors. Hypertension. 1992;19(2_supplement): II49.

14. Costagliola C, Di Benedetto R, De Caprio L, Verde R, Mastropasqua L. Effect of oral captopril (SQ 14225) on intraocular pressure in man. European Journal of Ophthalmology. 1995;5(1):19-25.

15. Mehta A, Iyer L, Parmar S, Shah G, Goyal R. Oculohypotensive effect of perindopril in acute and chronic models of glaucoma in rabbits. Canadian Journal of Physiology and Pharmacology. 2010;88(5):595-600.

16. Watkins RW, Baum T, Cedeno K, Smith EM, Yuen P, Ahn H, et al. Topical ocular hypotensive effects of the novel angiotensin converting enzyme inhibitor SCH 33861 in conscious rabbits. Journal of Ocular Pharmacology and Therapeutics. 1987;3(4):295-307.

17. Loftsson T, Thorisdóttir S, Fridriksdóttir H, Stefánsson E. Enalaprilat and enalapril maleate eyedrops lower intraocular pressure in rabbits. Acta Ophthalmologica. 2010;88(3):337-41.

18. Rachmani R, Lidar M, Levy Z, Ravid M. Effect of enalapril on the incidence of retinopathy in normotensive patients with type 2 diabetes. European Journal of Internal Medicine. 2000;11(1):48-50.

19. Manschot SM, Gispen WH, Kappelle LJ, Biessels GJ. Nerve conduction velocity and evoked potential latencies in streptozotocin-diabetic rats: effects of treatment with an angiotensin converting enzyme inhibitor. Diabetes/Metabolism Research and Reviews. 2003;19(6):469-77.

20. Choudhary R, Kapoor MS, Singh A, Bodakhe SH. Therapeutic targets of renin-angiotensin system in ocular disorders. Journal of Current Ophthalmology. 2017;29(1):7-16.

21. Nagai N, Oike Y, Izumi-Nagai K, Koto T, Satofuka S, Shinoda H, et al. Suppression of choroidal neovascularization by inhibiting angiotensin-converting enzyme: minimal role of bradykinin. Investigative Ophthalmology & Visual Science. 2007;48(5):2321-6.

22. Ritz E, Haxsen V. Diabetic nephropathy and anaemia. European Journal of Clinical Investigation. 2005;35 Suppl 3:66-74.

23. Israili ZH, Hall WD. Cough and angioneurotic edema associated with angiotensin-converting enzyme inhibitor therapy: a review of the literature and pathophysiology. Annals of Internal Medicine. 1992;117(3):234-42.

24. Fraňová S, Nosáľová G, Antošová M, Nosáľ S. Enalapril and diltiazem co-administration and respiratory side effects of enalapril. Physiological Research. 2005;54:515-20.

25. Stanisz B. Kinetics of degradation of quinapril hydrochloride in tablets. International Journal of Pharmaceutical Sciences. 2003;58(4):249-51.

26. Lin SY, Wang SL, Chen TF, Hu TC. Intramolecular cyclization of diketopiperazine formation in solid-state enalapril maleate studied by thermal FT-IR microscopic system. European Journal of Pharmaceutics and Biopharmaceutics. 2002;54(2):249-54.

27. Timmins P, Jackson IM, Wang YC. Factors affecting captopril stability in aqueous solution. International Journal of Pharmaceutics. 1982;11(4):329-36.

28. Thakur AB, Morris K, Grosso JA, Himes K, Thottathil JK, Jerzewski RL, et al. Mechanism and kinetics of metal ion-mediated degradation of fosinopril sodium. Pharmaceutical Research. 1993;10(6):800-9.

29. Choudhury S, Mitra AK. Kinetics of aspirin hydrolysis and stabilization in the presence of 2-hydroxypropyl-β-cyclodextrin. Pharmaceutical Research. 1993;10(1):156-9.

30. Ong J, Sunderland V, McDonald C. Influence of hydroxypropyl β-cyclodextrin on the stability of benzylpenicillin in chloroacetate buffer. Journal of Pharmacy and Pharmacology. 1997;49(6):617-21.

31. Yap KL, Liu X, Thenmozhiyal JC, Ho PC. Characterization of the 13-cis-retinoic acid/cyclodextrin inclusion complexes by phase solubility, photostability, physicochemical and computational analysis. European Journal of Pharmaceutical Sciences. 2005;25(1):49-56.

จุฬาลงกรณ์มหาวิทยาลัย
Chulalongkorn University

32. Pourmokhtar M, Jacobson G. Enhanced stability of sulfamethoxazole and trimethoprim against oxidation using hydroxypropyl-β-cyclodextrin. Pharmazie. 2005;60(11):837-9.

33. Szejtli J. Introduction and general overview of cyclodextrin chemistry. Chemical Reviews. 1998;98(5):1743-54.

34. Loftsson T, Brewster ME. Pharmaceutical applications of cyclodextrins. 1. Drug solubilization and stabilization. Journal of Pharmaceutical Sciences. 1996;85(10):1017-25.

35. Loftssona T, Järvinen T. Cyclodextrins in ophthalmic drug delivery. Advanced Drug Delivery Reviews. 1999;36(1):59-79.

36. Loftsson T, Stefánsson E. Effect of cyclodextrins on topical drug delivery to the eye. Drug Development and Industrial Pharmacy. 1997;23(5):473-81.

37. Boyd BJ. Past and future evolution in colloidal drug delivery systems. Expert Opinion on Drug Delivery. 2008;5(1):69-85.

38. Moghassemi S, Hadjizadeh A. Nano-niosomes as nanoscale drug delivery systems: An illustrated review. Journal of Controlled Release. 2014;185:22-36.

39. Uchegbu IF, Vyas SP. Non-ionic surfactant based vesicles (niosomes) in drug delivery. International Journal of Pharmaceutics. 1998;172(1):33-70.

40. Carafa M, Santucci E, Alhaique F, Coviello T, Murtas E, Riccieri FM, et al. Preparation and properties of new unilamellar non-ionic/ionic surfactant vesicles. International Journal of Pharmaceutics. 1998;160(1):51-9.

41. Vyas S, Mysore N, Jaitely V, Venkatesan N. Discoidal niosome based controlled ocular delivery of timolol maleate. Pharmazie. 1998;53(7):466-9.

42. Abdelbary G, El-gendy N. Niosome-encapsulated gentamicin for ophthalmic controlled delivery. AAPS PharmSciTech. 2008;9(3):740-7.

จุฬาลงกรณ์มหาวิทยาลัย
Chulalongkorn University

43. Saettone M, Perini G, Carafa M, Santucci E, Alhaique F. Non-ionic surfactant vesicles as ophthalmic carriers for cyclopentolate. A preliminary evaluation. Journal of Drug Delivery Science and Technology. 1996;6(1):94-8.

44. Guinedi AS, Mortada ND, Mansour S, Hathout RM. Preparation and evaluation of reverse-phase evaporation and multilamellar niosomes as ophthalmic carriers of acetazolamide. International Journal of Pharmaceutics. 2005;306(1-2):71-82.

45. Abdelkader H, Wu Z, Al-Kassas R, Alany RG. Niosomes and discomes for ocular delivery of naltrexone hydrochloride: Morphological, rheological, spreading properties and photo-protective effects. International Journal of Pharmaceutics. 2012;433(1):142-8.

46. Kaur IP, Garg A, Singla AK, Aggarwal D. Vesicular systems in ocular drug delivery: an overview. International Journal of Pharmaceutics. 2004;269(1):1-14.

47. Jain S, Jain V, Mahajan S. Lipid based vesicular drug delivery systems. Advances in Pharmaceutics. 2014;2014.

48. Kaur IP, Smitha R. Penetration enhancers and ocular bioadhesives: Two new avenues for ophthalmic drug delivery. Drug Development and Industrial Pharmacy. 2002;28(4):353-69.

49. Kwon YH, Fingert JH, Kuehn MH, Alward WL. Primary open-angle glaucoma. New England Journal of Medicine. 2009;360(11):1113-24.

50. Flammer J, Haefliger IO, Orgul S, Resink T. Vascular dysregulation: a principal risk factor for glaucomatous damage? J Glaucoma. 1999;8(3):212-9.

51. Hayreh SS. The role of age and cardiovascular disease in glaucomatous optic neuropathy. Survey of Ophthalmology. 1999;43 Suppl 1:S27-42.

52. Bonomi L, Marchini G, Marraffa M, Bernardi P, Morbio R, Varotto A. Vascular risk factors for primary open angle glaucoma: the Egna-Neumarkt study. Ophthalmology. 2000;107(7):1287-93.

53. Drance S, Anderson DR, Schulzer M. Risk factors for progression of visual field abnormalities in normal-tension glaucoma. American Journal of Ophthalmology. 2001;131(6):699-708.

54. Gottfredsdottir MS, Allingham RR, Shields MB. Physicians' guide to interactions between glaucoma and systemic medications. Journal of Glaucoma. 1997;6(6):377-83.

55. Brown NJ, Vaughan DE. Angiotensin-converting enzyme inhibitors. Circulation. 1998;97(14):1411-20.

56. Fletcher EL, Phipps JA, Ward MM, Vessey KA, Wilkinson-Berka JL. The renin–angiotensin system in retinal health and disease: Its influence on neurons, glia and the vasculature. Progress in Retinal and Eye Research. 2010;29(4):284-311.

57. Moravski CJ, Kelly DJ, Cooper ME, Gilbert RE, Bertram JF, Shahinfar S, et al. Retinal neovascularization is prevented by blockade of the renin-angiotensin system. Hypertension. 2000;36(6):1099-104.

58. Van Buggenum IH, Polak B, Reichert-Thoen J, De Vries-Knoppert W, Van Hinsbergh V, Tangelder G. Angiotensin converting enzyme inhibiting therapy is associated with lower vitreous vascular endothelial growth factor concentrations in patients with proliferative diabetic retinopathy. Diabetologia. 2002;45(2):203-9.

59. Smieško M, Remko M. Two-layer ONIOM calculation of gas-phase acidities of selected ACE inhibitors. Chemical Papers. 2004;58(2):71-8.

60. Schönherr D, Wollatz U, Haznar-Garbacz D, Hanke U, Box KJ, Taylor R, et al. Characterisation of selected active agents regarding pKa values, solubility concentrations and pH profiles by SiriusT3. European Journal of Pharmaceutics and Biopharmaceutics. 2015;92:155-70.

61. Šramko M, Remko M, Garaj V. Theoretical study of gas-phase acidities of selected angiotensin-converting enzyme inhibitors. Structural Chemistry. 2005;16(4):391-9.

62. Benet LZ. The role of BCS (Biopharmaceutics Classification System) and BDDCS (Biopharmaceutics Drug Disposition Classification System) in drug development. Journal of Pharmaceutical Sciences. 2013;102(1):34-42.

63. Wadworth AN, Brogden RN. Quinapril. Drugs. 1991;41(3):378-99.

64. Freed AL, Silbering SB, Kolodsick KJ, Rossi DT, Mahjour M, Kingsmill CA. The development and stability assessment of extemporaneous pediatric formulations of Accupril. International Journal of Pharmaceutics. 2005;304(1):135-44.

65. Gu L, Strickley RG. Diketopiperazine formation, hydrolysis, and epimerization of the new dipeptide angiotensin-converting enzyme inhibitor RS-10085. Pharmaceutical Research. 1987;4(5):392-7.

66. Wagstaff AJ, Davis R, McTavish D. Fosinopril. Drugs. 1996;51(5):777-91.

67. Narayanam M, Singh S. Characterization of stress degradation products of fosinopril by using LC-MS/TOF, MSn and on-line H/D exchange. Journal of Pharmaceutical and Biomedical Analysis. 2014;92:135-43.

68. Wang Z, Morris KR, Chu B. Aggregation behavior of fosinopril sodium — a new angiotensin-converting enzyme inhibitor. Journal of Pharmaceutical Sciences. 1995;84(5):609-13.

69. Moffat A, Osselton M, Widdop B, Watts J. Clarke's Analysis of Drugs and Poisons. 4th ed. London: Pharmaceutical Press; 2011.

70. Budavari S, O'Neil MJ, Smith A, Heckelman PE. The Merck index: an encyclopedia of chemicals, drugs and biologicals. 11th ed. USA: Merck Rahway NJ; 1989.

71. Ranade V, Somberg JC. Rapid determination of partition coefficients between n-octanol/water for cardiovascular therapies. American Journal of Therapeutics. 2002;9(1):19-24.

72. Suri R, Beg S, Kohli K. Target strategies for drug delivery by passing ocular barriers. Journal of Drug Delivery Science and Technology. 2020;55:101389.

73. Gaudana R, Ananthula HK, Parenky A, Mitra AK. Ocular Drug Delivery. AAPS PharmSciTech. 2010;12(3):348-60.

จุฬาลงกรณ์มหาวิทยาลัย
CHULALONGKORN UNIVERSITY

74. Barar J, Javadzadeh AR, Omidi Y. Ocular novel drug delivery: impacts of membranes and barriers. Journal of Expert Opinion on Drug Delivery. 2008;5(5):567-81.

75. Sunkara G, Kompella U. Ophthalmic Drug Delivery Systems. Membrane transport processes in the eye. Florida: CRC Press; 2003. p 34-79.

76. Prausnitz MR, Noonan JS. Permeability of cornea, sclera, and conjunctiva: a literature analysis for drug delivery to the eye. Journal of Pharmaceutical Sciences. 1998;87(12):1479-88.

77. Hämäläinen K, Kananen K, Auriola S, Kontturi K, Urtti A. Characterization of paracellular and aqueous penetration routes in cornea, conjunctiva, and sclera. Investigative Ophthalmology and Visual Science. 1997;38(3):627-34.

78. Saha P, Kim KJ, Lee VH. A primary culture model of rabbit conjunctival epithelial cells exhibiting tight barrier properties. Current Eye Research. 1996;15(12):1163-9.

79. Davies NM. Biopharmaceutical considerations in topical ocular drug delivery. Clinical and Experimental Pharmacology and Physiology. 2000;27(7):558-62.

80. Koevary SB. Pharmacokinetics of topical ocular drug delivery: potential uses for the treatment of diseases of the posterior segment and beyond. Current Drug Metabolism. 2003;4(3):213-22.

81. Loftsson T, Stefánsson E. Effect of cyclodextrins on topical drug delivery to the eye. Drug Development and Industrial Pharmacy. 2008;23(5):473-81.

82. Rajewski RA, Stella VJ. Pharmaceutical applications of cyclodextrins. 2. in vivo drug delivery. Journal of Pharmaceutical Sciences. 1996;85(11):1142-69.

83. Irie T, Uekama K. Pharmaceutical applications of cyclodextrins. III. Toxicological issues and safety evaluation. Journal of Pharmaceutical Sciences. 1997;86(2):147-62.

84. Szejtli J. Medicinal applications of cyclodextrins. Medicinal Research Reviews. 1994;14(3):353-86.

85. Saenger W, Jacob J, Gessler K, Steiner T, Hoffmann D, Sanbe H, et al. Structures of the common cyclodextrins and their larger analogues beyond the doughnut. Chemical Reviews. 1998;98(5):1787-802.

86. Zhou J, Ritter H. Cyclodextrin functionalized polymers as drug delivery systems. Polymer Chemistry. 2010;1(10):1552-9.

87. Loftsson T, Jarho P, Másson M, Järvinen T. Cyclodextrins in drug delivery. Expert Opinion on Drug Delivery. 2005;2(2):335-51.

88. Connors KA. The stability of cyclodextrin complexes in solution. Chemical Reviews. 1997;97(5):1325-57.

89. Mura P. Analytical techniques for characterization of cyclodextrin complexes in aqueous solution: A review. Journal of Pharmaceutical and Biomedical Analysis. 2014;101:238-50.

90. Mura P. Analytical techniques for characterization of cyclodextrin complexes in the solid state: A review. Journal of Pharmaceutical and Biomedical Analysis. 2015;113:226-38.

91. Loftsson T. Effects of cyclodextrins on the chemical stability of drugs in aqueous solutions. Drug Stability. 1995;1(1):22-3.

จุฬาลงกรณ์มหาวิทยาลัย
Chulalongkorn University

92. Anand S, Braga VML. Cyclodextrins in ocular drug delivery, In: Pathak Y, Sutariya V, Hirani A (eds). Nano-Biomaterials for Ophthalmic Drug Delivery. Switzerland: Springer; 2016. p 243-52.

93. Loftsson T, Stefánsson E. Cyclodextrins in ocular drug delivery: theoretical basis with dexamethasone as a sample drug. Journal of Drug Delivery Science and Technology. 2007;17(1):3-9.

94. Loftsson T, Friðriksdóttir H, Stefansson E, Thorisdottir S, Guðmundsson Ö, Sigthorsson T. Topically effective ocular hypotensive acetazolamide and ethoxyzolamide formulations in rabbits. Journal of Pharmacy and Pharmacology. 1994;46(6):503-4.

95. Saari KM, Nelimarkka L, Ahola V, Loftsson T, Stefánsson E. Comparison of topical 0.7% dexamethasone–cyclodextrin with 0.1%

dexamethasone sodium phosphate for postcataract inflammation. Graefe's Archive for Clinical and Experimental Ophthalmology. 2006;244(5):620.

96. Jarho P, Jarvinen K, Urtti A, Stella VJ, Jarvinen T. Modified β-cyclodextrin (SBE7-β-CyD) with viscous vehicle improves the ocular delivery and tolerability of pilocarpine prodrug in rabbits. Journal of Pharmacy and Pharmacology. 1996;48(3):263-9.

97. Loftsson T, Brewster ME. Pharmaceutical applications of cyclodextrins: effects on drug permeation through biological membranes. Journal of Pharmacy and Pharmacology. 2011;63(9):1119-35.

98. Uekama K, Adachi H, Irie T, Yano T, Saita M, Noda K. Improved transdermal delivery of prostaglandin E1 through hairless mouse skin: combined use of carboxymethyl-ethyl-beta-cyclodextrin and penetration enhancers. Journal of Pharmacy and Pharmacology. 1992;44(2):119-21.

99. Jansook P, Muankaew C, Stefánsson E, Loftsson T. Development of eye drops containing antihypertensive drugs: formulation of aqueous irbesartan/γCD eye drops. Pharmaceutical Development and Technology. 2015;20(5):626-32.

100. Loftsson T, Brewster ME. Pharmaceutical applications of cyclodextrins: effects on drug permeation through biological membranes. Journal of Pharmacy and Pharmacology. 2011;63(9):1119-35.

101. Popielec A, Loftsson T. Effects of cyclodextrins on the chemical stability of drugs. International Journal of Pharmaceutics. 2017;531(2):532-42.

102. Loftsson T, Björnsdóttir S, Pálsdóttir G, Bodor N. The effects of 2-hydroxypropyl-β-cyclodextrin on the solubility and stability of chlorambucil and melphalan in aqueous solution. International Journal of Pharmaceutics. 1989;57(1):63-72.

103. Loftsson T, Fridriksdóttir H. Degradation of lomustine (CCNU) in aqueous solutions. International Journal of Pharmaceutics. 1990;62(2):243-7.

104. Li J, Guo Y, Zografi G. The solid-state stability of amorphous quinapril in the presence of β-cyclodextrins. Journal of Pharmaceutical Sciences. 2002;91(1):229-43.

จุฬาลงกรณ์มหาวิทยาลัย
CHULALONGKORN UNIVERSITY

105. Wu W, Wu J, Bodor N. Effect of 2-hydroxypropyl-beta-cyclodextrin on the solubility, stability, and pharmacological activity of the chemical delivery system of TRH analogs. Pharmazie. 2002;57(2):130-4.

106. Alsarra IA, Ahmed MO, El-Badry M, Alanazi FK, Al-Mohizea AM, Ahmed SM. Effect of β-cyclodextrin derivatives on the kinetics of degradation of cefotaxime sodium in solution state. Journal of Drug Delivery Science and Technology. 2007;17(5):353-7.

107. Loftsson T, Johannesson H. The influence of cyclodextrins on the stability of cephalotin and aztreonam in aqueous solutions. Pharmazie. 1994;49(4):292-3.

108. Loftsson T, Ólafsdóttir BJ. Cyclodextrin-accelerated degradation of β-lactam antibiotics in aqueous solutions. International Journal of Pharmaceutics. 1991;67(2):R5-R7.

109. Mielcarek J. Photochemical stability of the inclusion complexes formed by modified 1,4-dihydropyridine derivatives with β-cyclodextrin. Journal of Pharmaceutical and Biomedical Analysis. 1997;15(6):681-6.

110. Lutka A, Koziara J. Interaction of trimeprazine with cyclodextrins in aqueous solution. Acta Poloniae Pharmaceutica. 2000;57(5):369-74.

111. Scalia S, Villani S, Casolari A. Inclusion complexation of the sunscreen agent 2-ethylhexyl-p-dimethylaminobenzoate with hydroxypropyl-β-cyclodextrin: effect on photostability. Journal of Pharmacy and Pharmacology. 1999;51(12):1367-74.

112. Lutka A. Investigation of interaction of promethazine with cyclodextrins. Acta Poloniae Pharmaceutica. 2002;59(1):45-52.

113. Brewster ME, Loftsson T, Estes KS, Lin J-L, Fridriksdóttir H, Bodor N. Effect of various cyclodextrins on solution stability and dissolution rate of doxorubicin hydrochloride. International Journal of Pharmaceutics. 1992;79(1):289-99.

114. Ma DQ, Rajewski RA, Vander Velde D, Stella VJ. Comparative effects of (SBE)7m-β-CD and HP-β-CD on the stability of two anti-neoplastic agents, melphalan and carmustine. Journal of Pharmaceutical Sciences. 2000;89(2):275-87.

115. Kang J, Kumar V, Yang D, Chowdhury PR, Hohl RJ. Cyclodextrin complexation: influence on the solubility, stability, and cytotoxicity of camptothecin, an antineoplastic agent. European Journal of Pharmaceutical Sciences. 2002;15(2):163-70.

116. Mahale NB, Thakkar PD, Mali RG, Walunj DR, Chaudhari SR. Niosomes: novel sustained release nonionic stable vesicular systems--an overview. Advances in Colloid and Interface Science. 2012;183-184:46-54.

117. Huang Y, Rao Y, Chen J, Yang VC, Liang W. Polysorbate cationic synthetic vesicle for gene delivery. Journal of Biomedical Materials Research Part A. 2011;96(3):513-9.

118. Azeem A, Anwer MK, Talegaonkar S. Niosomes in sustained and targeted drug delivery: some recent advances. Journal of Drug Targeting. 2009;17(9):671-89.

119. Sahin NO. Niosome as nanocarrier systems. In: Mozafari MR (ed). Nanomaterials and nanosystems for biomedical. Switzerland: Springer; 2007. p 67-81.

120. Nasseri B. Effect of cholesterol and temperature on the elastic properties of niosomal membranes. International Journal of Pharmaceutics. 2005;300(1):95-101.

121. Hu C, Rhodes DG. Proniosomes: a novel drug carrier preparation. International Journal of Pharmaceutics. 1999;185(1):23-35.

122. Marianecci C, Rinaldi F, Esposito S, Di Marzio L, Carafa M. Niosomes encapsulating ibuprofen-cyclodextrin complexes: preparation and characterization. Current Drug Targets. 2013;14(9):1070-8.

123. Oommen E, Tiwari SB, Udupa N, Kamath R, Devi PU. Niosome entrapped β-cyclodextrin methotrexate complex as a drug delivery system. Indian Journal of Pharmacology. 1999;31(4):279-84.

124. Elmotasem H, Awad GEA. A stepwise optimization strategy to formulate in situ gelling formulations comprising fluconazole-hydroxypropyl-beta-cyclodextrin complex loaded niosomal vesicles and Eudragit nanoparticles for enhanced antifungal activity and prolonged ocular delivery. Asian Journal of Pharmaceutical Sciences. 2019.

125. D'souza S, Ray J, Pandey S, Udupa N. Absorption of ciprofloxacin and norfloxacin when administered as niosome-encapsulated inclusion complexes. Journal of Pharmacy and Pharmacology. 1997;49(2):145-9.

126. Chi L, Wu D, Li Z, Zhang M, Liu H, Wang C, et al. Modified release and improved stability of unstable BCS II drug by using cyclodextrin complex as carrier to remotely load drug into niosomes. Molecular Pharmaceutics. 2016;13(1):113-24.

127. Sheena I, Singh U, Aithal K, Udupa N. Pilocarpine β-cyclodextrin complexation and niosomal entrapment. Pharmaceutical Sciences. 1997;3(8):383-6.

128. Oommen E, Shenoy BD, Udupa N, Kamath R, Devi PU. Antitumour efficacy of cyclodextrin-complexed and niosome-encapsulated plumbagin in mice bearing melanoma B16F1. Pharmacy and Pharmacology Communications. 1999;5(4):281-5.

129. Loukas YL, Vraka V, Gregoriadis G. Drugs, in cyclodextrins, in liposomes: a novel approach to the chemical stability of drugs sensitive to hydrolysis. International Journal of Pharmaceutics. 1998;162(1):137-42.

130. Chen J, Lu WL, Gu W, Lu SS, Chen ZP, Cai BC, et al. Drug-in-cyclodextrin-in-liposomes: a promising delivery system for hydrophobic drugs. Expert Opinion on Drug Delivery. 2014;11(4):565-77.

131. Duchêne D, Ponchel G, Wouessidjewe D. Cyclodextrins in targeting: application to nanoparticles. Advanced Drug Delivery Reviews. 1999;36(1):29-40.

132. McCormack B, Gregoriadis G. Entrapment of cyclodextrin-drug complexes into liposomes: potential advantages in drug delivery. Journal of Drug Targeting. 1994;2(5):449-54.

133. Mura P. Advantages of the combined use of cyclodextrins and nanocarriers in drug delivery: A review. International Journal of Pharmaceutics. 2020;579:119181.

134. Job P. Formation and stability of inorganic complexes in solution. Annali di Chimica Applicata. 1928;9:113–203.

135. Benesi HA, Hildebrand JH. A spectrophotometric investigation of the interaction of iodine with aromatic hydrocarbons. Journal of the American Chemical Society. 1949;71(8):2703-7.

136. Loftsson T, Hreinsdóttir D, Másson M. Evaluation of cyclodextrin solubilization of drugs. International Journal of Pharmaceutics. 2005;302(1):18-28.

137. Khalil RM, Abdelbary GA, Basha M, Awad GEA, el-Hashemy HA. Enhancement of lomefloxacin Hcl ocular efficacy via niosomal encapsulation: in vitro characterization and in vivo evaluation. Journal of Liposome Research. 2017;27(4):312-23.

138. Müller-Goymann CC. Physicochemical characterization of colloidal drug delivery systems such as reverse micelles, vesicles, liquid crystals and nanoparticles for topical administration. European Journal of Pharmaceutics and Biopharmaceutics. 2004;58(2):343-56.

139. Aggarwal D, Kaur IP. Improved pharmacodynamics of timolol maleate from a mucoadhesive niosomal ophthalmic drug delivery system. International Journal of Pharmaceutics. 2005;290(1):155-9.

140. Kopp S. Stability testing of pharmaceutical products in a global environment. The Regulatory Affairs Journal Pharma. 2006;5:291-4.

141. Markens U, ASIA-PACIFIC RH. Conducting stability studies-recent changes to climatic zone IV. Life Science Technical Bulletin. 2009;13:1-4.

142. Udrescu L, Sbarcea L, Fuliaș A, Ledeți I, Vlase G, Barvinschi P, et al. Physicochemical analysis and molecular modeling of the fosinopril β-cyclodextrin inclusion complex. Journal of Spectroscopy. 2014;2014.

143. Ikeda Y, Motoune S, Matsuoka T, Arima H, Hirayama F, Uekama K. Inclusion complex formation of captopril with α-and β-cyclodextrins in aqueous solution: NMR spectroscopic and molecular dynamic studies. Journal of Pharmaceutical Sciences. 2002;91(11):2390-8.

144. Bratu I, Kacso I, Borodi G, Constantinescu DE, Dragan F. Inclusion compound of fosinopril with β-cyclodextrin. Spectroscopy. 2009;23(1):51-8.

จุฬาลงกรณ์มหาวิทยาลัย
CHULALONGKORN UNIVERSITY

145. Touw D, Vigneron J. Stability. In: Bouwman-Boer Y, Fenton-May V, Le Brun P (eds). Practical Pharmaceutics. 5th ed. Switzerland: Springer; 2015. p 435-438.

146. Gibson M. Ophthalmic dosage forms. In: Gibson M (ed). Pharmaceutical Preformulation and Formulation: A Practical Guide from Candidate Drug Selection to Commercial Dosage Form. 2nd ed. New York, London: CRC Press; 2016. p 459-488.

147. Thompson JE, Davidow LW. A Practical Guide to Contemporary Pharmacy Practice. Antioxidants. 3rd ed. Philadelphia, United States: Lippincott Williams & Wilkins; 2009. p 216-23.

148. Ang ZY, Boddy M, Liu Y, Sunderland B. Stability of apomorphine in solutions containing selected antioxidant agents. Drug Design, Development and Therapy. 2016;10:3253-65.

149. Schneider H-J, Hacket F, Rüdiger V, Ikeda H. NMR studies of cyclodextrins and cyclodextrin complexes. Chemical Reviews. 1998;98(5):1755-86.

150. Greatbanks D, Pickford R. Cyclodextrins as chiral complexing agents in water, and their application to optical purity measurements. Magnetic Resonance in Chemistry. 1987;25(3):208-15.

151. Do Thi T, Nauwelaerts K, Froeyen M, Baudemprez L, Van Speybroeck M, Augustijns P, et al. Comparison of the complexation between methylprednisolone and different cyclodextrins in solution by 1H-NMR and molecular modeling studies. Journal of Pharmaceutical Sciences. 2010;99(9):3863-73.

152. Ali SM, Upadhyay SK. Complexation studies of pioglitazone hydrochloride and β-cyclodextrin: NMR (1 H, ROESY) spectroscopic study in solution. Journal of Inclusion Phenomena and Macrocyclic Chemistry. 2008;62(1-2):161-5.

153. Jansook P, Ritthidej GC, Ueda H, Stefánsson E, Loftsson T. γCD/HPγCD mixtures as solubilizer: solid-state characterization and sample dexamethasone eye drop suspension. Journal of Pharmacy & Pharmaceutical Sciences. 2010;13(3):336-50.

154. Jansook P, Kulsirachote P, Loftsson T. Cyclodextrin solubilization of celecoxib: solid and solution state characterization. Journal of Inclusion Phenomena and Macrocyclic Chemistry. 2018;90(1):75-88.

155. Manosroi A, Wongtrakul P, Manosroi J, Sakai H, Sugawara F, Yuasa M, et al. Characterization of vesicles prepared with various non-ionic surfactants mixed with cholesterol. Colloids and Surfaces B: Biointerfaces. 2003;30(1):129-38.

156. Pandey VP, Deivasigamani K. Preparation and characterization of ofloxacin non-ionic surfactant vesicles for ophthalmic use. Journal of Pharmacy Research. 2009;2(8):1330-4.

157. Mathis GA. Clinical ophthalmic pharmacology and therapeutics: ocular drug delivery, In: Gelatt KN (ed). Veterinary Ophthalmology. Florida: Lippincott Williams & Wilkins; 1999. p 291-297.

158. Yasin MN, Hussain S, Malik F, Hameed A, Sultan T, Qureshi F, et al. Preparation and characterization of chloramphenicol niosomes and comparison with chloramphenicol eye drops (0.5% w/v) in experimental conjunctivitis in albino rabbits. Pakistan Journal of Pharmaceutical Sciences. 2012;25(1):117-21.

159. Frisch D, Eyring H, Kincaid JF. Pressure and temperature effects on the viscosity of liquids. Journal of Applied Physics. 1940;11(1):75-80.

160. Kramer I, Haber M, Duis A. Formulation requirements for the ophthalmic use of antiseptics. Developments in Ophthalmology. 2002;33:85-116.

161. Danaei M, Dehghankhold M, Ataei S, Hasanzadeh Davarani F, Javanmard R, Dokhani A, et al. Impact of particle size and polydispersity index on the clinical applications of lipidic nanocarrier systems. Pharmaceutics. 2018;10(2):57-74.

162. Suwakul W, Ongpipattanakul B, Vardhanabhuti N. Preparation and characterization of propylthiouracil niosomes. Journal of Liposome Research. 2006;16(4):391-401.

163. Yoshioka T, Sternberg B, Florence AT. Preparation and properties of vesicles (niosomes) of sorbitan monoesters (Span 20, 40, 60 and 80) and

a sorbitan triester (Span 85). International Journal of Pharmaceutics. 1994;105(1):1-6.

164. Ruckmani K, Jayakar B, Ghosal SK. Nonionic surfactant vesicles (niosomes) of cytarabine hydrochloride for effective treatment of leukemias: encapsulation, storage, and in vitro release. Drug Development and Industrial Pharmacy. 2000;26(2):217-22.

165. Khazaeli P, Pardakhty A, Shoorabi H. Caffeine-loaded niosomes: characterization and in vitro release studies. Drug Delivery. 2007;14(7):447-52.

166. Guinedi AS, Mortada ND, Mansour S, Hathout RM. Preparation and evaluation of reverse-phase evaporation and multilamellar niosomes as ophthalmic carriers of acetazolamide. International Journal of Pharmaceutics. 2005;306(1):71-82.

167. Manconi M, Sinico C, Valenti D, Loy G, Fadda AM. Niosomes as carriers for tretinoin. I. Preparation and properties. International Journal of Pharmaceutics. 2002;234(1):237-48.

168. Tabbakhian M, Tavakoli N, Jaafari MR, Daneshamouz S. Enhancement of follicular delivery of finasteride by liposomes and niosomes: 1. In vitro permeation and in vivo deposition studies using hamster flank and ear models. International Journal of Pharmaceutics. 2006;323(1):1-10.

169. Hasan AA. Design and in vitro characterization of small unilamellar niosomes as ophthalmic carrier of dorzolamide hydrochloride. Pharmaceutical Development and Technology. 2014;19(6):748-54.

170. Abdelkader H, Ismail S, Kamal A, Alany RG. Design and evaluation of controlled-release niosomes and discomes for naltrexone hydrochloride ocular delivery. Journal of Pharmaceutical Sciences. 2011;100(5):1833-46.

171. Balakrishnan P, Shanmugam S, Lee WS, Lee WM, Kim JO, Oh DH, et al. Formulation and in vitro assessment of minoxidil niosomes for enhanced skin delivery. International Journal of Pharmaceutics. 2009;377(1):1-8.

จุฬาลงกรณ์มหาวิทยาลัย
Chulalongkorn University

172. Bayindir ZS, Yuksel N. Characterization of niosomes prepared with various nonionic surfactants for paclitaxel oral delivery. Journal of Pharmaceutical Sciences. 2010;99(4):2049-60.

173. Valente AJ, Söderman O. The formation of host–guest complexes between surfactants and cyclodextrins. Advances in Colloid and Interface Science. 2014;205:156-76.

174. Tsianou M, Fajalia AI. Cyclodextrins and surfactants in aqueous solution above the critical micelle concentration: where are the cyclodextrins located? Langmuir. 2014;30(46):13754-64.

175. Machado ND, Silva OF, de Rossi RH, Fernández MA. Cyclodextrin modified niosomes to encapsulate hydrophilic compounds. Royal Society of Chemistry Advances. 2018;8(52):29909-16.

176. Zubairu Y, Negi LM, Iqbal Z, Talegaonkar S. Design and development of novel bioadhesive niosomal formulation for the transcorneal delivery of anti-infective agent: in-vitro and ex-vivo investigations. Asian Journal of Pharmaceutical Sciences. 2015;10(4):322-30.

177. Junyaprasert VB, Teeranachaideekul V, Supaperm T. Effect of charged and non-ionic membrane additives on physicochemical properties and stability of niosomes. AAPS PharmSciTech. 2008;9(3):851.

178. Silva OF, Correa NM, Silber JJ, de Rossi RH, Fernández MA. Supramolecular assemblies obtained by mixing different cyclodextrins and AOT or BHDC reverse micelles. Langmuir. 2014;30(12):3354-62.

179. Zhou C, Cheng X, Zhao Q, Yan Y, Wang J, Huang J. Self-assembly of nonionic surfactant tween 20@ 2β-CD inclusion complexes in dilute solution. Langmuir. 2013;29(43):13175-82.

180. Essa EA. Effect of formulation and processing variables on the particle size of sorbitan monopalmitate niosomes. Asian Journal of Pharmaceutics 2014;4(4):227-33.

181. Kumar GP, Rajeshwarrao P. Nonionic surfactant vesicular systems for effective drug delivery—an overview. Acta Pharmaceutica Sinica B. 2011;1(4):208-19.

182. Jaehnig F, Harlos K, Vogel H, Eibl H. Electrostatic interactions at charged lipid membranes. Electrostatically induced tilt. Biochemistry. 1979;18(8):1459-68.

183. Paul BK, Ghosh N, Mondal R, Mukherjee S. Contrasting effects of salt and temperature on niosome-bound norharmane: direct evidence for positive heat capacity change in the niosome: β-cyclodextrin interaction. The Journal of Physical Chemistry B. 2016;120(17):4091-101.

184. Hao Y-M, Li Ka. Entrapment and release difference resulting from hydrogen bonding interactions in niosome. International Journal of Pharmaceutics. 2011;403(1):245-53.

185. El-Ridy MS, Abdelbary A, Essam T, Abd EL-Salam RM, Aly Kassem AA. Niosomes as a potential drug delivery system for increasing the efficacy and safety of nystatin. Drug Development and Industrial Pharmacy. 2011;37(12):1491-508.

186. Zhang L, Zhang Q, Wang X, Zhang W, Lin C, Chen F, et al. Drug-in-cyclodextrin-in-liposomes: A novel drug delivery system for flurbiprofen. International Journal of Pharmaceutics. 2015;492(1):40-5.

187. Wax MB, Camras CB, Fiscella RG, Girkin C, Singh K, Weinreb RN. Emerging perspectives in glaucoma: optimizing 24-hour control of intraocular pressure. American Journal of Ophthalmology. 2002;133(6, Supplement 1):S1-S10.

188. Barar J, Javadzadeh AR, Omidi Y. Ocular novel drug delivery: impacts of membranes and barriers. Expert opinion on drug delivery. 2008;5(5):567-81.

189. Loftsson T, Sigurđsson HH, Konráđsdóttir F, Gisladottir S, Jansook P, Stefansson E. Topical drug delivery to the posterior segment of the eye: anatomical and physiological considerations. International Journal of Pharmaceutical Sciences. 2008;63(3):171-9.

190. Hämäläinen KM, Kananen K, Auriola S, Kontturi K, Urtti A. Characterization of paracellular and aqueous penetration routes in cornea, conjunctiva, and sclera. Investigative Ophthalmology and Visual Science. 1997;38(3):627-34.

จุฬาลงกรณ์มหาวิทยาลัย
Chulalongkorn University

191. Loch C, Zakelj S, Kristl A, Nagel S, Guthoff R, Weitschies W, et al. Determination of permeability coefficients of ophthalmic drugs through different layers of porcine, rabbit and bovine eyes. European Journal of Pharmaceutical Sciences. 2012;47(1):131-8.

192. Ahmed I, Patton TF. Importance of the noncorneal absorption route in topical ophthalmic drug delivery. Investigative Ophthalmology and Visual Science. 1985;26(4):584-7.

193. Gharib R, Greige-Gerges H, Fourmentin S, Charcosset C, Auezova L. Liposomes incorporating cyclodextrin–drug inclusion complexes: Current state of knowledge. Carbohydrate Polymers. 2015;129:175-86.

194. Bates TR, Nightingale CH, Dixon E. Kinetics of hydrolysis of polyoxyethylene (20) sorbitan fatty acid ester surfactants. Journal of Pharmacy and Pharmacology. 1973;25(6):470-7.

195. Kopermsub P, Mayen V, Warin C. Potential use of niosomes for encapsulation of nisin and EDTA and their antibacterial activity enhancement. Food Research International. 2011;44(2):605-12.

196. Khan MI, Madni A, Peltonen L. Development and in-vitro characterization of sorbitan monolaurate and poloxamer 184 based niosomes for oral delivery of diacerein. European Journal of Pharmaceutical Sciences. 2016;95:88-95.

จุฬาลงกรณ์มหาวิทยาลัย
Chulalongkorn University

APPENDIX
HPLC VALIDATION

1. Specificity

The chromatograms of PBS (pH 7.4), γCD, Na-MS, EDTA, blank niosome, mobile phase and various concentration of FOS standard solutions are displayed in Figure A-1 and Figure A-2. FOS was eluted with the retention time of 4.3 to 4.5 minutes and the solvent peak was found with retention time of 1.0 to 3.0 minutes. Therefore, no interference peaks of excipients to FOS was found when injected as the same condition.

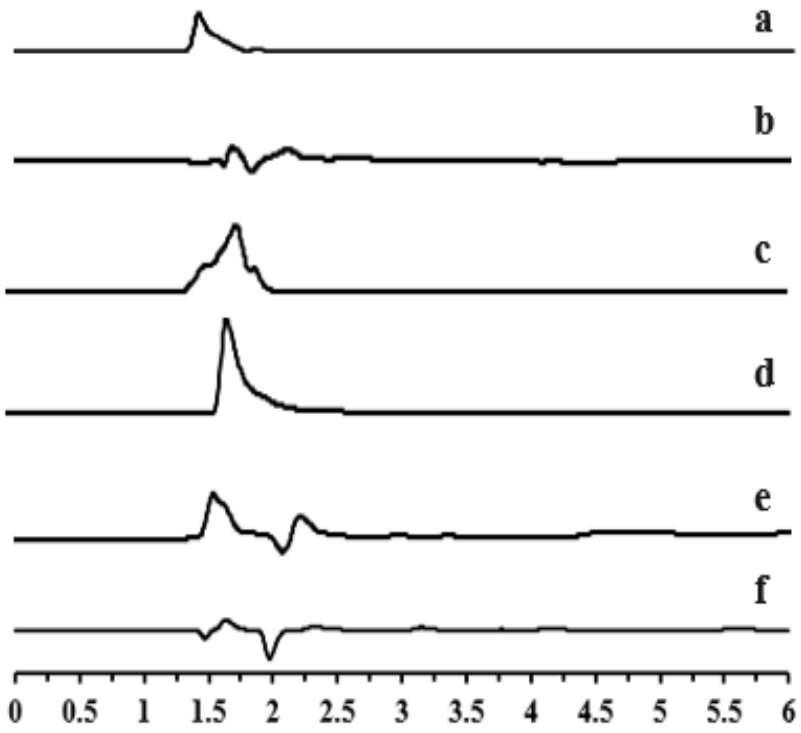

Figure A- 1 The HPLC chromatograms of (a) PBS pH 7.4, (b) γCD, (c) Na-MS, (d) EDTA, (e) blank niosome and (f) mobile phase in acetonitrile : water (70:30 v/v)

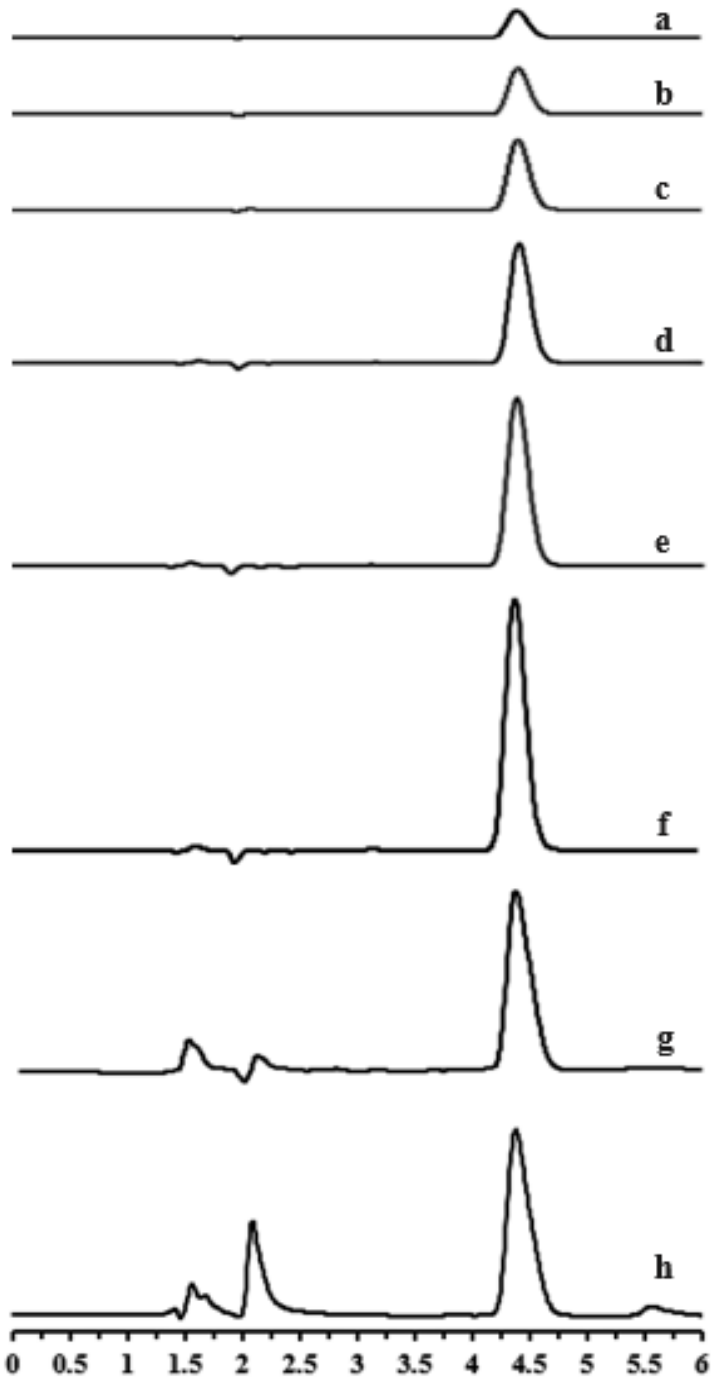

Figure A- 2 The HPLC chromatograms of the standard solution of FOS (a) 20 µg/ml, (b) 40 µg/ml, (c) 80 µg/ml, (d) 120 µg/ml, (e) 160 µg/ml, (f) 200 µg/ml, (g) FOS loaded niosome and (h) FOS/γCD loaded niosome in acetonitrile : water (70:30 v/v)

2. Linearity

The chromatograms of FOS standard solution are shown in Figure A-2. The retention time of FOS was about 4.3 to 4.5 minutes. The calibration curve was plotted between the peak area and concentration of FOS (µg/mL). The results are presented in Table A-1, A-2, A-3 and Figure A-3, A-4 and A-5. The linear regression analysis was performed with coefficient of determination (R^2) and resulted as 0.9997-1.0000. The result indicated that this HPLC condition was acceptable to analyze the concentration of FOS in formulation.

Table A-1. Data of calibration curve of FOS standard solutions (No.1)

FOS conc. (µg/mL)	Peak area			Mean	SD	% CV
	n 1	n 2	n 3			
20.12	732.0	733.0	736.4	733.8	2.30	0.31
40.24	1439.1	1445.9	1460.2	1448.4	10.76	0.74
80.48	2905.4	2895.0	2916.8	2905.7	10.03	0.37
120.72	4398.9	4424.4	4423.4	4415.5	14.44	0.32
160.96	5841.2	5841.8	5852.0	5845.0	60.06	0.10
201.2	7336.5	7360.3	7337.3	7344.7	13.51	0.18

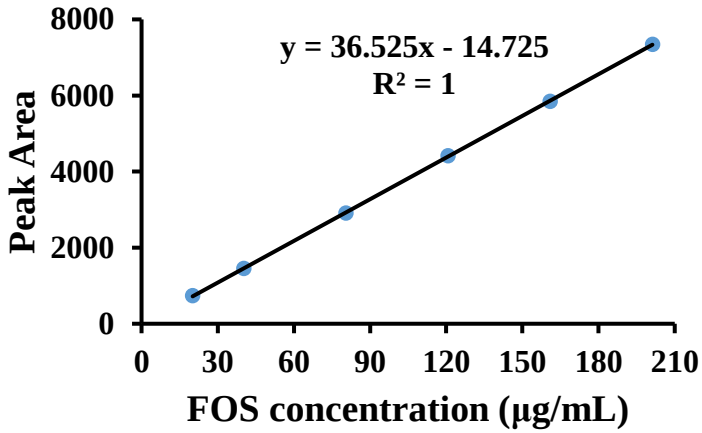

Figure A- 3 Calibration curve of standard FOS solutions by HPLC method (No.1)

Table A-2. Data of calibration curve of FOS standard solutions (No.2)

FOS conc. (µg/mL)	Peak area			Mean	SD	% CV
	n 1	n 2	n 3			
20.08	740.2	744.8.0	751.3	745.43	5.57	0.74816
40.16	1477.2	1480.6	1486.4	1481.40	4.65	0.314019
80.32	2895.3	2907.0	2909.2	2903.83	7.47	0.257298
120.48	4354.6	4367.0	4372.7	4364.76	9.25	0.212024
160.64	5833.1	5856.2	5866.7	5852.00	17.18	0.293733
200.8	7316.2	7332.4	7324.4	7324.33	8.10	0.110593

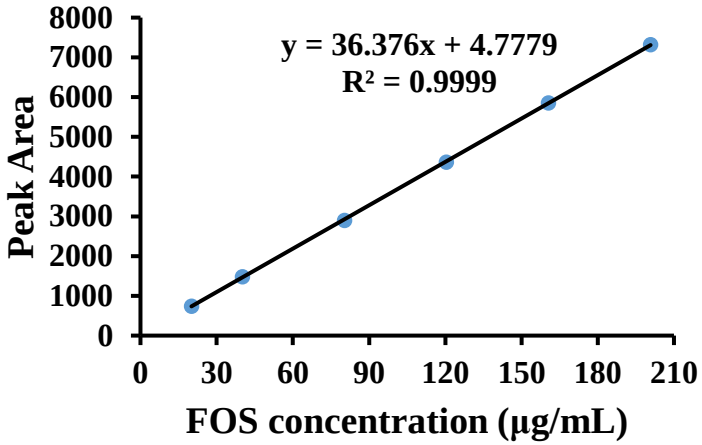

Figure A- 4 Calibration curve of standard FOS solutions by HPLC method (No.2)

Table A-3. Data of calibration curve of FOS standard solutions (No.3)

FOS conc. (µg/mL)	Peak area			Mean	SD	%CV
	n 1	n 2	n 3			
20.13	740.2	747.5	747.7	745.13	3.48	0.468285
40.26	1472.1	1483.8	1463.4	1473.10	8.35	0.567391
80.52	2922.1	2922.3	2921.2	2921.86	0.47	0.016374
120.78	4465.6	4481.7	4470.0	4472.43	6.79	0.151915
161.04	5944.6	5965.2	5926.4	5945.40	15.85	0.266595
201.3	7492.7	7458.3	7466.2	7472.40	14.71	0.196886

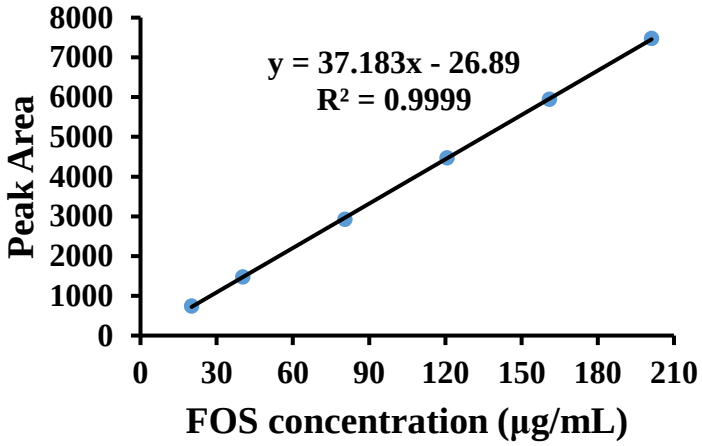

Figure A- 5 Calibration curve of standard FOS solutions by HPLC method (No.3)

3. Precision

For validating precision, analysis of within run (intra-day precision) and between run (inter-day precision) were performed. The data of analysis are demonstrated in Table A-4 and Table A-5. The low percentage of coefficient of variation (% CV) values of peak area were found in both within run (0.29 - 0.75 %) and between run (0.14 - 1.16 %). Therefore, this HPLC method could be used to analyze FOS over a period of time.

Table A-4. Data of within run precision of FOS analyzed by HPLC method

FOS conc. (μg/mL)	Peak area					Mean	SD	%CV
	n 1	n 2	n 3	n 4	n 5			
20.12	732.0	737.5	740.7	735.3	746.7	738.44	5.60	0.75
80.48	2905.4	2922.3	2921.2	2926.3	2925.4	2920.12	8.49	0.29
201.2	7336.5	7348.3	7366.2	7380.4	7464.3	7379.14	50.47	0.68

จุฬาลงกรณ์มหาวิทยาลัย
Chulalongkorn University

Table A-5. Data of between run precision of FOS analyzed by HPLC method

FOS conc. (μg/mL)		Peak area			Mean	SD	% CV
	N	Day1	Day2	Day 3			
20.12	n 1	732	744.7	748.5	741.73	8.64	1.16
	n 2	737.5	742.9	744.5	741.63	3.66	0.49
	n 3	740.7	743.8	745.1	743.20	2.26	0.30
	n 4	735.3	738.3	740.6	738.06	2.65	0.36
	n 5	746.7	750.4	754.1	750.40	3.70	0.49
	Average	738.4	744.0	746.5	743.00	4.15	0.55
80.48	n 1	2905.4	2912.1	2942.1	2919.86	19.54	0.66
	n 2	2922.3	2937.3	2962.3	2940.63	20.20	0.68
	n 3	2921.2	2932.2	2945.8	2933.06	12.32	0.42
	n 4	2930.3	2926.3	2936.4	2931.00	5.08	0.17
	n 5	2935.4	2945.2	2955.4	2945.33	10.00	0.33
	Average	2922.9	2930.6	2948.4	2933.98	13.06	0.44
201.2	n 1	7336.5	7352.7	7392.7	7360.63	28.92	0.39
	n 2	7348.3	7478.3	7458.3	7428.30	70.00	0.94
	n 3	7366.2	7486.2	7496.5	7449.63	72.43	0.97
	n 4	7370.4	7380.4	7495.7	7415.50	69.63	0.93
	n 5	7364.1	7378.3	7384.3	7375.56	10.37	0.14
	Average	7357.1	7415.1	7445.5	7405.92	44.92	0.60

จุฬาลงกรณ์มหาวิทยาลัย
Chulalongkorn University

4. Accuracy

The percentage of analytical recovery in each FOS concentration with three determinations are shown in Table A-6, A-7 and A-8. The mean percent recoveries were 100.12 %, 100.05 % and 99.87 % with low % CV values of 0.59 %, 0.98% and 0.71% respectively. This result concluded that the HPLC method could be used to determine FOS content within the concentration range of 20 - 200 μg/mL.

Table A-6. Data of accuracy of FOS analyzed by HPLC method (No.1)

FOS conc. (μg/mL)	Peak area				Mean analytical concentration (μg/mL)	% recovery
	n 1	n 2	n 3	Mean		
121.68	4420.8	4378.9	4482.6	4427.4	121.58	99.91
162.24	5831.4	5917.2	5912.6	5887.0	161.70	99.67
202.8	7414.4	7408.8	7498.7	7440.6	204.41	100.79
					Mean	100.12
					SD	0.59
					%CV	0.59

จุฬาลงกรณ์มหาวิทยาลัย
Chulalongkorn University

Table A-7. Data of accuracy of FOS analyzed by HPLC method (No.2)

FOS conc. (μg/mL)	Peak area				Mean analytical concentration (μg/mL)	% recovery
	n 1	n 2	n 3	Mean		
121.68	4394.0	4390.5	4374.5	4386.3	120.45	98.99
162.24	5864.9	5951.4	5941.0	5919.1	162.58	100.21
202.8	7385.2	7517.4	7452.2	7451.6	204.71	100.94
					Mean	100.05
					SD	0.98
					%CV	0.98

Table A-8. Data of accuracy of FOS analyzed by HPLC method (No.3)

FOS conc. (μg/mL)	Peak area				Mean analytical concentration (μg/mL)	% recovery
	n 1	n 2	n 3	Mean		
121.68	4389.2	4371.7	4408.5	4389.8	120.54	99.06
162.24	5880.6	5909.4	5947.0	5912.3	162.40	100.10
202.8	7404.4	7423.1	7416.8	7414.7	203.70	100.44
					Mean	99.87
					SD	0.71
					%CV	0.71

จุฬาลงกรณ์มหาวิทยาลัย
Chulalongkorn University

VITA

NAME	Hay Marn Hnin
DATE OF BIRTH	23 July 1993
PLACE OF BIRTH	Myanmar
INSTITUTIONS ATTENDED	University of Pharmacy,Yangon
HOME ADDRESS	179/2 Phetchaburi soi 5, Thung Phaya Thai, Ratchathewi, Bangkok 10400
PUBLICATION	-
AWARD RECEIVED	-

จุฬาลงกรณ์มหาวิทยาลัย
Chulalongkorn University